

Private Fuel Storage, LLC

*P.O. Box C4010, La Crosse, WI 54602-4010
John D. Parkyn, Chairman of the Board
(608) 787-1236*

November 21, 2001

U.S. Nuclear Regulatory Commission
ATTN: Document Control Desk
Washington, D.C. 20555-0001

LICENSE APPLICATION AMENDMENT No. 23
DOCKET NO. 72-22/TAC NO. L22462
PRIVATE FUEL STORAGE FACILITY
PRIVATE FUEL STORAGE L.L.C.

- References:
1. PFS letter, Parkyn to the U.S. NRC, "License Application Amendment No. 22", dated March 30, 2001
 2. April 18, 2001 meeting between PFS and the NRC in San Antonio, Texas
 3. NRC letter, Brach to Parkyn, "March 30, 2001 License Application Amendment", dated May 7, 2001
 4. PFS letter, Donnell to the U.S. NRC, "Response to April 18, 2001 Meeting Issues", dated May 1, 2001
 5. PFS letter, Parkyn to the U.S. NRC, "Data Needed for NRC Review of License Amendment #22, dated May 31, 2001
 6. PFS letter, Donnell to the U.S. NRC, "PFSF Site Specific HI-STORM Evaluation", dated May 31, 2001
 7. PFS letter, Donnell to the U.S. NRC, "Commitment Resolution Letter #37", dated August 7, 2001
 8. PFS letter, Donnell to the U.S. NRC, "PFSF Site Specific Cask Stability Analysis", dated August 20, 2001
 9. PFS letter, Donnell to the U.S. NRC, "Proprietary PFSF Site Specific HI-STORM Drop/Tipover Analyses", dated October 30, 2001
 10. PFS letter, Donnell to the U.S. NRC, "EIS Commitment Resolution Letter #13", dated September 25, 2001
 11. PFS letter, Donnell to the U.S. NRC, "Update of PFS Utilities", dated November 1, 2001

NMSS 01 P 10/21/01

U.S. NRC Document Control Desk

Page 2

November 21, 2001

This letter submits Amendment No. 23 to the Private Fuel Storage Facility (PFSF) License Application. The primary purpose of this amendment is to update the PFSF licensing documents to include information that PFS has previously submitted to the NRC in response to requests for additional information (RAI) that were associated with the previous Amendment No. 22 to the PFSF License Application (Reference 1). The NRC requested information in regards to Amendment No. 22 at the Reference 2 meeting and in Reference 3. PFS responded to the RAIs in References 4 and 5, and submitted Reference 6 to address effects related to the site-specific HI-STORM storage cask tipover analyses. Reference 7 provided additional information regarding the storage cask stability analysis, while References 8 and 9 submitted the latest updates of Holtec's HI-STORM cask stability and cask drop/tipover analyses, respectively. In Reference 10, PFS committed to expand upon the PFSF cask array dose rate information in Section 7.6 of the Safety Analysis Report (SAR) and Section 4.2.9 of the Environmental Report (ER), by adding information to these sections already contained in Section 7.3.3.5 of the SAR. Information from References 4 through 10 has been included in Amendment No. 23 to the PFSF License Application.

In addition to the above, Section 2.2 of the SAR has been revised to reflect the July 2001 addendum to the aircraft crash hazard analysis. ER Chapter 9 has been revised to include information in accordance with the Utah Contention T Settlement Agreement between PFS and the State of Utah regarding permits, licenses, approvals and other entitlements which may be necessary in connection with the PFSF. Chapter 1 of the License Application (LA) was revised to reflect changes in the PFS Board of Managers, and ER Chapter 1 was likewise revised to identify the current PFS member utilities (Reference 11). Appendix C of the License Application, "Commitment Letters" has been revised to include the latest PFS commitment resolution letters (References 7 and 10).

If you have any questions regarding this submittal, please contact me at 608-787-1236 or Mr. J. L. Donnell, Project Director, at 303-741-7009.

Sincerely,



John D. Parkyn, Chairman
Private Fuel Storage L.L.C.

JDP:JRJ
Enclosure

PREFACE

PRIVATE FUEL STORAGE FACILITY

LICENSE APPLICATION

AMENDMENT 23

Enclosed are the following revisions to the Private Fuel Storage Facility License Application documents:

License Application – Revision 14

Safety Analysis Report – Revision 22

Environmental Report – Revision 14

DOCUMENT CONTROL

PAGE	REVISION
a	14
b	14
c	14
d	14
License Application Tab	
i	0
ii	6
1-1	10
1-2	0
1-3	13
1-4	13
1-5	13
1-6	13
1-7	13
1-8	13
1-9	13
1-10	13
1-11	14
1-12	6
Figure 1-1	2
2-1	10
2-2	10
3-1	10
3-2	0
4-1	0
4-2	10
4-3	10
4-4	0
5-1	0
5-2	0
6-1	0
6-2	0
7-1	0
7-2	0
8-1	0
8-2	0

DOCUMENT CONTROL

PAGE	REVISION
9-1	0
9-2	0
10-1	10
10-2	0
11-1	0
11-2	0
12-1	0
12-2	0
13-1	0
13-2	0
Appendix A Tab - Proposed Technical Specifications Tab	
TS-i	12
TS-ii	12
TS-1	9
TS-2	9
TS-3	9
TS-4	9
TS-5	9
TS-6	9
TS-7	9
TS-8	9
TS-9	9
TS-10	9
TS-11	9
TS-12	9
TS-13	9
TS-14	9
TS-15	9
TS-16	9
TS-17	9
TS-18	9
TS-19	9
TS-20	9
TS-21	9
TS-22	9
TS-23	9
TS-24	9

DOCUMENT CONTROL

PAGE	REVISION
TS-25	9
TS-26	13
TS-27	13
TS-28	13
TS-28a	11
TS-28b	10
TS-29	9
TS-30	9
TS-31	9
TS-32	9
TS-33	9
TS-34	9
TS-35	13
TS-36	13
TS-37	10
TS-38	10
Appendix B Tab -	
Preliminary Decommissioning Plan Tab	
i	0
ii	0
1-1	0
1-2	0
2-1	0
2-2	0
2-3	0
2-4	0
3-1	0
3-2	0
4-1	4
4-2	10
4-3	10
4-4	4
4-5	10
4-6	13
4-7	13
4-8	13
5-1	0
5-2	4
5-3	4
5-4	4
6-1	0
6-2	10
6-3	0
6-4	0
7-1	0

DOCUMENT CONTROL

PAGE	REVISION
7-2	0
Appendix C Tab - Commitment Letters	
i	14
ii	14
iii	14
iv	14
v	14
vi	14

PRIVATE FUEL STORAGE L.L.C.

Board of Managers

November, 2001

Ronald Cocherell Southern Nuclear Operating Company	J. A. Stall Florida Power and Light Company
Paul Grigaux GPU Nuclear	Frank Rives Entergy Corporation
John D. Parkyn Genoa FuelTech, Inc.	Paul D. Myers Southern California Edison
Doug Malin Indiana Michigan Power	Scott Northard Xcel Energy Inc.

Principal Officer of the Company

John D. Parkyn
Chairman of the Board

Chapter 1 References

Gaukler, P.A., Shaw Pittman. Private Fuel Storage – Docket No. 72-22 – ASLB No. 97-732-02. Letter to the E.M. Julian, U.S. Nuclear Regulatory Commission, December 3, 1999.

Parkyn, J.D., Private Fuel Storage Limited Liability Company. Supplemental Response to RAIs. Letter to Director, Office of Nuclear Material Safety and Safeguards, U.S. Nuclear Regulatory Commission, Docket No. 72-22, September 15, 1998.

TABLE OF CONTENTS

**SAFETY ANALYSIS REPORT COMMITMENT LETTERS
ISSUED SUBSEQUENT TO THE FINAL RAI RESPONSES**

TITLE	DATE	SUBJECT
Commitment Resolution	March 17, 1999	Thermal/Seismic/Explosion Analysis/Geotechnical
Commitment Resolution Letter #2	March 19, 1999	Flooding Analysis
Commitment Resolution Letter #3	April 2, 1999	Seismic Program
Commitment Resolution Letter #4	April 14, 1999	Geotechnical
Commitment Resolution Letter #5	April 16, 1999	Emergency Plan-Offsite Assistance
Commitment Resolution Letter #6	May 10, 1999	Flooding Analysis
Commitment Resolution Letter #7	June 24, 1999	Geotechnical/Aircraft Hazards
Submittal of Commitment Resolution Letter #8 Information	July 9, 1999	Seismic Analysis
Commitment Resolution Letter #9	July 14, 1999	Aircraft Hazards
Commitment Resolution Letter #10	July 22, 1999	Seismic Analysis/ Aircraft Hazards
Commitment Resolution Letter #11	July 26, 1999	Aircraft Hazards
Commitment Resolution Letter #12	July 28, 1999	Geotechnical
Commitment Resolution Letter #13	July 30, 1999	Field Investigation Evaluation Report/Business Plan
Commitment Resolution Letter #14	August 6, 1999	Design Earthquake/ Geotechnical
Commitment Resolution Letter #15	August 6, 1999	Emergency Plan
Commitment Resolution Letter #16	August 10, 1999	Seismic Struts/Crane Uplift

TABLE OF CONTENTS

**SAFETY ANALYSIS REPORT COMMITMENT LETTERS
ISSUED SUBSEQUENT TO THE FINAL RAI RESPONSES**

TITLE	DATE	SUBJECT
Commitment Resolution Letter #17	September 3, 1999	Aircraft Hazards
Commitment Resolution Letter #18	October 13, 1999	Aircraft Hazards
Submittal of Commitment Resolution Letter #19 Information	October 15, 1999	Cask Storage Pad Sliding Analysis
Commitment Resolution Letter #22	November 19, 1999	Geotechnical/Aircraft Hazards
Commitment Resolution Letter #23	January 7, 2000	Geotechnical
Commitment Resolution Letter #24	January 14, 2000	SER Open Items
Commitment Resolution Letter #25	January 18, 2000	Aircraft Hazards
Commitment Resolution Letter #26	February 23, 2000	Seismic Hazards
Commitment Resolution Letter #27	March 10, 2000	Fire/Explosion Hazards and Meteorological Items
Commitment Resolution Letter #28	March 28, 2000	Geotechnical Issues
Commitment Resolution Letter #29	April 10, 2000	Postulated Fires in the Canister Transfer Building
Commitment Resolution Letter #30	April 7, 2000	Postulated Propane Vapor Cloud Explosion
Commitment Resolution Letter #31	April 14, 2000	Meteorological Data for the PFSF

NOTE: Commitment Resolution Letters #20 and #21 are not included above since they only provided additional information in response to the commitments made in Commitment Resolution Letter #18.

TABLE OF CONTENTS

**SAFETY ANALYSIS REPORT COMMITMENT LETTERS
ISSUED SUBSEQUENT TO THE FINAL RAI RESPONSES**

TITLE	DATE	SUBJECT
Commitment Resolution Letter #32	April 18, 2000	Dugway Hazards
Commitment Resolution Letter #33	May 17, 2000	PFSF Cost Estimates
Commitment Resolution Letter #34	June 2, 2000	Geotechnical, Cranes, Cask Transporter Stability, Onsite Explosions/Fires, and Aircraft Hazards
Commitment Resolution Letter #35	June 17, 2000	Aircraft Hazards
Commitment Resolution Letter #36	September 20, 2000	Aircraft Hazards
Commitment Resolution Letter #37	August 7, 2001	Storage Cask Stability Analysis

TABLE OF CONTENTS

ENVIRONMENTAL REPORT COMMITMENT LETTERS
ISSUED SUBSEQUENT TO THE FINAL RAI RESPONSES

TITLE	DATE	SUBJECT
EIS Commitment Resolution Letter #1	November 12, 1999	Water Sources/RR Right of Way/Air Emissions/Dose Rates/Photographic Equipment/Cost Benefit
EIS Commitment Resolution Letter #2	November 19, 1999	Water Sources/ Cost Benefit
EIS Commitment Resolution Letter #3	December 7, 1999	Meteorological Data/Wyoming Site Doses
EIS Commitment Resolution Letter #4	January 26, 2000	Cost Benefit Analysis
EIS Commitment Resolution Letter #5	February 15, 2000	Environmental Report Issues
EIS Commitment Resolution Letter #6	February 22, 2000	Environmental Report Issues
EIS Commitment Resolution Letter #7	February 25, 2000	Environmental Report Issues
EIS Commitment Resolution Letter #8	March 9, 2000	Cost Benefit Analysis
EIS Commitment Resolution Letter #9	April 28, 2000	PFSF Radiation Dose Estimates
EIS Commitment Resolution Letter #10	April 28, 2000	Cost Benefit Analysis
EIS Commitment Resolution Letter #11	May 3, 2000	PFSF Radiation Dose Estimates
DEIS Commitment Resolution Letter #1	September 15, 2000	Water Sources

DEIS Commitment Resolution
Letter #2

November 1, 2000

Rail Line Access During
Construction

EIS Commitment Resolution
Letter #12

February 7, 2001

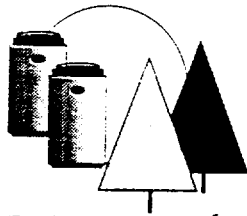
Removal of Water from the
Detention Basin

EIS Commitment Resolution
Letter #13

September 25, 2001

PFSF Cask Array Dose Rate
Information

THIS PAGE INTENTIONALLY LEFT BLANK



Private Fuel Storage, L.L.C.

7677 East Berry Ave., Englewood, CO 80111-2137

Phone 303-741-7009 Fax: 303-741-7806

John L. Donnell, P.E., Project Director

U.S. Nuclear Regulatory Commission
ATTN: Document Control Desk
Washington, D.C. 20555-0001

August 7, 2001

COMMITMENT RESOLUTION LETTER #37
DOCKET NO. 72-22 / TAC NO. L22462
PRIVATE FUEL STORAGE FACILITY
PRIVATE FUEL STORAGE L.L.C.

In accordance with our July 31, 2001 conference call, Private Fuel Storage (PFS) submits the following resolution to NRC/CNWRA questions and comments regarding the stability analysis for the cask storage pads.

NRC Question/Comment

PFS should provide a basis for the conclusions contained within the SAR that the storage casks do not tip over, collide, nor slide off the storage pad during the seismic event, taking into consideration the potential movement of the cask storage pads of up to 6".

PFS Response

A formal evaluation has been performed for PFS by Holtec International to assess the impact of potential movement of the cask storage pads during a seismic event on the PFS Site Specific HI-STORM Drop/Tipover Analyses, (Holtec Report No. HI-2012653, Revision 1, dated May 7, 2001). The Holtec evaluation is attached for your use.

The results of the evaluation demonstrate that the current conclusions reached in the PFSF Safety Analysis Report remain valid and are bounding for the response of the casks relative to the pad.

August 7, 2001

If you have any questions regarding this response, please contact me at 303-741-7009.

Sincerely,

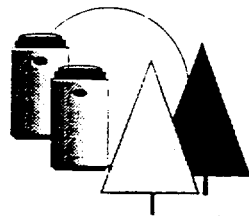
A handwritten signature in black ink that reads "John L. Donnell". The signature is written in a cursive style with a large initial "J" and "D".

John L. Donnell
Project Director
Private Fuel Storage L.L.C.

Enclosure

Copy to:

Mark Delligatti-1/1
John Parkyn-1/1
Jay Silberg-1/1
Sherwin Turk-1/1
Asadul Chowdhury-1/1
Scott Northard-1/1
Denise Chancellor-1/1
Richard E. Condit-1/1
John Paul Kennedy-1/1
Joro Walker-1/1
Duncan Steadman-1/1
Utah Document file (D. Bird)-1/1



Private Fuel Storage, L.L.C.

7677 East Berry Ave., Englewood, CO 80111-2137

Phone 303-741-7009 Fax: 303-741-7806

John L. Donnell, P.E., Project Director

U.S. Nuclear Regulatory Commission
ATTN: Document Control Desk
Washington, D.C. 20555-0001

September 25, 2001

EIS COMMITMENT RESOLUTION LETTER #13
DOCKET NO. 72-22 / TAC NO. L22462
PRIVATE FUEL STORAGE FACILITY
PRIVATE FUEL STORAGE L.L.C.

Reference: September 24, 2001 telephone call between the NRC and Stone and Webster (S&W)

During the above referenced telephone call, Mr. Mike Waters of the NRC requested that Private Fuel Storage L.L.C. (PFS) include a change to Section 4.2.9.1.1 of the Private Fuel Storage Facility (PFSF) Environmental Report (ER) in the next amendment to the PFSF License Application. ER Section 4.2.9.1.1 states the following:

“As described in Section 7.6 of the PFSF SAR, a maximum dose rate of 2.10 mrem/yr (assuming a 2,000 hour annual occupancy) was calculated at the OCA boundary fence 600 meters from the RA fence at its closest points of approach. This dose rate is comprised of direct and scattered gamma and neutron radiation assumed to emanate from 4,000 HI-STORM storage casks and is based on the assumption that all 4,000 casks contain typical fuel expected to be received at the PFSF with 35-GWd/MTU burnup and 20-year cooling time.”

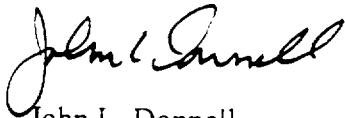
The PFSF storage cask array dose assessment evaluated dose rates at the north and west owner controlled area (OCA) boundaries, both of which are a minimum distance of 600 meters out from the restricted area fence. The dose assessment determined that the maximum dose rate occurs at the north OCA boundary. Section 7.3.3.5 of the PFSF SAR presents dose rates from the PFSF cask array at the OCA boundary, based on the full complement of 4,000 HI-STORM storage casks, assuming that all the casks contain 1) relatively hot fuel having 40 GWd/MTU burnup and 10-year cooling time, and 2) fuel having 35 GWd/MTU burnup and 20-year cooling time, which is considered to be representative of typical fuel expected to be received at the PFSF as explained in SAR Section 7.3.3.5. The dose rates at the OCA boundary for the relatively hot fuel were calculated to be 5.85 mrem/yr at a point on the boundary 600 meters north of the RA

fence, and 4.35 mrem/yr at a point on the boundary 600 meters west of the RA fence, assuming a hypothetical individual spends 2,000 hours per year at the OCA boundary. Dose rates will be lower at points along the south and east sides of the OCA boundary, since these points are further from the storage casks than the north and west OCA boundaries. The annual dose at the north OCA boundary (maximum) for typical fuel expected to be received at the PFSF (having 35 GWd/MTU burnup and 20-year cooling time) was calculated to be 2.10 mrem, again assuming that a hypothetical individual spends 2,000 hours per year at the boundary. Section 4.2.9.1.1 of the ER identifies the 2.10 mrem annual dose at the OCA boundary, based on the stated assumption that all 4,000 casks contain typical fuel expected to be received at the PFSF with 35-GWd/MTU burnup and 20-year cooling time. The NRC requested that PFS revise this section of the ER to include the higher calculated annual dose of 5.85 mrem, based on the assumption that all 4,000 HI-STORM storage casks contain the relatively hot fuel assumed to have 40 GWd/MTU burnup and 10-year cooling time.

PFS will revise ER Section 4.2.9.1.1 to incorporate the 5.85 mrem calculated annual dose at the OCA boundary that is based on the assumption that all 4,000 storage casks contain the relatively hot fuel, and PFS will make a similar revision to SAR Section 7.6, which contains essentially the same information as ER Section 4.2.9.1.1. These revisions will be included in the next amendment to the PFSF License Application.

If you have any questions regarding this response, please contact me at 303-741-7009.

Sincerely,



John L. Donnell
Project Director
Private Fuel Storage L.L.C.

Copy to (with enclosure):

Mark Delligatti
Scott Flanders
John Parkyn
Jay Silberg
Sherwin Turk
Greg Zimmerman
Scott Northard
Denise Chancellor
Richard E. Condit
John Paul Kennedy
Joro Walker

DOCUMENT CONTROL

PAGE	REVISION
Document Control Tab	
a	22
b	22
c	22
d	22
e	22
f	22
g	22
h	22
i	22
j	22
k	22
l	22
m	22
n	22
o	22
p	22
q	22
r	22
s	22
t	22
u	22
v	22
w	22
x	22
y	22
z	22
aa	22
bb	22
Table of Contents Tab	
i	10
ii	0
iii	9
iv	13
Chapter 1 Tab	
1-i	0
1-ii	17
1.1-1	0
1.1-2	21
1.1-3	21
1.1-4	0
1.2-1	17

DOCUMENT CONTROL

PAGE	REVISION
1.2-2	17
1.3-1	17
1.3-2	17
1.3-3	17
1.3-4	0
1.4-1	17
1.4-2	4
1.5-1	17
1.5-2	0
1.6-1	17
1.6-2	0
1.7-1	17
1.7-2	17
Figure 1.1-1	3
Figure 1.1-2	21
Figure 1.2-1	21
Figure 1.3-1	12
Figure 1.3-2 (deleted)	17
Chapter 2 Tab	
2-i	19
2-ii	19
2-iii	12
2-iv	22
2-v	22
2-vi	11
2-vii	11
2-viii	12
2-ix	22
2-x	11
2-xi	11
2-xii	22
2-xiii	11
2-xiv	11
2.1-1	0
2.1-2	0
2.1-3	6
2.1-4	10
2.1-5	0
2.1-6	0
2.2-1	9
2.2-2	10
2.2-3	9
2.2-4	9

DOCUMENT CONTROL

PAGE	REVISION
2.2-5	9
2.2-6	22
2.2-7	22
2.2-8	16
2.2-9	19
2.2-10	19
2.2-11	22
2.2-12	22
2.2-13	19
2.2-14	22
2.2-15	22
2.2-16	19
2.2-17	19
2.2-18	22
2.2-19	19
2.2-20	22
2.2-21	22
2.2-22	22
2.2-23	19
2.2-24	19
2.2-25	20
2.2-26	20
2.3-1	0
2.3-2	0
2.3-3	0
2.3-4	0
2.3-5	0
2.3-6	0
2.3-7	0
2.3-8	0
2.3-9	0
2.3-10	0
2.3-11	0
2.3-12	12
2.3-13	12
2.3-14	12
2.3-15	12
2.3-16	12
2.3-17	12
2.3-18	12
2.3-19	12
2.3-20	12
2.3-21	12
2.3-22	12

DOCUMENT CONTROL

PAGE	REVISION
2.4-1	0
2.4-2	0
2.4-3	3
2.4-4	3
2.4-5	6
2.4-6	3
2.4-7	11
2.4-8	11
2.4-9	11
2.4-10	11
2.4-11	11
2.4-12	11
2.4-13	11
2.4-14	11
2.4-15	11
2.4-16	11
2.5-1	0
2.5-2	3
2.5-3	3
2.5-4	3
2.5-5	21
2.5-6	3
2.6-1	3
2.6-2	22
2.6-3	22
2.6-4	21
2.6-5	21
2.6-6	21
2.6-7	6
2.6-8	21
2.6-9	3
2.6-10	21
2.6-11	21
2.6-12	21
2.6-13	21
2.6-14	21
2.6-15	21
2.6-16	21
2.6-17	21
2.6-18	21
2.6-19	21
2.6-20	15
2.6-21	8
2.6-22	22

DOCUMENT CONTROL

PAGE	REVISION
2.6-22a	22
2.6-22b	22
2.6-23	22
2.6-24	22
2.6-25	22
2.6-26	8
2.6.26a	8
2.6.26b	21
2.6.26c	22
2.6.26d	22
2.6-26e	22
2.6-26f	22
2.6-27	21
2.6-28	9
2.6-29	21
2.6-30	22
2.6-31	22
2.6-31a	22
2.6-31b	21
2.6-32	13
2.6-33	21
2.6-34	22
2.6-35	22
2.6-36	22
2.6-36a	22
2.6-36b	22
2.6-36c	21
2.6-36d	22
2.6-36e	22
2.6-36f	22
2.6-37	13
2.6-38	9
2.6-39	11
2.6-40	11
2.6-41	21
2.6-42	21
2.6-43	11
2.6-44	11
2.6-44a	21
2.6-44b	11
2.6-44c	13
2.6-44d	13
2.6-45	21
2.6-46	22

DOCUMENT CONTROL

PAGE	REVISION
2.6-47	22
2.6-48	21
2.6-49	21
2.6-50	22
2.6-51	22
2.6-52	9
2.6-53	9
2.6-54	22
2.6-55	22
2.6-56	21
2.6-57	22
2.6-58	21
2.6-59	22
2.6-60	22
2.6-61	22
2.6-62	22
2.6-63	22
2.6-64	22
2.6-65	22
2.6-66	22
2.6-67	22
2.6-67a	22
2.6-67b	22
2.6-67c	22
2.6-67d	22
2.6-67e	22
2.6-67f	22
2.6-68	22
2.6-69	9
2.6-70	21
2.6-71	21
2.6-72	21
2.6-72a	22
2.6-72b	15
2.6-73	21
2.6-74	21
2.6-75	21
2.6-76	21
2.6-77	22
2.6-78	22
2.6-79	22
2.6-80	22
2.6-81	22
2.6-81a	22

DOCUMENT CONTROL

PAGE	REVISION
2.6-81b	22
2.6-81c	22
2.6-81d	22
2.6-82	21
2.6-83	21
2.6-84	9
2.6-85	9
2.6-86	21
2.6-87	21
2.6-88	21
2.6-89	9
2.6-90	9
2.6-91	22
2.6-91a	22
2.6-91b	10
2.6-92	21
2.6-93	21
2.6-94	21
2.6-95	21
2.6-96	21
2.6-97	9
2.6-98	13
2.6-99	11
2.6-100	21
2.6-100a	11
2.6-100b	11
2.6-101	9
2.6-102	9
2.6-103	22
2.6-104	22
2.6-105	22
2.6-106	9
2.6-107	22
2.6-108	22
2.6-108a	22
2.6-108b	22
2.6-109	22
2.6-110	22
2.6-111	22
2.6-112	22
2.6-113	22
2.6-114	22
2.6-115	22
2.6-116	22

DOCUMENT CONTROL

PAGE	REVISION
2.6-117	22
2.6-118	22
2.6-119	22
2.6-120	22
2.6-121	22
2.6-122	22
2.7-1	11
2.7-2	21
2.8-1	11
2.8-2	21
2.8-3	11
2.8-4	21
2.8-5	11
2.8-6	19
2.8-7	22
2.8-8	22
2.8-9	22
2.8-10	22
2.8-11	22
2.8-12	22
2.8-13	22
2.8-14	11
Table 2.3-1	0
Table 2.3-2	0
Table 2.3-3	12
Table 2.3-4	12
Table 2.3-5	12
Table 2.3-6	0
Table 2.3-7	0
Table 2.3-8	1
Table 2.3-9	0
Table 2.3-10	0
Table 2.3-11	12
Table 2.6-1	21
Table 2.6-2	21
Table 2.6-3	21
Table 2.6-4 (1 of 14)	0
Table 2.6-4 (2 of 14)	0
Table 2.6-4 (3 of 14)	0
Table 2.6-4 (4 of 14)	0
Table 2.6-4 (5 of 14)	0
Table 2.6-4 (6 of 14)	0
Table 2.6-4 (7 of 14)	0
Table 2.6-4 (8 of 14)	0

DOCUMENT CONTROL

PAGE	REVISION
Table 2.6-4 (9 of 14)	0
Table 2.6-4 (10 of 14)	0
Table 2.6-4 (11 of 14)	0
Table 2.6-4 (12 of 14)	0
Table 2.6-4 (13 of 14)	0
Table 2.6-4 (14 of 14)	0
Table 2.6-5	6
Table 2.6-6	21
Table 2.6-7	21
Table 2.6-8	21
Table 2.6-9	21
Table 2.6-10	21
Table 2.6-11	22
Table 2.6-12	11
Table 2.6-13	22
Figure 2.1-1	0
Figure 2.1-2 (1 of 2)	21
Figure 2.1-2 (2 of 2)	0
Figure 2.3-1	0
Figure 2.3-2	0
Figure 2.3-3	0
Figure 2.3-4	0
Figure 2.3-5	0
Figure 2.3-6	0
Figure 2.4-1	3
Figure 2.4-2	3
Figure 2.4-3	21
Figure 2.4-4	3
Figure 2.4-5	3
Figure 2.5-1	3
Figure 2.6-1	0
Figure 2.6-2 (1 of 2)	21
Figure 2.6-2 (2 of 2)	0
Figure 2.6-3	0
Figure 2.6-4	0
Figure 2.6-5 (1 of 14)	21
Figure 2.6-5 (2 of 14)	21
Figure 2.6-5 (3 of 14)	21
Figure 2.6-5 (4 of 14)	21
Figure 2.6-5 (5 of 14)	21
Figure 2.6-5 (6 of 14)	21
Figure 2.6-5 (7 of 14)	21
Figure 2.6-5 (8 of 14)	21
Figure 2.6-5 (9 of 14)	21

DOCUMENT CONTROL

PAGE	REVISION
Figure 2.6-5 (10 of 14)	21
Figure 2.6-5 (11 of 14)	21
Figure 2.6-5 (12 of 14)	21
Figure 2.6-5 (13 of 14)	21
Figure 2.6-5 (14 of 14)	21
Figure 2.6-6	0
Figure 2.6-7	0
Figure 2.6-8	0
Figure 2.6-9	0
Figure 2.6-10	0
Figure 2.6-11	0
Figure 2.6-12	0
Figure 2.6-13A	21
Figure 2.6-13B	21
Figure 2.6-13C	21
Figure 2.6-14A	21
Figure 2.6-14B	21
Figure 2.6-14C	21
Figure 2.6-15	0
Figure 2.6-16	0
Figure 2.6-17	6
Figure 2.6-18	6
Figure 2.6-19	22
Figure 2.6-20 (1 of 2)	6
Figure 2.6-20 (2 of 2)	6
Figure 2.6-21	6
Figure 2.6-22	6
Figure 2.6-23	6
Figure 2.6-24	6
Figure 2.6-25	11
Figure 2.6-26	6
Figure 2.6-27	6
Figure 2.6-28	6
Figure 2.6-29	6
Figure 2.6-30 (1 of 6)	8
Figure 2.6-30 (2 of 6)	8
Figure 2.6-30 (3 of 6)	8
Figure 2.6-30 (4 of 6)	8
Figure 2.6-30 (5 of 6)	8
Figure 2.6-30 (6 of 6)	8
Figure 2.6-31	11

DOCUMENT CONTROL

PAGE	REVISION
Appendix 2A Tab	
Reports	22
Appendix 2B Tab	
Survey	0
Appendix 2C Tab	
Analysis	0
Appendix 2D Tab	
Deleted	3
Appendix 2E Tab	
Analysis	0
Appendix 2F Tab	
Report	9
Appendix 2G Tab	
Evaluation	21
Chapter 3 Tab	
3-i	9
3-ii	17
3-iii	17
3-iv	17
3-v	17
3-vi	0
3.1-1	17
3.1-2	17
3.1-3	17
3.1-4	17
3.1-5	17
3.1-6	0
3.2-1	0
3.2-2	17

DOCUMENT CONTROL

PAGE	REVISION
3.2-3	17
3.2-4	1
3.2-5	9
3.2-5a	9
3.2-5b	9
3.2-6	0
3.2-7	17
3.2-8	9
3.2-8a	9
3.2-8b	9
3.2-9	7
3.2-10	5
3.2-11	21
3.2-12	17
3.2-13	21
3.2-14	9
3.2-14a	21
3.2-14b	3
3.2-15	17
3.2-16	17
3.2-17	0
3.2-18	1
3.2-19	17
3.2-20	17
3.2-21	17
3.2-22	17
3.2-23	21
3.2-24	21
3.2-25	5
3.2-26	1
3.2-27	1
3.2-28	21
3.2-29	21
3.2-30	1
3.2-31	1
3.2-32	1
3.3-1	17
3.3-2	17
3.3-3	21
3.3-4	17
3.3-5	12
3.3-6	1
3.3-7	13
3.3-8	13

DOCUMENT CONTROL

PAGE	REVISION
3.3-9	13
3.3-10	10
3.3-11	10
3.3-12	10
3.4-1	0
3.4-2	17
3.4-3	17
3.4-4	9
3.4-5	9
3.4-6	17
3.4-7	17
3.4-8	9
3.5-1	0
3.5-2	17
3.6-1	0
3.6-2	0
3.7-1	22
3.7-2	22
3.7-3	12
3.7-4	12
Table 3.1-1 (deleted)	12
Table 3.1-2 (deleted)	12
Table 3.1-3 (1 of 2, deleted)	17
Table 3.1-3 (2 of 2) (deleted)	17
Table 3.2-1	12
Table 3.2-2	12
Table 3.2-3 (deleted)	17
Table 3.4-1	17
Table 3.6-1 (1 of 5)	17
Table 3.6-1 (2 of 5)	21
Table 3.6-1 (3 of 5)	22
Table 3.6-1 (4 of 5)	17
Table 3.6-1 (5 of 5)	17
Chapter 4 Tab	
4-i	4
4-ii	17
4-iii	10
4-iv	22
4-v	9
4-vi	17
4-vii	17
4-viii	17
4-ix	17

DOCUMENT CONTROL

PAGE	REVISION
4-x	17
4.1-1	17
4.1-2	17
4.1-3	0
4.1-4	16
4.2-1	17
4.2-2	0
4.2-3	12
4.2-4	12
4.2-5	22
4.2-6	12
4.2-7	12
4.2-8	21
4.2-9	22
4.2-10	22
4.2-10a	22
4.2-10b	22
4.2-10c	22
4.2-10d	22
4.2-11	21
4.2-12	21
4.2-13	22
4.2-13a	22
4.2-13b	22
4.2-14	21
4.2-15	21
4.2-16	21
4.2-16a	21
4.2-16b	21
4.2-16c	21
4.2-16d	21
4.2-17	8
4.2-18	22
4.2-19	22
4.2-20	22
4.2-20a	22
4.2-20b	12
4.2-21	4
4.2-22	17
4.2-23	21
4.2-24	21
4.2-25	17
4.2-26	17
4.2-27	21

DOCUMENT CONTROL

PAGE	REVISION
4.2-28	21
4.2-29	22
4.2-30	21
4.2-31	21
4.2-32	22
4.2-33	22
4.2-34	17
4.3-1	9
4.3-2	9
4.3-3	12
4.3-4	13
4.3-5	13
4.3-6	9
4.3-7	10
4.3-8	13
4.3-9	13
4.3-10	10
4.3-11	22
4.3-12	16
4.3-13	10
4.3-14	16
4.3-15	16
4.3-16	10
4.3-17	10
4.3-18	10
4.3-19	16
4.3-20	13
4.3-21	13
4.3-22	10
4.4-1	0
4.4-2	0
4.5-1	17
4.5-2	17
4.5-3	17
4.5-4	8
4.5-5	17
4.5-6	17
4.6-1	0
4.6-2	0
4.7-1	17
4.7-2	13
4.7-3	22
4.7-3a	22
4.7-3b	22

DOCUMENT CONTROL

PAGE	REVISION
4.7-4	0
4.7-5	21
4.7-6	15
4.7-6a	21
4.7-6b	21
4.7-6c	21
4.7-6d	21
4.7-6e	21
4.7-6f	22
4.7-7	22
4.7-8	22
4.7-8a	22
4.7-8b	22
4.7-8c	22
4.7-8d	21
4.7-8e	21
4.7-8f	21
4.7-8g	22
4.7-8h	22
4.7-9	3
4.7-10	2
4.7-11	3
4.7-12	17
4.7-12a	17
4.7-12b	17
4.7-13	21
4.7-13a	21
4.7-13b	21
4.7-13c	6
4.7-13d	6
4.7-13e	6
4.7-13f	6
4.7-13g	6
4.7-13h	6
4.7-13i	9
4.7-13j	6
4.7-14	0
4.7-15	12
4.7-16	0
4.7-17	12
4.7-18	0
4.7-19	21
4.7-20	12
4.7-21	12

DOCUMENT CONTROL

PAGE	REVISION
4.7-22	12
4.7-23	17
4.7-24	17
4.7-25	21
4.7-26	17
4.8-1	22
4.8-2	22
4.8-3	22
4.8-4	9
4.8-5	22
4.8-6	22
4.8-7	22
4.8-8	22
4.8-9	22
4.8-10	22
4.8-11	22
4.8-12	22
Table 4.1-1 (1 of 7)	17
Table 4.1-1 (2 of 7)	17
Table 4.1-1 (3 of 7)	17
Table 4.1-1 (4 of 7)	17
Table 4.1-1 (5 of 7)	17
Table 4.1-1 (6 of 7)	0
Table 4.1-1 (7 of 7)	0
Table 4.2-1	7
Table 4.2-2	12
Table 4.2-3	12
Table 4.2-4 (deleted)	17
Table 4.2-5 (deleted)	17
Table 4.2-6 (deleted)	17
Table 4.2-7	21
Table 4.2-8	21
Table 4.7-1	12
Table 4.7-2	4
Table 4.7-3 (deleted)	17
Figure 4.1-1	21
Figure 4.1-2	0
Figure 4.1-3	0
Figure 4.1-4	0
Figure 4.2-1	12
Figure 4.2-2 (1 of 3)	12
Figure 4.2-2 (2 of 3)	12
Figure 4.2-2 (3 of 3)	12
Figure 4.2-3	12

DOCUMENT CONTROL

PAGE	REVISION
Figure 4.2-4 (deleted)	17
Figure 4.2-5 (1 of 4) (deleted)	17
Figure 4.2-5 (2 of 4) (deleted)	17
Figure 4.2-5 (3 of 4) (deleted)	17
Figure 4.2-5 (4 of 4) (deleted)	17
Figure 4.2-6 (deleted)	17
Figure 4.2-7	22
Figure 4.2-8	0
Figure 4.3-1	21
Figure 4.5-1 (1 of 2)	12
Figure 4.5-1 (2 of 2)	12
Figure 4.5-2 (deleted)	17
Figure 4.5-3 (1 of 2)	11
Figure 4.5-3 (2 of 2)	2
Figure 4.5-4	17
Figure 4.5-5	17
Figure 4.5-6 (1 of 4)	3
Figure 4.5-6 (2 of 4)	3
Figure 4.5-6 (3 of 4)	3
Figure 4.5-6 (4 of 4)	3
Figure 4.7-1 (1 of 3)	21
Figure 4.7-1 (2 of 3)	21
Figure 4.7-1 (3 of 3)	21
Figure 4.7-2	0
Figure 4.7-3 (deleted)	17
Figure 4.7-4	0
Figure 4.7-5	3
Figure 4.7-6	3
Figure 4.7-7	21
Figure 4.7-8	21
Chapter 5 Tab	
5-i	0
5-ii	7
5-iii	0
5-iv	17
5-v	17
5-vi	0
5.1-1	17
5.1-2	0
5.1-3	3
5.1-4	2
5.1-5	17
5.1-6	17

DOCUMENT CONTROL

PAGE	REVISION
5.1-7	13
5.1-8	17
5.1-9	17
5.1-10	13
5.2-1	17
5.2-2	17
5.2-3	17
5.2-4	17
5.2-5	17
5.2-6	17
5.3-1	0
5.3-2	0
5.4-1	0
5.4-2	0
5.5-1	1
5.5-2	0
5.6-1	0
5.6-2	0
5.7-1	17
5.7-2	0
Table 5.1-1 (1 of 2)	6
Table 5.1-1 (2 of 2)	6
Table 5.1-2 (1 of 2) (deleted)	17
Table 5.1-2 (2 of 2) (deleted)	17
Figure 5.1-1	1
Figure 5.1-2	0
Figure 5.1-3 (deleted)	17
Figure 5.1-4 (deleted)	17
Figure 5.1-5	0
Chapter 6 Tab	
6-i	0
6-ii	0
6.1-1	17
6-1-2	13
6.2-1	1
6.2-2	0
6.3-1	0
6.3-2	0
6.4-1	17
6.4-2	7
6.4-3	7
6.4-4	7

DOCUMENT CONTROL

PAGE	REVISION
6.5-1	13
6.5-2	0
6.6-1	17
6.6-2	0
Chapter 7 Tab	
7-i	17
7-ii	17
7-iii	17
7-iv	17
7-v	0
7-vi	0
7.1-1	0
7.1-2	0
7.1-3	0
7.1-4	0
7.1-5	17
7.1-6	0
7.1-7	0
7.1-8	13
7.1-9	3
7.1-10	3
7.1-11	3
7.1-12	3
7.2-1	17
7.2-2	17
7.2-3	17
7.2-4	17
7.2-5	17
7.2-6	17
7.3-1	0
7.3-2	0
7.3-3	9
7.3-3a	13
7.3-3b	13
7.3-4	17
7.3-5	17
7.3-6	22
7.3-6a	22
7.3-6b	22
7.3-7	17
7.3-8	17
7.3-9	17
7.3-10	17

DOCUMENT CONTROL

PAGE	REVISION
7.3-11	21
7.3-12	21
7.3-13	21
7.3-14	17
7.3-15	17
7.3-16	17
7.4-1	21
7.4-2	21
7.4-3	21
7.4-4	12
7.5-1	3
7.5-2	0
7.5-3	8
7.5-4	8
7.5-5	8
7.5-6	8
7.5-7	8
7.5-8	8
7.6-1	22
7.6-2	0
7.6-3	13
7.6-4	13
7.7-1	17
7.7-2	21
7.7-3	21
7.7-4	22
Table 7.3-1	10
Table 7.3-2 (deleted)	17
Table 7.3-3	10
Table 7.3-4 (deleted)	17
Table 7.3-5	10
Table 7.3-6	17
Table 7.3-7	21
Table 7.3-8 (deleted)	17
Table 7.4-1 (1 of 4)	10
Table 7.4-1 (2 of 4)	10
Table 7.4-1 (3 of 4)	10
Table 7.4-1 (4 of 4)	10
Table 7.4-2 (1 of 4) (deleted)	17
Table 7.4-2 (2 of 4) (deleted)	17
Table 7.4-2 (3 of 4) (deleted)	17
Table 7.4-2 (4 of 4) (deleted)	17
Figure 7.3-1	0
Figure 7.3-2	17

DOCUMENT CONTROL

PAGE	REVISION
Chapter 8 Tab	
8-i	0
8-ii	7
8-iii	16
8-iv	9
8-v	9
8-vi	13
8.1-1	9
8.1-2	17
8.1-3	0
8.1-4	17
8.1-5	17
8.1-6	17
8.1-7	7
8.1-8	17
8.1-9	17
8.1-10	17
8.1-11	0
8.1-12	21
8.1-13	21
8.1-14	17
8.1-15	17
8.1-16	17
8.1-17	13
8.1-18	17
8.1-19	7
8.1-20	7
8.2-1	9
8.2-2	3
8.2-3	21
8.2-4	21
8.2-5	21
8.2-6	22
8.2-7	21
8.2-8	17
8.2-9	17
8.2-10	17
8.2-11	7
8.2-12	17
8.2-13	3
8.2-14	17
8.2-15	17
8.2-15a	17

DOCUMENT CONTROL

PAGE	REVISION
8.2-15b	17
8.2-16	17
8.2-17	22
8.2-17a	22
8.2-17b	22
8.2-18	17
8.2-19	17
8.2-20	17
8.2-21	10
8.2-22	13
8.2-23	11
8.2-23a	17
8.2-23b	13
8.2-23c	17
8.2-23d	11
8.2-23e	11
8.2-23f	13
8.2-23g	13
8.2-23h	13
8.2-23i	14
8.2-23j	13
8.2-23k	14
8.2-23l	14
8.2-23m	14
8.2-23n	14
8.2-23o	14
8.2-23p	16
8.2-23q	16
8.2-23r	16
8.2-24	13
8.2-25	13
8.2-26	11
8.2-27	11
8.2-28	13
8.2-29	17
8.2-29a	17
8.2-29b	17
8.2-29c	17
8.2-29d	11
8.2-29e	17
8.2-29f	18
8.2-29g	18
8.2-29g1	18
8.2-29g2	18

DOCUMENT CONTROL

PAGE	REVISION
8.2-29h	11
8.2-29i	11
8.2-29j	11
8.2-29k	11
8.2-29l	11
8.2-29m	13
8.2-29n	17
8.2-29o	17
8.2-29p	13
8.2-29q	17
8.2-29r	11
8.2-30	21
8.2-31	22
8.2-32	22
8.2-32a	22
8.2-32b	22
8.2-32c	22
8.2-32d	22
8.2-32e	22
8.2-32f	22
8.2-32g	22
8.2-32h	22
8.2-33	21
8.2-34	21
8.2-35	21
8.2-36	17
8.2-37	17
8.2-38	17
8.2-39	17
8.2-40	17
8.2-41	17
8.2-42	17
8.2-43	13
8.2-44	17
8.2-45	17
8.2-46	17
8.2-47	17
8.2-48	17
8.2-49	7
8.2-50	17
8.2-51	17
8.2-52	9
8.3-1	7
8.3-2	7

DOCUMENT CONTROL

PAGE	REVISION
8.4-1	17
8.4-2	17
8.4-3	9
8.4-4	9
8.4-5	9
8.4-6	9
8.4-7	17
8.4-8	17
8.4-9	9
8.4-10	13
8.4-11	17
8.4-12	10
8.5-1	17
8.5-2	9
8.5-3	17
8.5-4	9
8.5-5	9
8.5-6	21
8.5-7	17
8.5-8	17
8.5-9	21
8.5-10	22
Table 8.1-1	17
Table 8.1-2	17
Table 8.2-1	17
Figure 8.2-1	15
Chapter 9 Tab	
9-i	0
9-ii	1
9-iii	4
9-iv	4
9-v	0
9-vi	0
9.1-1	0
9.1-2	0
9.1-3	0
9.1-4	4
9.1-5	4
9.1-6	4
9.1-7	4
9.1-8	4
9.1-9	4
9.1-10	13

DOCUMENT CONTROL

PAGE	REVISION
9.1-10a	13
9.1-10b	13
9.1-10c	13
9.1-10d	13
9.1-11	13
9.1-12	4
9.1-13	13
9.1-14	0
9.1-15	1
9.1-16	1
9.1-16a	1
9.1-16b	1
9.1-17	0
9.1-18	0
9.1-19	0
9.1-20	0
9.1-21	0
9.1-22	0
9.1-23	0
9.1-24	3
9.1-25	4
9.1-26	4
9.1-27	4
9.1-28	4
9.1-29	4
9.1-30	4
9.2-1	13
9.2-2	13
9.2-2a	1
9.2-2b	1
9.2-3	17
9.2-4	17
9.2-5	0
9.2-6	0
9.2-7	1
9.2-8	1
9.2-8a	17
9.2-8b	1
9.3-1	4
9.3-2	4
9.3-3	13
9.3-4	4
9.3-5	4
9.3-6	4

DOCUMENT CONTROL

PAGE	REVISION
9.3-7	4
9.3-8	4
9.4-1	3
9.4-2	4
9.4-2a	4
9.4-2b	4
9.4-3	3
9.4-4	3
9.4-5	3
9.4-6	3
9.4-7	3
9.4-8	3
9.5-1	0
9.5-2	13
9.5-3	0
9.5-4	0
9.6-1	0
9.6-2	0
9.7-1	0
9.7-2	0
9.7-3	0
9.7-4	0
Figure 9.1-1	4
Figure 9.1-2	4
Figure 9.1-3	12
Chapter 10 Tab	
10-i	13
10-ii	13
10.1-1	13
10.1-2	13
Appendix 10A Tab	
Technical Specification Bases	13
Chapter 11 Tab	
11-i	0
11-ii	0
11.1-1	4
11.1-2	4
11.1-3	4
11.1-4	0

DOCUMENT CONTROL

PAGE	REVISION
11.1-5	0
11.1-6	0
11.1-7	0
11.1-8	0
11.1-9	0
11.1-10	0
11.2-1	0
11.2-2	0

TABLE OF CONTENTS (cont.)

SECTION	TITLE	PAGE
2.3.3	Onsite Meteorological Measurement Program	2.3-19
2.3.4	Diffusion Estimates	2.3-22
2.4	SURFACE HYDROLOGY	2.4-1
2.4.1	Surface Hydrologic Description	2.4-1
2.4.1.1	Site and Structures	2.4-3
2.4.1.2	Hydrosphere	2.4-3
2.4.2	Floods	2.4-5
2.4.2.1	Flood History	2.4-5
2.4.2.2	Flood Design Considerations	2.4-6
2.4.2.3	Effects of Local Intense Precipitation	2.4-10
2.4.3	Potential Maximum Flood on Streams and Rivers	2.4-14
2.4.4	Potential Dam Failures (Seismically Induced)	2.4-14
2.4.5	Probable Maximum Surge and Seiche Flooding	2.4-15
2.4.6	Probable Maximum Tsunami Flooding	2.4-15
2.4.7	Ice Flooding	2.4-15
2.4.8	Flooding Protection Requirements	2.4-15
2.4.9	Environmental Acceptance of Effluents	2.4-15
2.5	SUBSURFACE HYDROLOGY	2.5-1
2.5.1	Regional Characteristics	2.5-1
2.5.2	Site Characteristics	2.5-4
2.5.3	Contaminant Transport Analysis	2.5-6

TABLE OF CONTENTS (cont.)

SECTION	TITLE	PAGE
2.6	GEOLOGY AND SEISMOLOGY	2.6-1
2.6.1	Basic Geologic and Seismic Information	2.6-1
2.6.1.1	Site Geomorphology	2.6-5
2.6.1.2	Geologic History of Site and Region	2.6-7
2.6.1.2.1	Bedrock	2.6-7
2.6.1.2.2	Site Area Structural Geology and Geologic History	2.6-10
2.6.1.2.3	Surficial (Basin-fill deposits)	2.6-13
2.6.1.3	Site Geology	2.6-15
2.6.1.4	Geologic Map of Site Area	2.6-18
2.6.1.5	Facility Plot Plan and Geologic Investigations	2.6-19
2.6.1.6	Relationship of Major Foundations to Subsurface Materials	2.6-22a
2.6.1.7	Excavations and Backfill	2.6-27
2.6.1.8	Engineering-Geology Features Affecting ISFSI Structures	2.6-28
2.6.1.9	Site Groundwater Conditions	2.6-28
2.6.1.10	Geophysical Surveys	2.6-30
2.6.1.11	Static and Dynamic Soil and Rock Properties at the Site	2.6-31a
2.6.1.11.1	Pad Emplacement Area	2.6-32
2.6.1.11.2	Canister Transfer Building Area	2.6-36
2.6.1.11.3	Pad Emplacement and Canister Transfer Building Areas	2.6-37
2.6.1.11.4	Collapse Potential of High Void Ratio Soils	2.6-42
2.6.1.11.5	Dynamic Strength of Cohesive Soils	2.6-44b
2.6.1.12	Stability of Foundations for Structures and Embankments	2.6-45
2.6.1.12.1	Stability and Settlement Analyses—Cask Storage Pads	2.6-46
2.6.1.12.2	Stability and Settlement Analyses—Canister Transfer Building	2.6-72

TABLE OF CONTENTS (cont.)

SECTION	TITLE	PAGE
2.6.1.12.3	Allowable Bearing Capacity—Other Structures	2.6-83
2.6.2	Vibratory Ground Motion	2.6-85
2.6.2.1	Engineering Properties of Materials for Seismic Wave Propagation and Soil-Structure Interaction Analyses	2.6-87
2.6.2.2	Earthquake History	2.6-88
2.6.2.3	Determining the Design Basis Ground Motion	2.6-91
2.6.2.3.1	Capable Faults	2.6-92
2.6.2.3.2	Maximum Earthquake	2.6-94
2.6.3	Surface Faulting	2.6-95
2.6.4	Stability of Subsurface Materials	2.6-96
2.6.4.1	Geologic Features That Could Affect Foundations	2.6-96
2.6.4.2	Properties of Underlying Materials	2.6-97
2.6.4.3	Plot Plan	2.6-97
2.6.4.4	Soil and Rock Characteristics	2.6-97
2.6.4.5	Excavations and Backfill	2.6-97
2.6.4.6	Groundwater Conditions	2.6-98
2.6.4.7	Response of Soil and Rock to Dynamic Loading	2.6-98
2.6.4.8	Liquefaction Potential	2.6-106
2.6.4.9	Design Basis Ground Motion	2.6-107
2.6.4.10	Static Analyses	2.6-107
2.6.4.11	Techniques to Improve Subsurface Conditions	2.6-108
2.6.4.12	Criteria and Design Methods	2.6-120
2.6.5	Slope Stability	2.6-121

2.7	SUMMARY OF SITE CONDITIONS AFFECTING CONSTRUCTION AND OPERATING REQUIREMENTS	2.7-1
2.8	REFERENCES	2.8-1

TABLE OF CONTENTS (cont.)

LIST OF TABLES

TABLE	TITLE
2.6-5	SUMMARY OF BLOW COUNTS IN LAYER 1 IN STORAGE PAD AREA
2.6-6	SUMMARY – ALLOWABLE BEARING CAPACITY OF CASK STORAGE PADS; Based on Static Loads
2.6-7	SUMMARY – ALLOWABLE BEARING CAPACITY OF CASK STORAGE PADS; Based on Inertial Forces Due to Design Basis Ground Motion: PSHA 2,000-Yr Return Period
2.6-8	SUMMARY – ALLOWABLE BEARING CAPACITY OF CASK STORAGE PADS; Based on Maximum Cask Driving Forces Due to Design Earthquake: PSHA 2,000-Yr Return Period for Loading Case IV: 40% N S, 100% Vertical (Downward), and 40% E-W
2.6-9	SUMMARY – ALLOWABLE BEARING CAPACITY OF CANISTER TRANSFER BUILDING; Based on Static Loads
2.6-10	SUMMARY – ALLOWABLE BEARING CAPACITY OF CANISTER TRANSFER BUILDING; Based on Dynamic Loads Due to Design Basis Ground Motion: PSHA 2,000-Yr Return Period
2.6-11	FOUNDATION LOADINGS FOR THE CANISTER TRANSFER BUILDING; Based on Dynamic Loads Due to Design Basis Ground Motion: PSHA 2,000-Yr Return Period
2.6-12	RESULTS OF CONSOLIDATION TESTS IN ORDER OF DECREASING VOID RATIO
2.6-13	SLIDING STABILITY OF CANISTER TRANSFER BUILDING USING SHEAR STRENGTH ALONG BOTTOM OF PLANE FORMED BY 1.5 DEEP PERIMETER KEY AND RESISTANCE FROM SOIL CEMENT

TABLE OF CONTENTS (cont.)

LIST OF FIGURES

FIGURE	TITLE
2.1-1	POPULATION DISTRIBUTION WITHIN 5 MILES OF PFSF
2.1-2	SITE AND ACCESS ROAD LOCATION PLAN (2 SHEETS)
2.3-1	WIND ROSE, SALT LAKE CITY; 1988-1992, WINTER
2.3-2	WIND ROSE, SALT LAKE CITY; 1988-1992, SPRING
2.3-3	WIND ROSE, SALT LAKE CITY; 1988-1992, SUMMER
2.3-4	WIND ROSE, SALT LAKE CITY; 1988-1992, AUTUMN
2.3-5	WIND ROSE, SALT LAKE CITY; 1988-1992
2.3-6	METEOROLOGICAL TOWER LOCATION RELATIVE TO THE PFSF SITE
2.4-1	WATERSHED BASINS IN THE VICINITY OF THE PFSF SITE
2.4-2	PFSF SITE PMF BERM PLAN & PROFILE
2.4-3	PFSF RAIL LINE PLAN & PROFILE
2.4-4	PFSF ACCESS ROAD PLAN & PROFILE
2.4-5	PFSF ACCESS ROAD PMF BERM PLAN & PROFILE
2.5-1	WATER WELLS WITHIN 5 MILES (8 KM) OF PFSF SITE
2.6-1	PHYSIOGRAPHY OF UTAH
2.6-2	PLOT PLAN AND LOCATIONS OF GEOTECHNICAL INVESTIGATIONS (SHEETS 1 & 2)
2.6-3	GEOLOGIC MAP OF UTAH
2.6-4	SURFICIAL GEOLOGY AND PFSF SITE
2.6-5	PAD EMPLACEMENT AREA FOUNDATION PROFILE— LOOKING NORTHEAST (SHEETS 1-14)
2.6-6	RATE OF SECONDARY COMPRESSION VS STRESS RATIO

TABLE OF CONTENTS (cont.)

LIST OF FIGURES

FIGURE	TITLE
2.6-7	STATIC AND DYNAMIC LATERAL EARTH PRESSURES
2.6-8	LATERAL EARTH PRESSURE COEFFICIENTS VS WALL MOVEMENT
2.6-9	COMPACTION-INDUCED LATERAL STRESSES
2.6-10	GROSS ALLOWABLE BEARING PRESSURE VS FOOTING WIDTH & DEPTH FOR STRIP FOOTINGS
2.6-11	GROSS ALLOWABLE BEARING PRESSURE VS FOOTING WIDTH & DEPTH FOR SQUARE FOOTINGS
2.6-12	INTERMOUNTAIN SEISMIC BELT HISTORICAL EARTHQUAKES, MAGNITUDE ≥ 6.0
2.6-13A	STRAIN-COMPATIBLE SHEAR-WAVE VELOCITY PROFILE – LOW RANGE PROPERTIES
2.6-13B	STRAIN-COMPATIBLE SHEAR-WAVE VELOCITY PROFILE – BEST-ESTIMATE PROPERTIES
2.6-13C	STRAIN-COMPATIBLE SHEAR-WAVE VELOCITY PROFILE – HIGH RANGE PROPERTIES
2.6-14A	STRAIN-COMPATIBLE DAMPING RATIO PROFILE – LOW RANGE PROPERTIES
2.6-14B	STRAIN-COMPATIBLE DAMPING RATIO PROFILE – BEST-ESTIMATE PROPERTIES
2.6-14C	STRAIN-COMPATIBLE DAMPING RATIO PROFILE – HIGH RANGE PROPERTIES

TABLE OF CONTENTS (cont.)

LIST OF FIGURES

FIGURE	TITLE
2.6-15	MAGNITUDE \geq 3.0 EARTHQUAKES WITHIN 100 MILES OF PFSF, 1850—1996
2.6-16	QUATERNARY STRUCTURES AND SEISMICITY, 1884 TO 1989
2.6-17	STRATIGRAPHIC COLUMN FOR SKULL VALLEY AREA
2.6-18	LOCATION OF GEOTECHNICAL INVESTIGATIONS FOR CANISTER TRANSFER BUILDING
2.6-19	LOCATIONS OF GEOTECHNICAL INVESTIGATIONS IN PAD EMPLACEMENT AREA
2.6-20	SOIL PROPERTIES VS DEPTH IN STORAGE PAD AREA (2 SHEETS)
2.6-21	CANISTER TRANSFER BUILDING FOUNDATION PROFILE 1-1'— LOOKING NORTH
2.6-22	CANISTER TRANSFER BUILDING FOUNDATION PROFILE 2-2'— LOOKING NORTH
2.6-23	CANISTER TRANSFER BUILDING FOUNDATION PROFILE 3-3'— LOOKING EAST
2.6-24	EFFECT OF TIME OF LOADING ON STRESS-STRAIN RELATION FOR CAMBRIDGE CLAY
2.6-25	TYPICAL FAILURE RESPONSE FOR COHESIVE SOIL — “DYNAMIC” VS “RAPID STATIC” TESTING RATES
2.6-26	STANDARDIZED DISPLACEMENT FOR NORMALIZED EARTHQUAKES — SYMMETRICAL RESISTANCE

by common carrier along Skull Valley Road, but the safe packaging of those shipments is strictly regulated by the Department of Transportation so as to prevent a release even in the event of an accident. Hazardous wastes shipped from Dugway Proving Ground do not include chemical agent but rather only chemically neutralized agent, which is far less hazardous and would not threaten the PFSF even if spilled on Skull Valley Road.

Unexploded ordnance would not pose a significant hazard to the PFSF in that 1) it is extremely unlikely that such ordnance would explode spontaneously or accidentally and 2) even if it did, the PFSF is far enough away that the material in the round would not pose a significant hazard. Unexploded ordnance is not likely to be found off Dugway Proving Ground close enough to pose a risk to the PFSF, in that the firing ranges at Dugway are all at least 15 miles away and Army records of where munitions were fired at Dugway give no indication that munitions were fired elsewhere.

The Dugway Proving Ground receives and ships conventional Army weapons approximately 95 times a year. Some of these shipments could travel the Skull Valley Road, which present the only credible potential for an explosion near the PFSF. An accident associated with the transportation of explosives along the Skull Valley Road would be a minimum of 1.9 miles from the Canister Transfer Building and 2 miles from the nearest cask storage pad. Based on the methodology of Regulatory Guide 1.91, the Skull Valley Road is located much further from the PFSF than the distances required to exceed 1 psi overpressure for detonation of explosives transported by highway, as discussed in Section 8.2.4.

The Tooele Army Depot facilities, where toxic gas munitions are stored and incinerated, are located west and south, respectively, of Tooele City. The North Tooele Army Depot is 17 miles east-northeast of the PFSF and the South Tooele Army Depot is 21 miles

east-southeast of the PFSF. The Stansbury Mountains, with an elevation of approximately 8,000 feet, lie between the PFSF and the Tooele Army Depots. The activities and materials at the Tooele Army Depots will therefore present no credible hazard to the PFSF, because of their relative distance and the intervening Stansbury Mountains.

2.2.2 Hazards from Air Crashes

Aircraft flights in the vicinity of the PFSF take place to and from Michael Army Airfield on Dugway Proving Ground, on and around the Utah Test and Training Range (UTTR), and on federal airways J-56 and V-257. While there are no civilian airports within 25 miles of the PFSF, minimal general aviation traffic may also transit the region. The annual probability of an aircraft crashing into the PFSF has been conservatively calculated to be less than $4.17 \text{ E-}7$ per year and qualitative factors indicate that the true probability of an aircraft impacting the PFSF is significantly lower. (PFS August 2000) This is an extremely low probability, well below the $1 \text{ E-}6$ regulatory standard the NRC has promulgated for above ground facilities at geologic repositories (which are similar to ISFSIs) (61 Fed. Reg. 64,257, 64,261-62, 64,265-66 (1996)). Therefore, aircraft crashes do not present a credible hazard to the PFSF and the facility does not need to be designed to withstand the impact of an aircraft crash.

2.2.2.1 Michael Army Airfield and Airway IR-420

Michael Army Airfield is located on the Dugway Proving Ground, 17 miles south-southwest of the PFSF. This military airfield has a 13,125 foot runway, and can accommodate all operative aircraft in the Department of Defense inventory, although the majority of the aircraft flying to and from Michael AAF, other than F-16 aircraft from Hill Air Force Base (AFB) which are accounted for in Section 2.2.2.2.1 below, are large cargo aircraft such as the C-5, C-17, and C-141. The airspace over the Dugway

Proving Ground is restricted. Military airway IR-420 passes near the PFSF site area. The methods of NUREG-0800 Section 3.5.1.6 were used to estimate the probability of an aircraft impacting the PFSF from this airway, using the equation:

$$P = C \times N \times A / w, \text{ where}$$

P = probability per year of an aircraft crashing into the PFSF

C = in-flight crash rate per mile

N = number of flights per year along the airway

A = effective area of the PFSF in square miles

w = width of airway in miles

NUREG-0800 states the in-flight crash rate as 4 E-10 per mile, which is appropriate to apply to the types of aircraft flying to and from Michael AAF addressed here. (PFS August 2000) Information provided by the Dugway Proving Ground indicates that approximately 414 flights annually can be taken as an upper bound for this airfield. The effective area of the PFSF is 0.2116 mi², calculated using Department of Energy (DOE) formulas. (DOE 1996) The width of the airway is 10 nautical miles (nm), or 10nm x 1.15 mile/nm = 11.5 miles. The probability of an aircraft impacting the PFSF is therefore 3.0 E-9 per year. Because of the distance from the PFSF to Michael Army Airfield, takeoff and landing operations at Michael pose a negligible hazard to the PFSF.

Consideration was given to the plans for landing the X-33 aircraft at Michael Army Airfield. The X-33 is an unmanned half-scale demonstrator launch vehicle planned to test critical components for the next generation space transport system. The X-33 will not pose a hazard to the PFSF because, first, tests for the X-33 at Michael Army Airfield

are scheduled to be completed by mid-2000, before the PFSF would be operational, and second, the X-33's flight plan does not take it over Skull Valley, let alone the PFSF.

2.2.2.2 Utah Test and Training Range

The UTTR is an Air Force training and testing range over which the airspace is restricted to military operations. It is divided into a North Area, located on the western shore of the Great Salt Lake, north of Interstate 80, and a South Area, located to the west of the Cedar Mountains, south of Interstate 80 and northwest of Dugway Proving Ground. (PFS August 2000) The airspace over the UTTR extends somewhat beyond the range's land boundaries and is divided into military operating areas (MOAs) and restricted areas. The MOAs on the UTTR are located on the edges of the range, adjacent to the restricted areas. The PFSF site is located over 18 statute miles east of the eastern land boundary of the UTTR South Area and 8.5 statute miles northeast of the northeastern boundary of Dugway Proving Ground. The site lies within the Sevier B MOA, two statute miles to the east of the edge of restricted airspace. (PFS August 2000)

Military aircraft flying in or around the UTTR South Area comprise three groups: 1) F-16 fighter aircraft flying from Hill Air Force Base (AFB), near Ogden, Utah, down Skull Valley en route to the range (Section 2.2.2.2.1); 2) aircraft conducting training in the restricted airspace on the range (Section 2.2.2.2.2); and 3) aircraft departing the range via the Moser Recovery to return to Hill AFB (Section 2.2.2.2.3). Aircraft flying in or around the UTTR North Area pose no credible hazard to the PFSF because of the distance from the facility.

calculate the probability that such ordnance would impact the PFSF. The fraction of the 5,870 F-16s transiting Skull Valley per year that would be carrying ordnance was determined from Air Force data to be 2.556 percent. Thus the number of aircraft carrying ordnance through Skull Valley per year, N , would be 150. The crash rate for the F-16s, C , was taken to be $2.736 \text{ E-}8$ per mile, as above. Nonetheless, the pilot was assumed to jettison ordnance in only 90 percent of all crashes, the fraction of the crashes, e , assumed to be attributable to engine failure or some other event leaving him in control of the aircraft (in crashes attributable to other causes it was assumed that the pilot would eject quickly and would not jettison ordnance). Skull Valley was treated as an airway with a width, w , of 10 miles. As with the calculation for F-16s transiting Skull Valley, PFS conservatively assumed that the F-16s are uniformly distributed across the 10 miles, despite the fact that their predominant route of flight is down the eastern side of the valley and that, according to the Air Force, aircraft carrying live ordnance avoid flying over populated areas to the maximum extent possible. The area of the PFSF, from the perspective of a piece of ordnance jettisoned from an aircraft flying from north to south over the site, A , was taken to be the product of the width and the depth of the cask storage area (assuming a full facility with 4,000 casks) plus the product of the width and depth of the canister transfer building, in that the pieces of ordnance are small relative to an aircraft and impact the ground at a steep angle. Thus, the area of the PFSF was calculated to be 0.08763 mi^2 . The probability that the ordnance would impact the PFSF is given by $P = N \times C \times e \times A/w$, or:

$$P = 150 \times 2.736 \text{ E-}8 \times 0.90 \times 0.08763 / 10 = 3.2 \text{ E-}8$$

In addition to the potential hazard posed by direct impacts of crashing aircraft and jettisoned ordnance, PFS also calculated the hazard to the PFSF posed by jettisoned live ordnance that might land near the facility and explode on impact, as well as the hazard posed by a potential explosion of live ordnance carried aboard a crashing aircraft that might impact the ground near the PFSF. (PFS August 2000) At the outset,

aircraft transiting Skull Valley near the PFSF do not carry armed live ordnance. Furthermore, the U.S. Air Force has indicated that the likelihood that unarmed live ordnance would explode when impacting the ground after being jettisoned is "remote" and the Air Force has no records of such incidents in the last 10 years. Thus, it is highly unlikely that jettisoned live ordnance or live ordnance carried aboard a crashing aircraft that did not directly impact the PFSF would damage the facility. Nevertheless, to calculate a numerical hazard to the facility, PFS assumed that such ordnance would have a 1 percent chance of exploding and assessed that damage to the PFSF would result if an explosion occurred close enough that the blast overpressure would damage a storage cask or the Canister Transfer Building, without hitting either one. The explosive overpressure limit for a storage cask was taken to be 10 psi. The limit for the Canister Transfer Building was taken to be 1.5 psi. PFS assumed that the ordnance in question was a 2,000 lb. bomb, the largest single piece of ordnance carried by the F-16s that transit Skull Valley. The Air Force indicated that 193 F-16s transited Skull Valley in 1998 with live ordnance. PFS calculated the probability that an F-16 carrying live ordnance would crash and jettison the ordnance so as to impact near the PFSF, or crash near the PFSF without jettisoning the ordnance, following the same method it used to calculate the probability that an F-16 would crash and impact the facility. The results of PFS's final calculation showed that the annual probability that a storage cask or the Canister Transfer Building would be damaged by an explosion of live ordnance jettisoned from a crashing aircraft or carried aboard a crashing aircraft that impacted the ground near the PFSF was equal to $2.43 \text{ E-}10$. If this probability is adjusted to reflect 1) the additional sorties expected to be flown by F-16s from Hill AFB, based on FY99 and FY00 data, and the stationing of the 12 additional F-16s at Hill AFB, and 2) the decreased usage of ordnance in FY99 and FY00, the probability would fall below $1 \text{ E-}10$. This is exceedingly low and is insignificant relative to the other aircraft crash and jettisoned ordnance impact hazards calculated for the PFSF.

2.2.2.2.2 Aircraft Training on the UTTR

According to the Air Force, 8,284 sorties were flown over the UTTR South Area in 1998. (PFS August 2000) Those aircraft conducted a variety of activities, including air-to-air combat training, air-to-ground attack training, air-refueling training, and transportation to and from Michael Army Airfield (which is located beneath UTTR airspace). Hazards posed by aircraft flying to and from Michael Army Airfield are addressed in Section 2.2.2.1 above. Of the remaining aircraft, only fighter aircraft conducting air-to-air training represent a potential hazard to the PFSF, in that aircraft conducting air-to-ground attack training do so over targets that are located more than 20 miles from the PFSF site and aircraft conducting air refueling training do so on the far western side of the UTTR, over 50 miles from the site. The Air Force indicated 6,360 fighter sorties were flown on the UTTR South Area in 1998 and one-third, or approximately 2,120, involved fighter aircraft conducting air-to-air training.

The crash impact probability for fighter aircraft conducting air-to-air training on the UTTR was calculated as follows:

$$P = C_a \times A_c \times A/A_p \times R, \text{ where}$$

P = annual crash impact probability

C_a = total air-to-air training crash rate per square mile on the UTTR

A_c = the area of the UTTR from which aircraft could credibly impact the PFSF in the event of a crash

A = effective area of the PFSF in square miles

A_p = the footprint area, in which a disabled aircraft could possibly hit the ground in the event of a crash

R = the probability that the pilot of a crashing aircraft would be able to take action to avoid hitting the PFSF

The total air-to-air training crash rate per square mile on the UTTR, C_a , was calculated from the total number of hours flown in air-to-air training on the UTTR South Area in 1998 (2,468), the crash rate per hour for fighter aircraft (the F-16) conducting the types of flight activity conducted within the portion of the restricted areas on the UTTR near the PFSF, the distribution of air operations over the sectors of the UTTR nearest the PFSF, and the ground areas of those sectors. PFS then updated its input data based on F-16 sortie information from Hill AFB for Fiscal Years 1999 and 2000, and a projected increase in the number of aircraft stationed at the base. (PFS August 2000) As with the F-16s transiting Skull Valley, 95 percent of the crashes on the UTTR attributable to engine failure or some other cause leaving the pilot in control of the aircraft were determined not to pose a hazard to the PFSF, in that the pilot would retain control of the aircraft and would be able to avoid the site. Based on Air Force data, 45 percent of all F-16 crashes occurring during combat training are attributable to engine failure; thus the factor R in the equation above was set equal to 0.573 (1-(45% x 95%)).

The area from which an aircraft could credibly impact the PFSF in the event of a crash, A_c , was taken to be the portion of the UTTR within 5 miles of the PFSF and outside a three-mile buffer zone assumed to exist on the edge of the UTTR restricted areas. Based on Air Force F-16 mishap data, a crashing aircraft more than 5 miles from the PFSF would have to be under control of the pilot in order to glide and reach the site, and the pilot would guide any such aircraft away from the site, which is outside the land boundaries and the restricted airspace of the UTTR. The buffer zone represents the fact that aircraft do not fly within three miles of the edges of the restricted areas while conducting training on the UTTR. Because the PFSF is located two miles from the edge of the closest restricted area, aircraft conducting air-to-air training on the UTTR would have practically no chance of hitting the PFSF in the event of a crash.

The site effective area, A , was determined as in Section 2.2.2.2.1 above for a facility at a full capacity of 4,000 storage casks. The footprint area, A_p , was calculated by assuming that a crashing aircraft could glide in any direction up to a distance equal to the product of its starting altitude above ground and its glide ratio. Accordingly, the aircraft conducting air-to-air training over the UTTR were divided into altitude bands and an impact probability calculated for each band. Aircraft too low to glide to the PFSF in the event of a mishap were calculated not to contribute to the crash impact hazard, in that they would have no chance of reaching the site.

The maximum annual air crash impact probability for aircraft conducting air-to-air training on the UTTR South Area was determined to be significantly less than $1 \text{ E-}8$, based primarily on the fact that practically no aircraft on the UTTR experiencing an in-flight mishap leading to a crash would be close enough to the PFSF site to impact it.

2.2.2.2.3 Aircraft Using the Moser Recovery

Most of the F-16s returning to Hill AFB from the UTTR South Area exit the northern edge of the range (away from the PFSF) in coordination with air traffic control. However, some aircraft returning to Hill from the UTTR South Area may use the Moser recovery route, which runs from the southwest to the northeast, approximately two miles from the PFSF site. (PFS August 2000) The Moser route is only used during marginal weather conditions or at night under specific wind conditions which require the use of Runway 32 at Hill AFB. Based on information from local air traffic controllers, conservatively estimated, the Moser recovery is used by less than five percent of the aircraft returning to Hill. According to the Air Force, 5,726 F-16 sorties were flown on the UTTR South Area in 1998, almost all of which flew from Hill AFB (not all aircraft transit Skull Valley en route to the South Area). Thus, fewer than 286 aircraft per year ($5\% \times 5,726$) were estimated to have used the Moser recovery on their return flights.

The annual crash impact probability for aircraft flying the Moser recovery was calculated using the NUREG-0800 method. The Moser recovery is defined as an airway with a

width, w , of 10 nautical miles (11.5 statute miles) (equal to the width of military airway IR-420). The number of aircraft, N , was conservatively taken to be 286; the crash probability, C , is equal to $2.736 \text{ E-}8$ per mile; the effective area of the site is 0.1337 mi^2 ; and it is calculated that 85.5 percent of all crashes would be attributable to events leaving the pilot in control of the aircraft, in which the pilot could direct the aircraft away from the PFSF (see Section 2.2.2.2.1). Thus, the annual crash impact probability was conservatively estimated to be $1.32 \text{ E-}8$. If this probability is increased to reflect the additional sorties expected to be flown by F-16s from Hill AFB, based on FY99 and FY00 data, and the stationing of the 12 additional F-16s at Hill AFB (Section 2.2.2.2.1), the probability would increase by a factor of 1.516 to $2.00 \text{ E-}8$.

2.2.2.3 Aircraft Flying Federal Airways

Federal airway J-56 runs east-northeast to west-southwest at a distance (from the airway centerline) of 11.5 miles north of the PFSF. (PFS August 2000) Local air traffic controllers have indicated that fewer than 12 aircraft per day use the airway. The crash impact probability for aircraft on the airway was calculated for the PFSF using the method of NUREG-0800. Using the standard width for federal airways, J-56 is 8 nautical miles (9.2 statute miles) wide and the closest edge of J-56 is 6.9 miles from the PFSF. For facilities outside an airway, the effective width of the airway, w , is equal to the actual width plus twice the distance from the facility to the closest edge. Thus, J-56 has an effective width of 23 miles. The number of aircraft, N , is conservatively taken to be 12 per day, the crash rate, C , from NUREG-0800 is $4 \text{ E-}10$ per mile, and the effective area of the PFSF for commercial airliners (the most common aircraft on the airway) is 0.2615 mi^2 , assuming a full facility with 4,000 casks. Accordingly, the maximum annual crash impact probability is $1.9 \text{ E-}8$. (PFS August 2000)

Federal airway V-257 runs north and south at a distance (from the airway centerline) of 19.5 miles east of the PFSF. (PFS August 2000) Local air traffic controllers have indicated that fewer than 12 aircraft per day use the airway. The crash impact probability for aircraft on the airway was calculated for the PFSF using the method of NUREG-0800. V-257 is 12 nautical miles (13.2 statute miles) wide and its closest edge is 12.6 miles from the PFSF. Thus, V-257 has an effective width of 39 miles. The number of aircraft, N , is conservatively taken to be 12 per day, the crash rate, C , is $4 \text{ E-}10$ per mile, and the effective area of the PFSF is 0.2615 mi^2 . Accordingly, the annual crash impact probability is $1.2 \text{ E-}8$. (PFS August 2000)

2.2.2.4 General Aviation

There are no civilian airports within 25 miles of the PFSF, the PFSF is located in a sparsely populated area, and the PFSF is located inside a military operating area (MOA) in which flight by civilian aircraft is limited while the MOA is being used by the Air Force (and which is avoided by general aviation pilots because of the military flight activity that takes place there). Thus, the general aviation traffic over Skull Valley is negligible; in fact F-16 pilots who have flown from Hill AFB through Skull Valley indicate never having seen any, or having seen only minimal, general aviation traffic there. Therefore, it is highly unlikely that a general aviation aircraft would crash into the PFSF. (PFS August 2000) PFS estimates that the probability would be less than $1 \text{ E-}8$ per year.

First, a conservative upper bound for the crash impact probability for general aviation aircraft was calculated using National Transportation Safety Board (NTSB) crash data and the population of general aviation aircraft in the state of Utah. (PFS August 2000) The crash impact probability is equal to $C_a \times A$, where C_a is the crash rate per square mile and A is the effective area of the PFSF. In 1995, the 182,600 general aviation aircraft in the United States suffered 412 fatal accidents. There are 1,218 general

aviation aircraft in the state of Utah, which covers an area of 84,094 mi². FAA crash data indicate, however, that only 15 percent of all general aviation crashes occur during the cruise mode of flight, which, because there are no airports nearby, is the mode in which general aviation aircraft would be flying near the PFSF. Furthermore, business jets experience 7.85 percent of all general aviation fatal crashes and they can be excluded from this calculation, in that they fly mostly on federal airways. The effective area of the PFSF with respect to general aviation aircraft crashes is 0.1173 mi² (assuming a fully loaded facility with 4,000 casks). Accordingly, the annual crash impact probability for general aviation aircraft is 5.25 E-7. (PFS August 2000)

The crash impact hazard to the PFSF, however, would be reduced below the calculated impact probability, in that the spent fuel storage casks would be able to withstand the crash impact of most general aviation aircraft. Fifty-five percent of all general aviation aircraft are single-engine piston types weighing less than 3,500 lbs. (PFS August 2000) Such aircraft typically fly at speeds under 100 knots (114 mph). Therefore, the impact of such aircraft at the PFSF would be bounded by the design basis tornado missile impact for the HI-STORM spent fuel storage casks, an automobile weighing 1800 kg (3,968 lbs.) moving at a speed of 126 mph. (p. 8.2-17) Thus, the impact of such light general aviation aircraft would not cause a radioactive release from a storage cask. Therefore, the calculated upper bound general aviation crash impact hazard to the PFSF can be reduced by 55 percent to 2.36 E-7 per year.

Based on the observations of F-16 pilots in Skull Valley, however, the general aviation traffic level there is significantly below the statewide average traffic level. Thus, the Skull Valley crash rate is significantly less than the statewide rate. The methodology of NUREG-0800, Section 3.5.1.6, can be used to correlate these observations with an associated hazard probability. (PFS August 2000)

The crash impact hazard posed by general aviation aircraft flying through Skull Valley is given, according to NUREG-0800, by $P = N \times C \times A/W$ (see Section 2.2.2.1). The fatal crash rate, C , for fixed wing, powered general aviation aircraft in the cruise mode of flight, is 3.82 E-8 per mile. For Skull Valley, the corridor width, W , is 10 miles, and the PFSF effective area, A , remains 0.1173 mi^2 . Therefore, if P is equal to 1 E-8 , then N must be 22 general aviation aircraft per year transiting Skull Valley in the neighborhood of the PFSF. This number, however, includes single-engine piston general aviation aircraft weighing less than 3,500 lbs., which account for at least 55 percent of all general aviation aircraft and which pose no hazard to the PFSF. Refining this calculation to exclude those aircraft, the required number of aircraft transiting Skull Valley becomes 49 per year, or approximately one flight every 7 days. It is reasonable to assume that if general aviation aircraft were transiting Skull Valley on a weekly basis, they would be seen by the F-16 pilots (e.g, in FY98 there were approximately 11 F-16 flights per day), but in fact the F-16 pilots have never, or seldom, seen them. (PFS August 2000) Thus, PFS concludes that the general aviation crash impact hazard to the PFSF is less than 1 E-8 .

Furthermore, the effective general aviation crash impact hazard posed by those aircraft whose impacts would not be bounded by the design basis tornado missile (i.e., the 45 percent of all general aviation impacts not excluded above) is shown to be even lower than 1 E-8 by PFS calculations demonstrating that such aircraft would not penetrate a spent fuel storage cask even in the remote event they were to impact the PFSF. PFS employed the methodology used by the Department of Energy to assess aircraft crash risks to hazardous facilities (DOE 1996; Davis et al. 1998) and determined that the engine of a general aviation aircraft, which would be the bounding component of a crashing aircraft, could not penetrate a storage cask. (PFS August 2000) General aviation aircraft other than jets may be modeled as having engines weighing between 230 and 800 lbs. and impacting at speeds between 67 and 280 miles per hour. (Kimura and Budnitz 1987) PFS calculations showed that an 800-lb. engine impacting at a

speed of 280 miles per hour would have substantially less energy than that required to penetrate a spent fuel storage cask. Therefore, PFS's assessment of the crash impact hazard posed by general aviation aircraft whose impacts would not be bounded by the design basis tornado missile is conservative.

2.2.2.5 Cumulative Air Crash Impact Probability

The cumulative maximum air crash impact probability is given in the table below.

Aircraft Crash Impact Probabilities	
Aircraft	Maximum Annual Probability
Skull Valley F-16s	3.11 E-7
Aircraft Using the Moser Recovery	2.00 E-8
UTTR Aircraft	<1 E-8
Aircraft on Airway J-56	1.9 E-8
Aircraft on Airway V-257	1.2 E-8
General Aviation Aircraft	<1 E-8
Aircraft on Airway IR-420	3.0 E-9
Cumulative Crash Probability	<3.85 E-7
Jettisoned Military Ordnance	3.2 E-8
Cumulative Hazard	<4.17 E-7

The table shows that the cumulative air crash impact probability is less than 1 E-6 for the PFSF. Qualitative factors discussed below show further that the true impact probability is significantly less than the calculated probability. Thus, air crash impact

does not pose a credible hazard to the PFSF and the PFSF does not need to be designed to withstand the effects of air crash impacts.

2.2.2.6 Projected Growth in Air Traffic

The Federal Aviation Administration projects that the number of commercial aviation flights in the United States will increase by approximately 66 percent between 1998 and 2025, that the number of general aviation flights will increase by approximately 14 percent over the same period, and that the number of military flights will not increase during this period. (FAA 1999) Furthermore, based on PFS assessment of Air Force operational policies, it is not expected that F-16s at Hill AFB will fly significantly more sorties per aircraft per year than were flown in FY00. (PFS August 2000) Because most of the air traffic near the PFSF site is military, the growth in commercial and general aviation projected by the FAA will have no material effect on the air crash impact probability calculated for the facility.

2.2.2.7 Conservatism in the PFSF Air Crash Impact Probabilities

While the calculated cumulative hazard for the PFSF is less than $4.17 \text{ E-}7$, qualitative factors indicate that the true probability of an aircraft or jettisoned ordnance impacting the site is significantly lower. (PFS August 2000) With respect to the F-16s transiting down Skull Valley en route to the UTTR South Area (and jettisoned military ordnance), these factors include the fact that, according to the U.S. Air Force, the predominant route of choice for the F-16s is the east side of the Valley, approximately five miles from the site. Thus, the uniform distribution assumed in calculations in Section 2.2.2.2.1 is conservative, especially considering the fact that the only aircraft that pose a real hazard to the site are those that are pointed directly toward it at the time of the incident leading to a crash. In addition, the Skull Valley F-16 calculations assume that F-16s will

crash at the 10-year average rate rather than the more recent and lower 5-year average rate.

Furthermore, the calculated cumulative hazard is conservative in three other major respects. First, the calculated probability is for a fully loaded, 4,000 cask facility, which would be the case for only a short period in the life of the PFSF. The average area of the PFSF site, and hence the average annual probability that an aircraft or jettisoned ordnance would impact the site, is 55 percent of that of the full facility. Thus, the average annual impact probability is roughly 2×10^{-7} .

Second, no credit was taken for the resistance to the effects of an air crash impact provided by the concrete storage casks in which the spent fuel canisters will be located (other than resistance to impacts of light general aviation aircraft). The cask construction is robust enough that a significant fraction of the potential air crash impacts at the PFSF would not cause a release of radioactivity. (Davis et al. 1998) The casks could withstand the direct impact of a jet fighter or commercial airliner at a speed of over 370 knots, which is significantly greater than typical air crash impact velocities, and the casks could withstand the impact of all general aviation aircraft that might overfly the PFSF. (PFS August 2000) This resistance of the casks to penetration further reduces significantly the calculated risk to the PFSF from aircraft crashes or jettisoned ordnance.

Third, PFS's assessment of the hazard posed by jettisoned ordnance is also conservative. The Air Force has indicated that the inert (i.e., dummy) variants of most of the munitions carried by F-16s transiting Skull Valley would not penetrate a spent fuel storage cask if they were to be jettisoned and impact a cask. (PFS August 2000) This assessment would also apply to any jettisoned live (but unarmed) munitions of the

2.6 GEOLOGY AND SEISMOLOGY

2.6.1 Basic Geologic and Seismic Information

Geological and seismological investigations for the PFSF site and area began in 1996 and included review of pertinent published and unpublished literature, consultation with geologists and seismologists familiar with the area, and reconnaissance level geologic mapping. In addition, a test boring program was conducted at the site at that time and along the 2.5-mile-long access road to characterize subsurface soil conditions. The drilling was performed by Earthcore, Inc. of Salt Lake City under the direct supervision of Stone & Webster Engineering Corporation (SWEC). Laboratory testing of soil for engineering properties was performed in SWEC's Soil Testing Laboratory in Boston, Massachusetts. Seismic reflection and refraction (both P- and S-wave) surveys were completed in 1996 in order to determine soil and rock stratigraphy, bedrock surface profiles, depth to the water table, seismic velocities of the underlying rock and soil, and engineering parameters of near-surface soils from shear wave velocities. This work was performed by Geosphere Midwest of Brooklyn Park, Minnesota, also under the direct supervision of Stone & Webster.

Professor Donald Currey of the University of Utah completed an evaluation of surficial linear features near the site at Stone & Webster's request. Drs. William Nash and Michael Perkins of the University of Utah analyzed volcanic ash samples from site borings and trench excavations for age correlation purposes.

Additional work was performed in 1998 in response to NRC Requests for Additional Information (RAI). This work included review of existing literature and data, and discussions with researchers knowledgeable with the structural and stratigraphic setting of Skull Valley. In addition, an extensive program of surface and subsurface

investigations was conducted under the direction of Geomatrix Consultants, Inc. and Stone and Webster. Their investigations included the following activities and are described in detail in Geomatrix Consultants, Inc. (2001a):

- photogeologic interpretation of aerial photos
- surficial and bedrock geologic mapping
- geomorphic mapping and interpretation
- geophysical investigations including interpretation of gravity data, conducting a magnetometer survey, reprocessing and interpretation of proprietary P-wave reflection data, and completing a high-resolution shear wave reflection survey (Bay Geophysical Associates, 1999).
- Trenching and test pit excavation and mapping
- Drilling and logging of boreholes
- Geochronologic analysis

As a result of these investigations and in response to recent changes to 10CFR50, Part 100 (100.23), as well as anticipated changes to Part 72 (SECY-98-126), probabilistic analyses were performed to evaluate the potential for fault displacement and ground shaking hazards at the PFSF. The design basis for vibratory ground motion was assessed at this time. The results of this effort are reported in Geomatrix Consultants, Inc. (2001a and b).

Stone and Webster also conducted a drilling program in 1998 in the area of the Canister Transfer Building (CTB) for engineering purposes. One of these borings reached a total depth of 225 ft. and a groundwater monitoring well was installed. Additional geotechnical investigations included cone penetrations tests, which were performed in April 1999, and test pits, which were excavated in the pad emplacement area in January 2001. Refer to Section 2.6.1.5 for additional details concerning these geotechnical investigations.

The site is situated in western Utah near the eastern boundary of the Basin and Range Physiographic Province with the Middle Rocky Mountain Province (Figure 2.6-1). This

area is characterized by a series of roughly north-south trending, tilted fault block ranges separated by down-faulted linear basins. The PFSF is located near the middle of the Skull Valley basin, at approximate elevation 4,465 ft, between the Stansbury Mountain range on the east and the Cedar Mountains on the west. The top 25 to 35 ft of surficial soils at the site are mainly lacustrine marly silts and clays. Below about 25 to 35 ft is a very dense fine sand with minor gravel and silt layers to at least 100 ft deep (Appendix 2A). The base of the late Pleistocene Bonneville alloformation is believed to be at a depth of about 45 ft. in the site area where the Promontory Soil was identified (Geomatrix Consultants, Inc., 2001a) and the soil blow-counts increase dramatically (Appendix 2A). The base of the Quaternary section is not well-constrained but the Tertiary "Walcott ash" is known in several borings at a depth of about 85 ft.

Bedrock was not encountered in the borings but is believed to occur at a depth of between 520 and 880 ft, based on seismic survey results (Appendix 2B). Bedrock outcroppings, about 1.5 miles south of the site at Hickman Knolls, have been mapped as the Fish Haven Dolomite of Late Ordovician age (Moore and Sorensen, 1979; Geomatrix Consultants, Inc., 2001a). As indicated in Section 2.4.1.2, the groundwater table is about 125 ft below grade at the site, based on the observation well and seismic refraction surveys.

The Stansbury fault, exposed along the base of the western escarpment of the Stansbury Mountains, is about 6 miles east of the site. The fault dips to the west and is projected beneath the PFSF site at a depth of 4.4 miles (55 degree dip assumed). The most recent events on the Stansbury fault displace late Pleistocene shorelines that are estimated to be about 18,000 years old. Arabasz et al. (1987) consider the Stansbury fault capable of a maximum magnitude 7.3 earthquake. Empirical relations by Wells and Coppersmith (1994) that relate surface rupture length to magnitude suggest the maximum earthquake magnitude on the Stansbury fault is 7.0 ± 0.28 (moment mag.). Helm (1995) has calculated that the next seismic event on the fault should be a $M_s 6.8-6.9 \pm 0.04$, based

on strain accumulation rates of previous events. Geomatrix Consultants, Inc. (2001a) calculate an expected value (mean) of **M** 7.0 for the maximum magnitude on the Stansbury fault.

Two unnamed faults were identified in the PFSF area and are informally named the East and West faults (Geomatrix Consultants Inc., 2001a). Late Pleistocene activity is indicated for both of these faults, based on geophysical and geomorphological studies. The East fault lies 0.9 km east of the site and the West is 2 km to the west. Mean maximum magnitudes for the East and West faults were calculated to be **M** 6.5 and **M** 6.4, respectively. The Stansbury, East, and West faults are the most important structures with respect to the assessment of seismic hazard in the PFSF vicinity. A transition zone or zone of distributive fault offset between the East and West faults was identified. The potential for surface fault displacement beneath the PFSF is evaluated in Geomatrix Consultants, Inc. (2001a).

The maximum "random" earthquake for this region has been defined by Pechmann and Arabasz (1995) as $M_L = 6.5$.

A probabilistic seismic hazard analysis was performed (Geomatrix Consultants, Inc., 2001a) to assess vibratory ground motion and fault displacement at the PFSF site. Peak ground accelerations for the design basis earthquake (2,000-yr return period) were calculated to be 0.711g horizontal and 0.695g vertical (Geomatrix Consultants, Inc., 2001b). Ground surface displacements associated with faults believed to exist beneath the site were determined to be less than 0.1 cm for the same return period.

The closest Quaternary igneous activity is 50 miles south of the PFSF site at Fumarole Butte on Crater Bench. Basaltic volcanic activity here is believed to be between 950,000 and 880,000 years old (Hecker, 1993) and does not present a threat to the integrity of the PFSF at that distance, if it were to become active.

or remains constant with depth, down to a depth of about 23 ft, at which point it increases markedly, as did the Standard Penetration Test blow counts in most of the borings in the pad emplacement area.

These data were interpreted to provide profiles of the variation of strength, which are plotted in Appendix D and listed in tabular form in Appendix F of ConeTec (1999). A review of the plots of the undrained shear strength, s_u , vs depth indicates that s_u measured in the CPTs increases with depth, and it generally exceeds 1 tsf. Note, this value corresponds with the lower bound of the values of s_u measured in the CU and UU tests. These plots indicate that s_u remains fairly constant in the depth range from ~15 ft to ~23 ft, and normally exceeds 2 tsf. Therefore, the lower blow count zone at approximately 20 ft has undrained shear strengths that are at least twice those used in the analyses of the stability of the cask storage pads.

In Phase 2 of the cone penetration testing program, dilatometer tests were performed to measure, in situ, the variation of compressibility of the soils vs depth at the locations identified in Phase 1 where the softer soils exist. The compressibility is reported as the constrained modulus, M , in the plots and tables included in Appendices G and H of ConeTec (1999).

The plots of M vs depth in Appendix G of ConeTec (1999) show that M generally is lowest near the surface of the site, increases with increasing depth to about 4 to 5m (13 to 16 ft), at which point it decreases, generally remaining fairly constant at a value that is equal to or greater than that near the top of the profile. This trend is evident on the plots of DMT-1, 2, 3, 4, 8, 9 (excluding the high modulus values above 2.5m), 11, 12, 14, 15, 16, 17, and 18. Although DMT-6 found a slight decrease in M from ~5.5m to 7m, the resulting values were higher than in the other DMTs in this depth range. DMT-

5, 7, and 13 show only slight increases in M with depth to ~4 to 5m, followed by slight drop in modulus to ~7.5 to 8m.

In general, DMT-10 had the lowest constrained modulus (i.e., highest compressibility) for the entire profile. DMT-10 is anomalous in that M remains fairly constant throughout the entire depth range of ~2m to 7.8m, with a minimum value of 130 bars (135.7 tsf). This DMT was located about half-way between Borings B-1 and C-1 at the northern edge of the pad emplacement area. Note, the consolidation tests reported in Attachment 2 of Appendix 2A were performed on samples obtained at a depth of 10 ft in Boring C-1 and C-2, which were near this location.

See Section 2.6.1.12.1 for discussion of incorporation of these CPT results in the bearing capacity and settlement analyses.

In January 2001, 16 test pits were excavated in the pad emplacement area to obtain bulk soil samples for tests required for design of the soil cement that will be constructed in the pad emplacement area and in the area surrounding the Canister Transfer Building. These test pits were excavated using a backhoe at the locations shown in Figure 2.6-19 to depths of approximately 6 ft. Logs of these test pits and the results of laboratory tests performed on these samples are included in Attachment 9 of Appendix 2A. The sample descriptions presented on these logs are based on visual observations made during excavation, as well as particle-size analyses and Atterberg limits test results. Solid horizontal lines are used on the test pit logs to designate the locations of the top of ground and the bottom of the test pits, as well as interfaces observed in the field between strata. The dashed horizontal lines indicate strata changes based on the results of the laboratory tests.

Geophysical surveys were conducted at the site and are discussed in Section 2.6.1.10.

2.6.1.6 Relationship of Major Foundations to Subsurface Materials

Figure 2.6-5, Sheets 1 through 14, present foundation profiles in the pad emplacement area, showing the locations of the proposed structures in relationship to the subsurface materials encountered in the borings. Based on the borings and laboratory test data, the generalized subsurface profile consists of three layers. The uppermost layer extends to a depth of between 25 and 35 ft below existing grade and is mainly interlayered silt, silty clay, and clayey silt. Standard Penetration Test (SPT) N-values for this layer vary between 1 and 20 blows per ft. The average N-value of 16 blows per ft and the median N-value of 14 blows per ft indicate that these are “stiff” or “medium dense” materials. The casks and the Canister Transfer Building will be placed on mat foundations, and the other proposed structures will be constructed on strip and spread footings founded on this layer.

Excluding the surficial samples, which need not be considered because they will be mixed with cement to form soil cement, only a few samples obtained from the pad emplacement area have N-values of less than 8 blows/ft. These were all obtained from the depth range of 5 to 7 ft, and they include Samples S-2 of the following:

**Samples Obtained Within Pad Emplacement Area That Have SPT N-values
Less Than 8 Blows/ft
(Excluding Surficial Samples, Which Will Be Replaced by Soil Cement)**

Boring	N-Value (Blows/ft)	LL (Liquid limit)	PI (Plasticity Index)
B-2	5	47.4	21.8
D-2	6	46.4	15.3
C-3	6	43.1	20.7
C-4	7	69.5	25.3
D-4	4	49.3	21.6

As indicated by the index property tests presented in Figure 2.6-20, the soils obtained from this depth interval (5 to 7 ft) typically are clayey silt/silty clay. Liquid limit values for these soils indicate they typically are high plasticity clays. Figure 4 of DM-7.1 (NAVFAC, 1982) indicates that clays of high plasticity with SPT N-values of 4 to 8 typically have unconfined compressive strengths of 1 to 2 tsf.

This result is further confirmed by the cone penetration tests performed in the pad emplacement area. All of these CPTs measured cone tip resistance values, Q_t , of the soils within the depth range of 5 to 7 ft, that exceed 15 tsf, as shown in the plots of Q_t vs depth in Appendix A of ConeTec (1999). Using an empirical cone factor, N_{kt} , of 12.5 to estimate the undrained shear strength, these tip resistance values result in undrained shear strengths that exceed 1 tsf, indicating the unconfined compressive strengths exceed 2 tsf.

Table 7.1 of Terzaghi & Peck (1967) indicates that clayey soils with strengths of 1 to 2 kg/cm² (~1 to ~2 tsf) are characterized as having "stiff" consistency. Therefore, existence of a few N-values that are less than 8 blows/ft for the soils within the pad emplacement area do not adversely impact the characterization of these soils as "stiff".

The value of standard penetration resistance, N, was determined to be approximately 15 blows/ft for the top 25 to 30-ft soil layer based on the data obtained in Borings A-1 through A-4, B-1 through B-4, C-1 through C-4, and D-1 through D-4. This set of borings represents all of the borings that were drilled over the entire proposed pad emplacement area, as shown in Figure 2.6-2. The blow count data are summarized in Table 2.6-5. As indicated in this table, the average blow count is 15.7 blows/ft, and the median value is 14.0 blows/ft. These two values were combined to obtain the value of ~15 blows/ft.

These blow count data are plotted versus elevation in Figure 2.6-27. The average blow count for each 5-ft elevation interval is plotted using an open circle, whereas the median value is plotted as an open square. Also shown, by the heavy dash-dot line, is the average value of all SPT blow counts in the upper 25 to 30-ft layer of silt, silty clay, and clayey silt, at $N = 15$.

A distinct change in material occurs at about 25 to 35 ft, where refusal ($N > 100$ blows per 6 inches) conditions are often encountered. The following 25 to 30 ft consists of very dense, dry, fine sand. Thin layers of fine gravel and coarse sand also are evident. A few clayey zones were encountered, but they had no apparent effect on the blow counts. The borings that were drilled to a depth of 100 ft or more (Borings A-1, D-4, CTB-1, and CTB-5) indicate that this layer is mainly underlain by very dense silt, silty sand, and sandy silt with occasional layers of clayey silt. Several layers of volcanic ash were also encountered in these borings.

A groundwater observation well was installed in Boring CTB-5(OW) in early 1999 in the vicinity of the Canister Transfer Building. Initial readings from this well indicate the groundwater table is about 125 ft below ground surface, approximate elevation 4,350 ft. Seismic refraction results (Appendix 2B) in the vicinity of the Storage Facility (see Figure 2.6-2, Seismic Lines 1 & 2) indicate the compression wave (P-wave) velocity changes from approximately 2,780 ft/sec to approximately 5,525 ft/sec at depths of between 90 and 131 ft below grade, which corroborates the depth to the water table measured in CTB-5(OW).

As indicated in Section 2.6.1.5, cone penetration tests were performed to further investigate the properties of the upper 25 to 30-ft thick layer at the site. There are some differences between the results of the cone penetration testing and the borings in regard to descriptions of the types of soils encountered, mostly in the 10 to 20-ft depth

range. The CPTs indicated that the soils between approximately 10 ft and 20 ft below existing grade at the site ***behave as though they are silty sands and sandy silts***.

This finding was not corroborated by the descriptions of the soils obtained from that zone in the borings, many of which are confirmed by laboratory test results.

The soil behavior type data presented in the CPT report (ConeTec, 1999) were determined using empirical correlations derived primarily from data collected from testing saturated and uncemented soils. Experience has shown that, typically, the cone penetration tip resistance is high in sands and low in clays and the friction ratio ($R_f = F_s/Q_t$) is low in sands and high in clays. This observation is incorporated in several soil classification charts. The correlations used to interpret the data measured in the CPTs performed at the site were developed by Robertson and Campanella (1988) and are presented in Figure 5, "Soil Behavior Type Classification Chart," of ConeTec (1999).

The soil descriptions shown in the CPT test results in ConeTec (1999) are based on the soil behavior type zones defined by the cone tip resistance and friction ratio values. The SBTs indicate that the soils within the 10 to 20-ft depth range generally behave like sandy silts or silty sand/sand, while the boring logs show the soils to be primarily a slightly to highly plastic silt. This difference is believed due to the partially saturated and weakly cemented soils encountered at the site. Many of the samples in this depth range had water contents near to or below the plastic limit. It is believed that, because of the low water contents and partial saturation effect, the slightly to highly plastic silts have low or no dynamic pore pressure response, which results in low measured sleeve friction values when penetrated by the cone. The cementation effect results in higher cone tip resistance values when penetrated by the cone and, likely, lower sleeve friction values. The higher tip resistance, in combination with measured sleeve friction values that are lower than they would otherwise be if they were saturated and uncemented, results in the interpretation that these soils behave like sandy soils when the SBT

classification chart developed by Robertson and Campanella (1988) is used. However, as observed in the borings and confirmed by the laboratory test results, most of these soils are clayey silts to silty clays.

As stated on page 51 of Robertson Campanella (1988),

“... CPT classification charts cannot be expected to provide accurate predictions of soil type based on grain size distribution but provide a guide to soil behaviour type. The CPT data provide a repeatable index of the aggregate behavior of the in situ soil in the immediate area of the probe.”

As indicated on page 8 of ConeTec (1999),

“It should be noted that it is not always possible to clearly identify a soil type based on Q_c , F_s and U_d .”

Factors such as changes in stress history, *in situ* stresses, sensitivity, stiffness, macrofabric, mineralogy, and void ratio will also influence the classification. As indicated on page 8 of ConeTec (1998),

“... the chart is global in nature and provides only a guide to soil behaviour type (SBT). Overlap in some zones should be expected and the zones should be adjusted somewhat based on local experience.

If no prior CPT experience exists in a given geologic environment it is advisable to obtain samples from appropriate locations to verify the classification and soil behaviour type.”

To appropriately use the cone penetration test results for soil classification at this site, the soil behavior type chart developed based on saturated uncemented soils must be recalibrated for the partially saturated and cemented soils encountered at the site. This was done by plotting the results of the soil classifications determined based on the borings and laboratory tests alongside plots of the soil behavior types from the CPT results. The borings and CPTs selected for this comparison were those that were performed within ~50 ft of each other, which included the following:

Boring	CPT	Distance Between (Ft)
CTB-4	CPT-37	4.2
CTB-5(OW)	CPT-38	4.2
C-1	CPT-39	5.5
A-2	CPT-34	15.0
B-3	CPT-20	29.8
A-3	CPT-32	50.9

developed from this program corroborated the conclusions drawn from the previous work.

The boring and trench data reported by Geomatrix (2001a) are stratigraphically very consistent across the storage pad area with the original boring data presented in Appendix 2A, both in the north-to-south and the east-to-west directions. The upper 30-ft (approximately) layer of soil is comprised of mixtures of silt, silty clay, clayey silt, and some sandy silt, that can be interpreted to represent stages in the cyclic history of Lake Bonneville (Geomatrix, 2001a). These stages are, from oldest to youngest, a Stansbury deepwater facies, a post-Stansbury transgressive and regressive facies, and the Provo and Bonneville deepwater facies.

Four borings (A-1, D-4, CTB-1, and CTB-5(OW)) were drilled to depths in excess of 100 ft and 25 borings were drilled to depths of approximately 50 to 75 ft (see Figure 2.6-5 sheets 1 through 14 and Figures 2.6-21 through 2.6-23). Logs of these borings are included in Attachment 1 of Appendix 2A. Standard penetration test (SPT) blow counts were obtained, generally, at 5-ft intervals in these borings. The data from these borings show a consistent picture across the site.

These site materials are consistent with what would be expected for deposits of a lacustrine environment, away from the direct influence of range-front alluvial fans. These deposits are overlain at the surface by thin, post-Provo eolian silt and recent playa deposits. They lie upon a uniform, fine sand that forms a nearly horizontal surface across the site at about elevation $4,440 \pm 5$ ft. This sand is the Stansbury transgressive facies, representing a series of shorelines and deltas that developed as Lake Bonneville initially occupied the area and rose to the deepwater Stansbury level. This sand is dense, having SPT blow counts generally in the range of 70 to over 100 blows/ft. At the base of the sand unit is an unconformity marked by the Promontory

soil, which developed on pre-Bonneville subaerial deposits. This gravelly layer occurs in the borings drilled in the storage pad area at a depth of about 45 to 50 ft (at about elevation 4410 to 4430 ft). Below the sandy gravel, the sediments are very hard silts, with some very dense sands. The SPT blow counts in these materials are generally well in excess of 100 blows/ft. Below a depth of approximately 90 ft, an ash marker horizon is encountered that indicates penetration into the Tertiary sediments of the Salt Lake Group.

As shown in the pad emplacement area foundation profiles (Figure 2.6-5, Sheets 1 through 14), the cask storage pads will be founded in the surficial eolian silt layer. The eolian silt, in its in situ loose state, is not suitable for founding the cask storage pads. Instead of excavating the eolian silt and replacing it with suitable structural fill, the eolian silt will be mixed with sufficient portland cement and water and compacted to form a strong soil-cement subgrade to support the cask storage pads. Soil cement will also be utilized around the Canister Transfer Building. The characteristics of the soil cement will be engineered during detailed design to meet the necessary strength requirements. See Section 2.6.4.11 for additional details about the soil cement.

As indicated in Section 2.6.1.5, in January 2001, 16 test pits were excavated at the PFSF site in the pad emplacement area to obtain soil samples for use in the laboratory analyses necessary to design the soil cement. It was observed from these test pits that the depth of the eolian silt was shallower than previously believed (approximately 2 ft on average, rather than 3 ft). The borings previously performed in this area obtained soil samples at depths from grade to 2 ft and from 5 ft to 7 ft. Therefore, as later observed in the test pits, the interface between the eolian silt and the silty clay/clayey silt fell between the samples collected in the borings. The soil unit descriptions from Trench T-2 in the pad emplacement area (Plate 3, Geomatrix, 2001a) also corroborates the soil-cement test pit observations; i.e., the fine sandy silt (eolian deposit) overlying

the sandy clayey silt (combic B soil horizon developed on Bonneville deep-water sediment) is not expected to extend much deeper than approximately 2 ft from the ground surface. Furthermore, these observations are verified by Atterberg limits tests that have recently been performed on the samples obtained from these test pits, which indicate that the soil samples collected below depths of 2 ft are exclusively cohesive clayey silt/silty clay with high plasticity indices.

The previous interpretation of the eolian silt boundary assumed that this boundary lay where the initial spike in the cone penetration tip resistance bottomed out. This assumption was made in order to obtain a conservative upper-bound estimate of the amount of soil cement required for the soil improvement of the noncohesive eolian silt. This increase in tip resistance was previously assumed to represent a layer of slightly cemented eolian silt. However, as observed in the January 2001 soil-cement test pits and in Trench T-2, the interface between the noncohesive eolian silt and the cohesive clayey silt/silty clay more closely corresponds to the initial increase in the cone tip resistance, along with an accompanying steep increase in the sleeve skin friction resistance. These observations are consistent with the experience of soil classification using electric CPT data, which indicate that sandy soils (noncohesive) tend to produce high cone resistance and low friction ratio, whereas soft clay soils (cohesive) tend to produce low cone resistance and high friction ratio (p.51, Lunne, Robertson and Powell, 1997). Therefore, it is expected that the transition from the noncohesive soil to the cohesive soil will be characterized by a steep increase of the cone skin friction resistance.

Based on the correlations and evaluations discussed above, the transitional boundary between the surficial noncohesive eolian silt and underlying cohesive clayey silt/silty clay presented in Figure 2.6-5, Sheets 1 through 14, was re-interpreted to make it consistent with the soil-cement test pit observations and laboratory classification test

results performed on soil samples from the test pits in the pad emplacement area. The interpretation also considered that the measurement of sleeve friction (f_s) is often less accurate and less reliable than the cone resistance (p.51, Lunne, Robertson and Powell, 1997). The boundary was re-interpreted based on consideration of the consistency between various cone penetration tests to obtain a smoothed boundary, instead of interpreting each cone penetration test discretely. This re-interpretation of the eolian silt boundary results in a reduction of the estimated amount of eolian silt, and a corresponding reduction in the amount of soil cement required under the cask storage pads (see Figure 4.2-7), minimizing environmental impacts associated with construction of the facility (i.e., fewer truck trips for cement deliveries, less water required to mix the soil cement, less dust associated with excavation, mixing, and compaction of soil cement, ...).

Refer to Sections 2.6.1.11 and 2.6.2.1 for a discussion of the engineering characteristics of these soils and to Section 2.6.4.11 for information concerning the soil cement.

and 6 miles southeast several wells flow at the surface (elevation 4,605 ft). A well at the Tekoi Rocket Engine Test Facility about 3 miles south of the site was drilled to 400 ft and has static water at 80 ft below ground surface (elevation about 4,480 ft). All the above-mentioned wells were completed in unconsolidated materials without drilling into the bedrock. The locations of all wells within 5 miles of the PFSF are identified in Figure 2.5-1. These data suggest that the main aquifer in the central part of Skull Valley is unconfined or semi-confined and occurs mainly within the fine-grained Tertiary Salt Lake Group deposits. These sediments interfinger with coarse-grained alluvial fan material along the toe of the fan and may create confined conditions where they overlap the fan deposits. The fan deposits are the main recharge zone for the valley aquifers and the main source for domestic water wells in the valley. The aquifer in the fans is unconfined for the most part, but becomes confined and under artesian conditions downslope where the lake and basinal deposits onlap the fan at depth. Water wells drilled near the lower edge of the fan, such as at the Rocket Engine Test Facility, may penetrate several hundred feet of sediments before encountering a coarse alluvial fan layer. Since the coarse layer is under artesian pressure, the level of water in the well will rise upward to the static condition or may flow at the surface, such as occurs just south of the Reservation.

Groundwater levels at the site appear to closely correlate with levels in the main valley aquifer. They do not appear to be affected by proximity to the alluvial fan. At this time it is believed an adequate quantity of suitable quality water can be developed within the site area for the PFSF needs. Specific properties of aquifer materials are unknown at this time. As discussed in ER Sections 4.5.5 - 4.5.7, based on initial testing of the site monitoring well, it is believed that groundwater withdrawals at the PFSF site would have no measurable impact on off-site wells, either up-gradient or down-gradient (SWEC, 1999b). Surface soil at the site has a permeability of 0.2 to 0.6 inch/hr, whereas the soil on the alluvial fan has a permeability of 6 to 20 inches/hr (USDA, unpub. data). As

discussed in ER Section 4.5.5, it is estimated that the average withdrawal rate from the well over a 42 year period will be approximately 2.040 gallons per day (1.4 gpm).

Groundwater quality in the area is variable, with the best quality associated with wells developed in the alluvial fans near the Stansbury Mountains. In general, water quality is lower in the valley bottom, but it is suitable for irrigation or stock watering without treatment. The main dissolved ions are sodium and chloride (Hood and Waddell, 1968). There is also a tendency for the quality to be lower farther north, down-valley, towards the Great Salt Lake, although there are exceptions to this trend. Total dissolved solids range from 1,600 to 7,900 mg/l at the northern end of the valley (Arabasz et al., 1987, App. F). Most sources of water in the valley are high in calcium and would be classified as very hard. Aquifer transmissivities range from 500 to 30,000 sq ft/day with an average for Skull Valley estimated at 5,000 sq ft/day (Arabasz et al., 1987, App. F).

2.6.1.10 Geophysical Surveys

Seismic Refraction and Reflection Surveys

Results of seismic refraction and reflection surveys performed at the site in 1996 are found in Appendix 2B. Engineering properties of site materials based on the geophysical investigations are discussed in Section 2.6.1.11. The results of 1998 geophysical surveys (seismic reflection, gravity, and magnetic) are discussed in Geomatrix Consultants, Inc. (2001a) and Bay Geophysical Associates (1999).

Seismic Cone Penetration Tests

Seismic cone penetration tests were performed at the locations designated as "SEIS CPT" on Figure 2.6-19. The purpose of these tests was to measure down-hole P and S-wave velocities. The results of these tests are presented in Appendix C of ConeTec (1999), and the average velocities vs depth are shown in Figure 2.6-28.

Shear wave velocities of soils are dependent on the effective stress, void ratio, and for clays, the plasticity index and overconsolidation ratio of the soils. If all of these parameters were the same, it would be expected that the shear wave velocities would increase with increasing depth in the profile. The apparent leveling off of the shear wave velocities at a depth of about 10 to 15 ft in the results of the seismic CPTs that were performed at the site (Appendix C of ConeTec, 1999) is an indication that one or more of these parameters have changed. A review of the Q_t plots, which are included on the left-hand side of the same pages that present the shear wave velocities vs depth, indicates that the tip resistance increases greatly in this zone. This increase in tip resistance is most likely associated with a change in soil type, as indicated by the SBT plots on the right-hand side of these same pages, as well as by a decrease in the void ratio of these soils. Therefore, it is not unexpected that the shear wave velocities would change within this zone.

A review of the shear wave velocities vs depth presented in Appendix C of ConeTec (1999) indicates that they do not level off with depth. The general trend in the data is to increase with respect to depth; however this trend is masked by the presence of the marked increase in the shear wave velocities in the "harder" zone that exists generally within the depth range of about 13 feet to about 20 feet. If the shear wave velocities associated with this harder zone are excluded, all of the plots of shear wave velocities show a general increase with respect to depth. This general increase in velocity with increasing depth is more readily observed in Figure 2.6-28.

Downhole Seismic Velocity Tests

Northland Geophysical (2001) conducted confirmatory downhole shear and compression wave velocity measurements in Borings CTB-5(OW) and CTB-5A to a maximum depth of 106.5 feet. The data from Boring CTB-5(OW) were measured in a PVC-cased boring to a maximum depth of 50.8 feet. The shear and compression wave velocity data from this boring are very consistent with the velocities obtained from the

seismic cone penetration tests in the depth range of 0 to 30 feet (Geomatrix, 2001c). The data from Boring CTB-5(OW) show a trend of gradually increasing velocity in the depth range of 30 to 50 feet. Boring CTB-5A was drilled adjacent to CTB-5(OW) using a hollow-stem auger, and shear wave velocities were measured with the geophones clamped within the auger stem. The measurements were initiated near the bottom of the hole at a depth of 106.5 feet and continued upward until the data quality began to deteriorate above 44 feet. As a result, there was a very limited range of overlap between the measurements in Borings CTB-5(OW) and CTB-5A. The velocities in the two borings were similar (see Figures 3 and 4 of Northland Geophysical, 2001). The data from Boring CTB-5A show fairly uniform velocities for the depth range of 55 to 95 feet and an increase in velocity below 95 feet. The results of the measurements taken in these downhole seismic velocity surveys have been incorporated into the analyses discussed in Section 2.6.2, Vibratory Ground Motion.

2.6.1.11 Static and Dynamic Soil and Rock Properties at the Site

Geotechnical laboratory tests were performed on samples obtained from the borings. The results of these tests are included in Appendix 2A and are summarized below. Figure 2.6-20 presents plots of the SPT blow counts vs depth in the pad emplacement area, on a row-by-row basis. This figure also presents the index properties that were measured for these soils, along with the results of triaxial testing. Dry densities of subsurface soils at the site are plotted vs depth in Figure 2.6-31. Comparison of these plots indicates that the soil properties are fairly consistent across the site.

to the seismic loading, and then shearing them rapidly to simulate conditions that will exist during the earthquake loading.

The original triaxial tests (results reported in Appendix 2A, Attachments 2, 4, and 5) were performed at confining stresses that represent the static conditions that will exist under the fully loaded pads. To demonstrate the cohesive nature of these soils, an additional consolidated-undrained triaxial compression test was performed at a confining stress of 1 ksf, which is representative of the minimum confining stresses expected to exist under the fully loaded pads when the maximum uplift forces due to the design basis ground motion occurs, and one test was performed at a confining stress of 0, which is essentially an unconfined compression test. The results of these tests are included in the total-stress strength parameters reported above, and details of these tests are included in Attachment 8 of Appendix 2A.

The dotted line shown in the plot of Mohr's circles of the results of CU tests performed on samples from Boring B-1 that is included in Attachment 8 of Appendix 2A is tangent to the Mohr's circle for Sample U-2B of Boring B-1. It indicates that the cohesion of this specimen is slightly less than that of the other specimens tested. This strength was lower because its dry density ($\gamma_d = 46.3$ pcf) was lower than that of the other specimens. As indicated by the plots of water content vs depth presented in Figure 2.6-20, most of the *in situ* soils in the upper ~25-ft layer at the site have $w_n < 50\%$, which is more like Samples U-2C and U-2D; hence the recommendation that $c = 1.4$ ksf for these soils.

For the partially saturated cohesive soils at the site, the strength of the soil is dependent on its apparent cohesion, friction angle, as well as the consolidation pressure. The strain rates are very high during the seismic event; therefore, the partially saturated cohesive soils will be stressed essentially under undrained

conditions. The effect of the pore pressure response, if any, during such tests, either positive or negative, will be manifested directly in the shear strength value measured. Because the strain rate of the laboratory tests is at least one order of magnitude slower than the rate associated with the design basis ground motion, the strength measured in the laboratory is a lower-bound estimate of the strength that will be available to resist the dynamic loadings during the seismic event. See Section 2.6.1.11.5, "Dynamic Strength of Cohesive Soils," for additional details.

The bearing capacity of the structures is dependent primarily on the strength of the soils in the upper ~25 to ~30-ft layer at the site. All of the borings drilled at the site indicate that the soils underlying this upper layer are very dense fine sands overlying silts with standard penetration test blow counts that exceed 100 blows/ft. The results of the cone penetration testing, presented in ConeTec(1999) and plotted in Figure 2.6-5, Sheets 1 to 14, illustrate that the strength of the soils in the upper layer are much greater at depths below ~10 ft than in the range of ~5 ft to ~10 ft, where most of the triaxial tests were performed.

In determining the bearing capacity of shallow foundations, the average shear strength of the soils along the anticipated bearing capacity failure slip surface should be used. This slip surface is normally confined to the zone within a depth below the footing equal to the minimum width of the footing. For the cask storage pads, the effective width of the footing is decreased because of the large eccentricity of the load on the pads due to the seismic loading. As indicated in Table 2.6-7, the minimum effective width of the cask storage pads occurs for Load Case II, where $B' = 15.6$ ft. For the load cases where the three components of the earthquake are combined in accordance with ASCE (1986), the minimum effective width of the cask storage pads occurs for Load Case IIIB, where $B' = 15.7$ ft. Figure 7 of Calculation 05996.02-G(B)-4 (SWEC, 2001b) illustrates that the anticipated slip surface of the bearing capacity failure for $B' \sim 15$ ft is limited to the soils within the upper two-thirds of the upper layer. Therefore, in the bearing

capacity analyses of the cask storage pads, the undrained strength measured in the triaxial tests was not increased to reflect the increase in strength measured for the deeper-lying soils in the cone penetration testing.

Table 6 of Calculation 05996.02-G(B)-5 (SWEC, 2000c) summarizes the results of the triaxial tests that were performed within depths of ~10 ft at the site. The undrained shear strengths measured in these tests are plotted vs confining pressure in Figure 11 of that calculation. This figure is annotated to indicate the vertical stresses existing prior to construction and following completion of construction. As indicated, the undrained strength of the soils within ~10 ft of grade was assumed to be 2.2 ksf. This value is the lowest strength measured in the UU tests, which were performed at confining stresses of 1.3 ksf. This confining stress corresponds to the in situ vertical stress existing near the middle of the upper layer prior to construction of these structures. It is much less than the final stresses that will exist under the cask storage pads and the Canister Transfer Building following completion of construction. Figure 11 of Calculation 05996.02-G(B)-5 (SWEC, 2000c) illustrates that the undrained strength of these soils increases as the loadings of the structures are applied; therefore, 2.2 ksf is a very conservative, lower-bound value for use in the dynamic bearing capacity analyses of these structures.

Effective-stress strength parameters are estimated to be $c = 0$ ksf, even though these soils may be somewhat cemented, and $\phi = 30^\circ$. This value of ϕ is based on the average PI value for these soils, which equaled 14%, as shown in the table presented above, and the relationship between ϕ and PI presented in Figure 18.1 of Terzaghi & Peck (1967).

Therefore, static bearing capacity analyses of the cask storage pads were performed using the following soil strengths:

Case IA Static using undrained strength: $\phi = 0^\circ$ & $c = 2.2$ ksf.

Case IB Static using effective-stress strength: $\phi = 30^\circ$ & $c = 0$.

The pads will be constructed on and within soil cement, as illustrated in Figure 4.2-7 and described in Sections 2.6.1.7 and 2.6.4.11. The unit weight of the soil cement is assumed to be 100 pcf in the bearing capacity analyses. The strength of the soil cement was conservatively ignored in the bearing capacity analyses.

Direct shear tests were performed on undisturbed specimens of the silty clay/clayey silt obtained at a depth of 5.7 ft to 6 ft in Boring C-2. These tests were performed at normal stresses that were essentially equal to the normal stresses expected:

- under the fully loaded pads before the earthquake,
- with all of the vertical forces due to the earthquake acting upward, and
- with all of the vertical forces due to the earthquake acting downward.

The results of these tests are presented in Attachment 7 of the Appendix 2A and they are plotted in Figure 7 of Calculation 05996.02-G(B)-5 (SWEC, 2000c). Because of the fine grained nature of these soils, they will not drain completely during the rapid cycling of loadings associated with the design basis ground motion. Therefore, sliding stability analyses of the cask storage pads constructed directly on the silty clay are performed using the shear strength measured in these direct shear tests for the normal stress that equals the vertical stress under the fully loaded cask storage pads prior to imposition of the dynamic loading due to the earthquake. As shown in Figure 7 of Calculation 05996.02-G(B)-5 (SWEC, 2000c), this shear strength is 2.1 ksf and the friction angle is set equal to 0° for the clayey soils underlying the cask storage pads.

2.6.1.11.2 Canister Transfer Building Area

The results of the tests of the silty clay/clayey silts obtained from the upper 25 to 30 ft layer in the Canister Transfer Building area are as follows:

Index Property:	Minimum	Maximum	Average
Water Content, %	7	86	40
Liquid Limit	28	83	51
Plastic Limit	18	48	30
Plasticity Index	4	38	20
Moist Unit Weight, pcf	73	118	92
Dry Unit Weight, pcf	40	98	65
Void Ratio	0.7	3.3	1.8
Saturation, %	40	88	71
Specific Gravity	2.71	2.73	2.72
Consolidation parameters:	Low	High	Average
Maximum past pressure, ksf:	6	26	13
Virgin compression ratio, CR:	0.13	0.37	0.31
Recompression ratio, RR:	0.014	0.020	0.018

Total-stress strength parameters are $\phi = 21.1^\circ$ and $c = 1.13$ ksf, based on the average values of the direct shear test results for samples from Borings CTB-6 & CTB-S, presented in Attachments 7 and 8 of Appendix 2A.

Table 6 of Calculation 05996.02-G(B)-5 (SWEC, 2000c) summarizes the results of the triaxial tests that were performed within depths of ~10 ft at the site. The undrained shear strengths measured in these tests are plotted vs confining pressure in Figure 11 of that calculation. This figure is annotated to indicate the vertical stresses existing prior to construction and following completion of construction. As indicated, the undrained strength of the soils within ~10 ft of grade was assumed to be 2.2 ksf. This value is the lowest strength measured in the UU tests, which were performed at confining stresses of 1.3 ksf. This confining stress corresponds to the in situ vertical stress existing near the middle of the upper layer prior

to construction of these structures. It is much less than the final stresses that will exist under the cask storage pads and the Canister Transfer Building following completion of construction. Figure 11 of Calculation 05996.02-G(B)-5 (SWEC, 2000c) illustrates that the undrained strength of these soils increases as the loadings of the structures are applied; therefore, 2.2 ksf is a very conservative, lower-bound shear strength value for use in the dynamic bearing capacity analyses of these structures.

The bearing capacity of the structures is dependent primarily on the strength of the soils in the upper ~25 to ~30-ft layer at the site. All of the borings drilled at the site indicate that the soils underlying this upper layer are very dense fine sands overlying silts with standard penetration test blow counts that exceed 100 blows/ft. The results of the cone penetration testing, presented in ConeTec (1999) and plotted in Figure 2.6-5, Sheets 1 to 14, illustrate that the strength of the soils in the upper layer are much greater at depths below ~10 ft than in the range of ~5 ft to ~10 ft, where most of the triaxial tests were performed.

In determining the bearing capacity of shallow foundations, the average shear strength of the soils along the anticipated bearing capacity failure slip surface should be used. This slip surface is normally confined to the zone within a depth below the footing equal to the minimum width of the footing. For the Canister Transfer Building, the effective width of the footing is decreased because of the large eccentricity of the load on the mat due to the seismic loading. As indicated in Table 2.6-10, the minimum effective width of the Canister Transfer Building occurs for Load Case IIIA, where $B' = 119.5$ ft. This is greater than the depth of the upper layer (~30 ft). Therefore, it is reasonable to use the average strength of the soils in the upper layer in the bearing capacity analyses of this structure, since all of the soils in the upper layer will be effective in resisting failure along the anticipated bearing capacity slip surface.

The undrained strength used in the bearing capacity analyses of the Canister Transfer Building is a weighted average strength that is applicable for the soils in the upper layer. This value is determined using the value of undrained shear strength of 2.2 ksf noted above for the soils tested at depths of ~10 ft and the relative strength increase measured for the soils below depths of ~12 ft in the cone penetration tests that were performed within the Canister Transfer Building footprint. As indicated on Figure 2.6-18, these included CPT-37 and CPT-38. Similar increases in undrained strength for the deeper lying soils were also noted in all of the other CPTs performed in the pad emplacement area.

Attachment B of Calculation 05996.02-G(B)-13 (SWEC, 2001c) presents copies of the plots of s_u vs depth for CPT-37 and CPT-38 (from Appendix D of ConeTec, 1999). These plots are annotated to identify the average undrained strength of the cohesive soils measured with respect to depth. As shown by the plot of s_u for CPT-37, the weakest zone exists between depths of ~5 ft and ~12 ft. The results for CPT-38 are similar, but the bottom of the weakest zone is at a depth of ~11 ft. The underlying soils are all much stronger. The average value of s_u of the cohesive soils for the depth range from ~18 ft to ~28 ft is ~2.20 tsf, compared to s_u ~1.34 tsf for the zone between ~5 ft and ~12 ft. Therefore, the undrained strength of the deeper soils in the upper layer was ~64% ($\Delta s_u = 100\% \times [(2.20 \text{ tsf} - 1.34 \text{ tsf}) / 1.34 \text{ tsf}]$) higher than the strength measured for the soils within the depth range of ~5 ft to ~12 ft. The relative strength increase was even greater than this in CPT-38.

Using 2.2 ksf, as measured in the UU triaxial tests performed on specimens obtained from depths of ~10 ft, as the undrained strength applicable for the weakest soils (i.e., those in the depth range of ~5 ft to ~12 ft), the average strength for the soils in the entire upper layer is calculated as shown in Figure 4 of that calculation (SWEC, 2001c). The resulting average value, weighted as a function of the depth, is s_u ~3.18 ksf. This

value would be much higher if the results from CPT-38 were used; therefore, this is considered to be a reasonable lower-bound value of the average strength applicable for the soils in the upper layer that underlie the Canister Transfer Building.

Further evidence that this is a conservative value of s_u for the soils in the upper layer is presented in Figure 11 of Calculation 05996.02-G(B)-5 (SWEC, 2000c), which presents a summary of the triaxial test results for soils obtained within ~10 ft of the ground surface at the site. This plot of s_u vs confining pressure illustrates that this weighted average value (3.18 ksf) is slightly less than the average value of s_u measured in the CU triaxial tests that were performed on specimens obtained from depths of ~10 ft at confining stresses of 2.1 ksf. As indicated in this figure, the confining stress of 2.1 ksf used to test these specimens is comparable to the vertical stress that will exist ~5 ft below the Canister Transfer Building mat following completion of construction. Since these tests were performed on specimens of the weakest soils underling the Canister Transfer Building mat (the deeper lying soils are stronger based on the SPT and the cone penetration test data), it is conservative to use the weighted average value of s_u of 3.18 ksf for the soils in the entire upper layer of the profile in the bearing capacity analyses of the Canister Transfer Building.

Effective-stress strength parameters are estimated to be $\phi = 30^\circ$ and $c = 0$ ksf, even though these soils may be somewhat cemented. This value of ϕ is based on the average PI value for the soils underlying the Canister Transfer Building, which equaled 20%, as shown in the table presented above, and the relationship between ϕ and PI presented in Figure 18.1 of Terzaghi & Peck (1967).

Therefore, static bearing capacity analyses are performed using the following soil strengths:

Case IA Static using undrained strength parameters: $\phi = 0^\circ$ & $c = 3.18$ ksf.

Case IB Static using effective-stress strength parameters: $\phi = 30^\circ$ & $c = 0$.

and dynamic bearing capacity analyses are performed using $\phi = 0^\circ$ & $c = 3.18$ ksf.

Direct shear tests were performed on undisturbed specimens of the silty clay/clayey silt obtained from Borings CTB-6 and CTB-S, which were drilled in the locations shown in Figure 2.6-18, within the footprint of the Canister Transfer Building. These specimens were obtained from Elevation ~4469, the elevation near the bottom of the perimeter key will be constructed at the base of Canister Transfer Building mat. Note, this key is being constructed around the perimeter of the mat to ensure that the full shear strength of the clayey soils is engaged to resist sliding of the structure due to loads from the design basis ground motion. These direct shear tests were performed at normal stresses that ranged from 0.25 ksf to 3.0 ksf. This range of normal stresses bounds the ranges of stresses expected for static and dynamic loadings from the design basis ground motion.

The results of these tests are presented in Attachments 7 and 8 of the Appendix 2A. Copies of these plots are included as Figures 9 and 10 of Calculation 05996.02-G(B)-5 (SWEC, 2000c), with annotations that identify the range of vertical stresses due to the design basis ground motion, as well as the shear strength used in the analysis of the sliding stability of the Canister Transfer Building founded on the in situ silty clay/clayey silt. Because of the fine grained nature of these soils, they will not drain completely during the rapid cycling of loadings associated with the design basis ground motion. Therefore, sliding stability analyses of the Canister Transfer Building constructed directly on the silty clay are performed using the average shear strength measured in these direct shear tests for the normal stress equal to the vertical stress under the building following completion of construction, but prior to imposition of the dynamic loading due to the earthquake. As shown in Figures 9 and 10 of Calculation

05996.02-G(B)-5 (SWEC, 2000c), this average shear strength is 1.8 ksf and the friction angle is set equal to 0°. No credit is taken in this sliding stability analysis for the increased frictional strength due to the increased normal force multiplied by $\tan \phi$ when the earthquake forces act downward, nor is credit taken for the strength increase that is typical for cohesive soils subjected to dynamic loadings.

For the sand or sandy soils layer in the Canister Transfer Building area found in some of the borings located at a depth of 8 to 20 ft:

Index Property	Minimum	Maximum	Average
Water Content, %	3	15	6
Moist Unit Weight, pcf	85	105	98
Dry Unit Weight, pcf	77	102	93
Void Ratio	0.64	1.2	0.83
Saturation, %	11	32	19
% Fines	9	38	23
Specific Gravity = 2.69			

2.6.1.12 Stability of Foundations for Structures and Embankments

All exterior footings will be founded at a depth of no less than 30 inches below finished grade to provide protection against frost, in accordance with local code requirements. Interior footings in heated areas may be founded at shallower depths, if desired.

The minimum factor of safety against a bearing capacity failure due to static loads (dead load plus maximum live loads) is 3.0.

In accordance with the requirements of NUREG-75/087, Section 3.8.5, "Foundations," Section II.5, "Structural Acceptance Criteria," the recommended minimum factor of safety against overturning or sliding failure from static loads (dead load plus maximum live loads) is 1.5 and due to static loads plus loads from extreme environmental conditions, such as the design basis ground motion, is 1.1. In addition, it is recommended that a factor of safety of 1.1 be used to design footings against a bearing capacity failure from static loads plus loads due to the design basis ground motion.

If the factor of safety against sliding is less than 1 due to the design basis ground motion, additional analyses of the displacements the structure may experience are performed using the method proposed by Newmark (1965) for estimating displacements of dams and embankments during earthquakes to demonstrate that such displacements, if they did occur, would not have an adverse impact on the performance of the Important-to-Safety structures.

Recommended design earth pressure distributions are presented in Figure 2.6-7. Lateral earth pressures for determining driving forces shall be based on K_0 , the at-rest earth pressure coefficient. These can be reduced to "active" earth pressures if the yield ratio exceeds 0.1%, where yield ratio, S/H , is defined as shown for the active case in Figure 2.6-8. In determining "passive" pressures resisting lateral movement, assume

the lateral earth pressure coefficient varies from K_0 at a yield ratio of 0% to a maximum of K_p at a yield ratio of 2%, where yield ratio, S/H , is defined as shown for the passive case in Figure 2.6-8. Compaction-induced lateral stresses are determined as shown in Figure 2.6-9.

2.6.1.12.1 Stability and Settlement Analyses—Cask Storage Pads

Bearing Capacity

The bearing capacity of the cask storage pads was determined using the general bearing capacity equation and associated shape, depth, and inclination factors, as presented in Winterkorn and Fang (1975). Refer to Calculation 05996.02-G(B)-04 (SWEC, 2001b) for details. These analyses are based only on the strength of the silty clay/clayey silts underlying the pads. They conservatively ignore the presence of the soil cement that will be constructed adjacent to and beneath the cask storage pads (Figure 4.2-7) and the dense sand layer at a depth of ~25 to 30 ft. Even with these conservative assumptions, they demonstrate that there is an adequate factor of safety against a bearing capacity failure for both static and dynamic loadings.

As indicated in Revision 7 of Calculation 05996.02-G(B)-04 (SWEC, 2001b), the soil cement could be designed to have sufficient strength to provide, in passive resistance alone, all of the horizontal resistance required to obtain a factor of safety against sliding that exceeds the criterion ($FS=1.1$) for dynamic loadings. The current version of this calculation demonstrates that the soil cement beneath the pads will have sufficient shear strength to resist all of the horizontal forces due to the earthquake; therefore, the soil cement adjacent to the pads is not required to resist sliding. However, soil cement will be constructed adjacent to the pads to provide an adequate subbase for support of the cask transporter, in lieu of placing and compacting structural fill. The unconfined compressive strength of this soil cement likely will be at least 250 psi to satisfy the durability requirements associated with environmental considerations (i.e., freeze/thaw and wet/dry cycles) within the frost zone (30 in. from the ground surface). The soil

cement adjacent to the pad will resist some of the horizontal loads due to the earthquake, which will minimize the effects of the angle of inclination of the vertical load on the allowable bearing capacity. The allowable bearing capacity is inversely related to the angle of inclination of the load, and it is markedly reduced for the inclination angles applicable for the dynamic horizontal loads from the design basis ground motion. The presence of the soil cement, therefore, will greatly enhance the bearing capacity of these foundations.

These analyses included determination of factors of safety against a bearing capacity failure of the foundation due to static loads and due to static plus dynamic loads from the design basis ground motion (PSHA 2,000-yr return period earthquake). The dynamic bearing capacity analyses are discussed in detail in the section below titled "*Dynamic Bearing Capacity of the Cask Storage Pads.*"

Static Bearing Capacity of the Cask Storage Pads

Table 2.6-6 presents the results of the bearing capacity analyses for the following static load cases. As indicated above, the minimum factor of safety for these static load cases is 3.

Case IA Static using undrained strength parameters ($\phi = 0^\circ$ & $c = 2.2$ ksf).

Case IB Static using effective-stress strength parameters ($\phi = 30^\circ$ & $c = 0$).

As indicated in this table, the gross allowable bearing pressure for the cask storage pads to obtain a factor of safety of 3.0 against a shear failure from static loads is greater than 4 ksf. However, loading the storage pads to this value may result in undesirable settlements. This minimum allowable value was obtained in analyses that conservatively use $\phi = 0^\circ$ and $c = 2.2$ ksf, as measured in the UU tests that are reported in Attachment 2 of Appendix 2A, to model the end of construction. Using the estimated effective-stress strength of $\phi = 30^\circ$ and $c = 0$ results in a higher allowable bearing pressure. As shown in Table 2.6-6, the gross allowable bearing capacity of the cask storage pads for static loads for the effective-stress soil strength is greater than 9 ksf.

Effect of Cohesionless Soils Underlying the Cask Storage Pads on Bearing Capacity

Unconsolidated-undrained triaxial test results included in Attachment 1 of Appendix 2A indicate that 2.2 ksf is a reasonable lower-bound value to use for bearing capacity analyses of the undrained conditions to represent the end-of-construction case. These triaxial tests were performed at confining pressures comparable to the in situ vertical stresses existing near the middle of the upper layer prior to the construction of the pads, thus, provide a realistic estimation of the minimum strength that will be available for resisting a bearing capacity failure at the end of construction.

As indicated in Section 2.6.1.6, based on the CPT program, most of the soils underlying the pad emplacement area are mischaracterized as soils that behave as "sandy" soils, rather than as cohesive soils. These soils were found to be mostly cohesive soils in the borings that were drilled in 1996, as indicated in Attachment 1 of Appendix 2A. The soil behavior types reported in ConeTec (1999) were determined based on correlations developed from testing saturated, uncemented soils. The soils at the site are partially saturated and cemented; thus, the soil behavior types determined from the cone penetration test data must be recalibrated to agree with the soil classifications determined based on samples obtained in the borings and tested in the laboratory.

Figure 2.6-30, Sheets 1 through 6, present comparisons of the boring and laboratory soil classifications plotted vs elevation alongside the soil behavior type data from nearby cone penetration tests. The differences shown under the column labeled Δ SBT represent the SBT zoning shift required to more correctly characterize these soils as a result of the effects of partial saturation and cementation, as discussed above.

Evaluation of these Δ SBT values leads to the conclusion that the soil behavior type values reported in ConeTec (1999) that are greater than 5 (i.e., sandier soils), as well as some of those equal to 5 (i.e., clayey silts), typically should be adjusted downward one or two zones to more accurately reflect the soil classifications that were determined

based on the borings and confirmed by the laboratory tests performed specifically for the purpose of classifying the soil types. Conservatively adjusting these data by subtracting 1 from the SBTs that were reported to be greater than 5 (i.e., "sandy" soils), as discussed in Section 2.6.1.6, results in the SBTs presented on the pad emplacement area foundation profiles, Sheets 2 through 14 of Figure 2.6-5. As shown on these figures, the subsurface soils that were reported in ConeTec (1999) as being silty sand/sand and sands are more correctly described as silts with some sandy silts. The following discussion is included to demonstrate that even if these soils are cohesionless soils, the factor of safety against a bearing capacity failure is much greater than that reported above for the clayey soils identified in the borings.

Whereas the bearing capacity of cohesive soils is a function of the strength of the soil, that of cohesionless soils is also a function of the width of the foundation. The foundations in question for this project have widths that are 30 ft or greater. Such large foundations, supported by soils having Standard Penetration Test blow counts that were measured for these soils, have much greater bearing capacities if they are founded on cohesionless soils than if supported by undrained cohesive soils. Therefore, characterizing the soils in the upper layer as cohesive even though some of these may be cohesionless provides a conservative estimate of the bearing capacity.

Analyses of bearing capacity were made in Calculation 05996.02-G(B)-4, (SWEC, 2001b), based on the assumption that the entire upper layer, approximately 25 to 30-ft thick, was comprised of cohesive soils similar to those tested at depths of 10 to 12 ft. In these analyses, the strength of the soils in the entire upper layer (~25 to 30-ft thick) was set equal to the minimum value measured in the UU tests ($s_u = 2.2$ ksf) that were performed on samples obtained from depths of approximately 10 to 12 feet. As indicated on Table 2.6-6 for Case IA, the factor of safety of the cask storage pad foundation is 7.0 using this undrained strength for the cohesive soils. The results for Case IB Table 2.6-6 illustrates that the factor of safety against a bearing capacity failure increases to greater than 15 when the effective-stress strength of $\phi = 30^\circ$ is used.

The friction angle used in the effective-stress strength analyses discussed above is less than the friction angle shown for the soils that behave as sandy soils (SBT>5) based on the CPT data presented in Appendix D of ConeTec (1999). These plots illustrate that most of the "Phi" values are between 35° and 40° for these soils, with very few values that are slightly less than 35°. Therefore, assuming that all of the soils underlying the cask storage pads are cohesionless, as represented by the preponderance of soils that behave as "sandy" soils based on the uncorrected CPT SBT data, the factor of safety against a bearing capacity failure will be much greater than 15.

Static Settlements of the Cask Storage Pads

Analyses were performed to estimate the maximum total settlement of the cask storage pads as a result of the weight of the pad and the weight of eight, fully loaded, Holtec HI-STORM casks (356.5 K) in Calculations 05996.02-G(B)-3 (SWEC, 1999e) and 05996.03-G(B)-21 (SWEC, 2001a). The actual bearing pressure for this case was about 1.9 ksf, and the estimated total settlement of the pad was determined to be about 1.7 inches. The maximum total settlement consists of the following three components:

• Elastic settlement	0.5 inches
• Primary consolidation settlement	0.8 inches
• Secondary compression	0.4 inches
<hr/>	
• Maximum total settlement	1.7 inches

The maximum differential settlement between the center of the crushed rock aisle and the center of the storage pads is 1-1/2 inches, when the 0.25 inches of immediate settlement of the pad emplacement area is removed. The estimated settlement of the storage pads at the long edge of the pads is approximately half that value, or 3/4 inch. The maximum differential settlement between the long edge of the storage pads and the center of the crushed rock aisle between the storage pads is therefore less than or equal to 3/4 inch (SWEC, 2001a).

The crushed rock surface materials will be installed flush with the top of the storage pads and removed as required in order to accommodate the actual settlement of the pads. Exposed edges of the pads will be chamfered and the compacted aggregate surface material will be feathered to meet the edges of the raised pads for transporter access, as shown in Figure 4.2-7.

This settlement represents an upper-bound estimate of the total compression, because it was developed assuming that the consolidation characteristics that were measured for the clayey soils at a depth of about 10 ft are applicable for the entire upper layer (~25 to 30 ft). The SPT data from the borings and the CPT results indicate that the soils become stiffer within the 10 to 20 ft depth zone. Additional consolidation tests performed on samples obtained from depths of about 25 ft in the Canister Transfer Building area, reported in Attachment 6 of Appendix 2A, indicate that the soils at that depth are less compressible than those used to estimate the settlements presented above. Further, based on the CPT program, most of the soils underlying the pad emplacement area are characterized as soils that **behave** as "sandy" soils, rather than as cohesive soils. Such soils are much less compressible than the clayey soils described above. Therefore, assuming that the entire upper layer at the site was comprised of soils whose compressibilities are similar to those measured at a depth of 10 to 12 ft conservatively overestimates the expected settlements.

Effect of Cohesionless Soils Underlying the Cask Storage Pads on Settlements

As discussed above, the soil behavior types determined from the cone penetration test data and reported in ConeTec (1999) must be recalibrated to agree with the soil classifications determined based on samples obtained in the borings and tested in the laboratory. Figure 2.6-30, Sheets 1 through 6, present comparisons of the boring and laboratory soil classifications plotted vs elevation alongside the soil behavior type data from nearby cone penetration tests. These figures illustrate that the soil behavior type values reported in ConeTec (1999) that are greater than 5 (i.e., sandier soils), as well

as some of those equal to 5 (i.e., clayey silts), typically should be adjusted downward one or two zones to more accurately reflect the soil classifications that were determined based on the borings and confirmed by the laboratory tests performed specifically for the purpose of classifying the soil types. The following discussion is included to demonstrate that even if these soils are cohesionless, the estimated settlements will be much less than those reported above assuming that the entire upper layer at the site was comprised of soils whose compressibilities are similar to those measured in consolidation tests performed on samples obtained at a depth of 10 to 12 ft.

A review of the CPT data (ConeTec, 1999) indicates that most of the soil behavior type (SBT) values represent soils whose behavior is similar to that of "sandy" soils. As indicated in Figure 5 of ConeTec (1999), these include SBT values that are greater than 5. A map was produced to show the thickness of those soils for which the soil behavior type values are greater than 5. The purpose of this map is to readily identify those areas where the subsurface profile differs from the assumption that the soils in the upper layer (~25 to 30 ft) are predominantly cohesive soils.

This map, titled "Contour Map Showing Thickness of Soils with CPT Soil Behavior Type > 5 (Sandy)", is included as Figure 2.6-29. The thickness of the soils beneath the cask storage pads that behave as "sandy" soils based on the CPT data are posted under the CPT identifiers shown on this plan view of the site. These values were calculated by subtracting the top three feet, to account for the proposed depth of the pads, as well as the total thickness of all zones where the SBT values were found to be less than 6, from the total depth of the CPT. The thicknesses were contoured to facilitate interpretation of the SBT > 5 data obtained in the CPT program. As indicated in the figure, the thickness of the soils that behave as sandy soils (SBT>5) based on the CPT data ranges from 13.8 feet at CPT-15, near the center of the pad emplacement area, to a

high of 26.4 feet at CPT-33 near the center of the western edge of the pad emplacement area. The thicknesses are generally about 20 to 25 feet.

Calculation 05996.02-G(B)-3 (SWEC, 1999e) incorporated the calculation of settlements for the soils whose behavior is similar to that of "sandy" soils based on the CPT data. In this analysis, settlements are calculated based on Equation 6-17 of Lunne, Robertson, and Powell (1997), which was developed by Schmertmann (1970, 1978). This method is applicable for estimating settlements of foundations over sand using CPT data. The Schmertmann method takes into account the depth of footing, time of loading (40 years was used in the analysis), shape of the footing, and strain influence factor, which varies with depth. The equivalent Young's modulus, which appears in the equation, is related to the cone penetration resistance by a factor, α . This factor is related to the degree of loading, soil density, stress history, cementation, age, grain shape, and mineralogy of the deposit. In this analysis, α was assumed to be 5, which is in the middle of the range recommended in ConeTec (1998) for aged (>1,000 years) normally consolidated sands.

Two sets of estimated settlements were calculated and are summarized in the table presented on Page 44 of the calculation. Because of the preponderance of soils whose behavior is similar to that of "sandy" soils based on the uncorrected CPT soil behavior type data, settlements were calculated assuming that the Schmertmann method is applicable to the entire upper layer. As indicated by the left-hand column of settlements reported on Page 44 of the calculation, the estimated settlements for this case varied from 0.34 inches at CPT-26 to 0.56 inches at CPT-38.

The analyses were repeated, excluding those soils whose behavior is not similar to "sandy" soils, since the Schmertmann method is applicable only for cohesionless soils. In this analysis, cohesionless soils were defined as those with SBT values greater than

5, which includes silts, sandy silts, silty sands, and sands. The estimated settlements for this case are presented in the right-hand column on Page 44 of the calculation and range from 0.24 inches at CPT-31 to 0.50 inches at CPT-10.

These results are posted on the map showing the locations of the CPTs on Page 46 of the calculation. As indicated, the differential settlements between CPT locations average less than 0.1 inches. The maximum difference between two adjacent (diagonally) CPTs is 0.19 inches, CPT-34 to CPT-29. Total and differential settlements of this magnitude are not significant in the design or performance of the cask storage pads. These results confirm that if the soils are actually "sandy" soils, as indicated by the uncorrected SBTs from the cone penetration testing (ConeTec, 1999), then the estimated settlements will be much less than those reported above assuming that the entire upper layer at the site was comprised of soils whose compressibilities are similar to those measured in consolidation tests performed on samples obtained at a depth of 10 to 12 ft.

Dynamic Bearing Capacity of the Cask Storage Pads

The dynamic bearing capacity of the cask storage pads was analyzed in Calculation 05996.02-G(B)-4 (SWEC, 2001b) using two different sets of dynamic forces. The dynamic forces used in the first set of analyses were the inertial forces applicable for the peak ground accelerations from the design basis ground motion. The second set of analyses used the maximum dynamic cask driving forces developed for use in the design of the pads in Calculation 05996.02-G(PO17)-2 (CEC, 2001) for the pad supporting 2 casks, 4 casks, and 8 casks. These latter dynamic forces represent the maximum force occurring at any time during the earthquake at each node in the model used to represent the cask storage pads. These forces, therefore, represent an upper bound of the dynamic forces that could act at the base of the pad. As in the structural analyses discussed in Section 4.7.1.5.3, "Structural Analysis," the seismic loads used in these analyses were combined using 100% of the enveloped zero period accelerations

(ZPA) in one direction with 40% of the enveloped ZPA in each of the other two directions.

Table 2.6-7 presents the results of the bearing capacity analyses for the following cases, which include static loads plus inertial forces due to the earthquake. Because the *in situ* fine-grained soils are not expected to fully drain during the rapid cycling of load during the earthquake, these cases are analyzed using the undrained strength that was measured in unconsolidated- undrained triaxial tests ($\phi = 0^\circ$ and $c = 2.2$ ksf). As indicated above, for these cases including dynamic loads from the design basis ground motion, the minimum acceptable factor of safety is 1.1.

Case II	100%	N-S direction,	0%	Vertical direction,	100%	E-W direction.
Case IIIA	40%	N-S direction,	-100%	Vertical direction,	40%	E-W direction.
Case IIIB	40%	N-S direction,	-40%	Vertical direction,	100%	E-W direction.
Case IIIC	100%	N-S direction,	-40%	Vertical direction,	40%	E-W direction.
Case IVA	40%	N-S direction,	100%	Vertical direction,	40%	E-W direction.
Case IVB	40%	N-S direction,	40%	Vertical direction,	100%	E-W direction.
Case IVC	100%	N-S direction,	40%	Vertical direction,	40%	E-W direction.

As indicated in Table 2.6-7, the minimum gross allowable bearing pressure for the cask storage pads to obtain a factor of safety of 1.1 against a shear failure from static loads plus the inertial loads due to the design basis ground motion is 4.8 ksf for all loading cases identified above. The minimum allowable value was obtained for Load Case II, wherein 100% of the earthquake loads were assumed to act in both horizontal directions at the same time and the vertical earthquake load was assumed to be 0. Combining the three components of the earthquake in accordance with ASCE (1986), the minimum allowable value was obtained for Load Case IIIB, wherein 100% of the earthquake loads act in the E-W direction, 40% acts in the N-S direction, and 40% acts in the vertical direction. The actual factor of safety for this condition is 1.2, which is greater than the criterion for dynamic bearing capacity ($FS \geq 1.1$).

In these dynamic bearing capacity analyses, the dynamic forces were based on the inertial forces due to the earthquake. The total vertical force shown in Table 2.6-7 includes the static weight of the pad and 8 fully loaded casks \pm the vertical inertial forces due to the earthquake. The vertical inertial force is calculated as $a_v \times [\text{pad} + \text{cask dead loads}]$, multiplied by the appropriate factor ($\pm 40\%$ or $\pm 100\%$) for the load case. In these analyses, the minus sign for the percent loading in the vertical direction signifies uplift forces, which tend to unload the pad. Similarly, the horizontal inertial forces are calculated as $a_h \times [\text{pad} + \text{cask dead loads}]$, multiplied by the appropriate factor (40% or 100%) for the load case. The horizontal inertial force from the casks was confirmed to be less than the maximum force that can be transmitted from the cask to the pad through friction for each of these load cases. This friction force was calculated based on the upper-bound value of the coefficient of friction between the casks and the storage pad considered in the HI-STORM cask stability analysis ($\mu = 0.8$, as shown in Section 8.2.1.2, Accident Analysis) \times the normal force acting between the casks and the pad.

The lower-bound friction case (discussed in Section 4.2.3.5.1B), wherein μ between the steel bottom of the cask and the top of the concrete storage pad = 0.2, results in lower horizontal forces being applied at the top of the pad. This decreases the inclination of the load applied to the pad, which results in increased bearing capacity. Therefore, bearing capacity analyses are not performed for $\mu = 0.2$ in Calculation 05996.02-G(B)-04 (SWEC, 2001b).

Table 2.6-8 presents a summary of the bearing capacity analyses that were performed using the maximum dynamic cask driving forces developed for use in the design of the pads in Calculation 05996.02-G(PO17)-2 (CEC, 2001) for the pad supporting 2 casks, 4 casks, and 8 casks. As indicated in this table, the gross allowable bearing pressure for the cask storage pads to obtain a factor of safety of 1.1 against a shear failure from

static loads plus the very conservative maximum dynamic cask driving forces due to the design basis ground motion is at least 10.5 ksf for the 2-cask, 4-cask, and 8-cask loading cases. The minimum allowable value was obtained for the 8-cask loading. The actual factor of safety for this case was 1.6, which is greater than the criterion for dynamic bearing capacity ($FS \geq 1.1$).

As indicated above, these maximum dynamic cask driving forces represent the upper bound of the dynamic forces that could act at the base of the pad. The horizontal forces from the casks were confirmed to be less than the maximum force that can be transmitted from the cask to the pad through friction acting at the base of the cask for each of these load cases. This friction force was calculated based on the upper-bound value of the coefficient of friction between the casks and the storage pad ($\mu = 0.8$, as shown in Section 8.2.1.2) x the normal force acting between the casks and the pad. These maximum dynamic cask driving forces can be transmitted to the pad through friction only when the inertial vertical forces act downward; therefore, these analyses are performed only for Load Case IVA. The width (30 ft) is less in the E-W direction than the length N-S (67 ft); therefore, the E-W direction is the critical direction with respect to a bearing capacity failure.

Because of the nature of the subsurface materials, dynamic settlements due to the design basis ground motion are not expected to occur. See Section 2.6.4.7 for more details.

Overturning Stability of the Cask Storage Pads

The factor of safety against overturning is defined as:

$$FS_{OT} = \Sigma M_{Resisting} \div \Sigma M_{Driving}$$

The resisting moment is calculated as the net effective weight of the pad and casks x the distance from one edge of the pad to the center of the pad in the direction of the minimum width. The net effective weight of the pad and casks is the static weight of pad and casks plus and minus the inertial force due to earthquake. The weight of the pad is calculated as 3 ft x 67 ft x 30 ft x 0.15 kips/ft³ = 905 K, and the weight of 8 casks is 8 x 356.5 K/cask = 2,852 K. The moment arm for the resisting moment equals ½ of 30 ft, or 15 ft. Therefore,

$$\Sigma M_{\text{Resisting}} = (1-0.695) \times [905 \text{ K} + 2,852\text{K}] \times 15 \text{ ft} = 17,188 \text{ ft-K.}$$

The driving moment includes the moments due to the horizontal inertial force of the pad x ½ the height of the pad and the horizontal force from the casks acting at the top of the pad x the height of the pad. The casks are simply resting on the top of the pads; therefore, this force cannot exceed the friction force acting between the steel bottom of the cask and the top of the concrete storage pad. This friction force was calculated based on the upper-bound value of the coefficient of friction between the casks and the storage pad ($\mu = 0.8$, as shown in Section 8.2.1.2) x the normal force acting between the casks and the pad. This force is maximum when the vertical inertial force due to the earthquake acts downward. However, when the vertical force from the earthquake acts downward, it acts in the same direction as the weight, tending to stabilize the structure. Therefore, the minimum factor of safety against overturning will occur when the dynamic vertical force acts in the upward direction, tending to unload the pad.

When the vertical inertial force due to the earthquake acts upward, the friction force between the casks and the storage pad = $0.8 \times (2,852\text{K} - 0.695 \times 2,852\text{K}) = 696 \text{ K}$. This is less than the maximum dynamic cask horizontal driving force of 2,212 K (Table D-1(c) in CEC, 2001). Therefore, the worst-case horizontal force that can occur when the vertical earthquake force acts upward is limited by the upper-bound value of the

coefficient of friction between the bottom of the casks and the top of the storage pad, and it equals 696K. Recalling that the pad height is 3 ft,

$$\Sigma M_{\text{Driving}} = 1.5 \text{ ft} \times 0.711 \times 905 \text{ K} + 3 \text{ ft} \times 696 \text{ K} = 3,050 \text{ ft-K.}$$

Therefore, $FS_{\text{OT}} = 17,188 \div 3050 = 5.63$

This is greater than the factor of safety criterion of 1.1; therefore, the cask storage pads have an adequate factor of safety against overturning due to dynamic loadings from the design basis ground motion.

Sliding Stability of the Cask Storage Pads

The sliding stability analyses of the cask storage pads are presented in Calculation 05996.02-G(B)-4 (SWEC, 2001b). These pads will be constructed on and within soil cement, as illustrated in Figure 4.2-7 and described in Sections 2.6.1.7 and 2.6.4.11. The following section discusses the sliding stability of these pads embedded in soil cement and demonstrates that embedding them in soil cement will greatly enhance their resistance to sliding due to dynamic loads from the design basis ground motion.

Subsequent sections demonstrate that sliding will not occur along deeper surfaces within the profile underlying the cask storage pads. First, the sliding resistance of the *in situ* silty clay/clayey silt layer is addressed to demonstrate that sliding will not occur along the interface between the bottom of the soil cement and those soils. As shown in the pad emplacement area foundation profiles (Figure 2.6-5), a layer, composed in part of sandy silt, underlies the clayey layer at a depth of about 10 ft below the cask storage pads. Sandy silts oftentimes are cohesionless; therefore, the subsequent section addresses the possibility that sliding may occur along a deep slip plane at the clayey soil/sandy soil interface as a result of the earthquake forces.

These analyses demonstrate there is an adequate factor of safety against sliding of the cask storage pads and along deeper surfaces beneath the storage pads due to the maximum loadings of design basis ground motion.

Sliding Stability of the Cask Storage Pads Founded on and Within Soil Cement

The cask storage pads will be constructed on and within soil cement, as shown in Figure 4.2-7. The analysis of sliding stability of the cask storage pads embedded in soil cement is included in Calculation 05996.02-G(B)-4 (SWEC, 2001b). This analysis demonstrates that the static, undrained strength of the in situ clayey soils is sufficient to preclude sliding (FS = 1.27 vs minimum required value of 1.1), provided that the full strength of the clayey soils is engaged.

The soil-cement layer beneath the pads provides an "engineered mechanism" to ensure that the full, static, undrained strength of the clayey soils is engaged in resisting sliding forces. This soil cement will be designed to have a minimum unconfined compressive strength of 40 psi. The bond between this soil-cement layer and the base of the concrete pad will be stronger than the static, undrained strength of the in situ clayey soils. The factor of safety against sliding between the concrete at the base of the pad and the surface of the underlying soil cement is greater than 1.98, which exceeds the factor of safety between the bottom of the soil cement and the underlying clayey soils. Therefore, the minimum factor of safety against sliding of the overall cask storage pad design is at least 1.27.

As indicated in Figure 4.2-7, the soil cement will extend at least 1 ft below all of the cask storage pads. As shown in Figure 2.6-5, the pad emplacement area foundation profiles, it typically will nominally extend 2 ft below the bottoms of the pads (it will be a

minimum of 1 ft thick and shall have a maximum thickness of 2 ft). Shear resistance will be transferred through the approximately 2-ft thick soil-cement layer and into the underlying silty clay/clayey silt subgrade. Additional resistance will be provided by the continuous layer of soil cement under and between the pads; thus, the area available to resist sliding will greatly exceed that of the embedded portion of the pads alone, as was used in the analysis described above. Shear resistance requirements at the soil cement/clayey silt interface, therefore, will be lower than those required to construct the pads directly on the silty clay/clayey silt without the proposed soil-cement layer.

The soil cement will have higher shear strength than the underlying silty clay/clayey silt layer; therefore, the resistance to sliding on that interface will be limited by the shear strength of the silty clay/clayey silt. Direct shear tests on samples of the soils from the pad emplacement area (presented in Attachments 7 and 8 of Appendix 2A) indicate the shear strength available to resist sliding from loads due to the design basis ground motion is 2.1 ksf, as shown in Figure 7 of Calc 05996.02-G(B)-5 (SWEC, 2000c). The following section indicates that there is an adequate factor of safety against sliding of the pads, postulating that they are constructed directly on the silty clay/clayey silt and neglecting the passive resistance provided by the soil cement that will be surrounding the pads. The factor of safety against sliding along the soil cement/silty clay interface will be much greater than this, because the shearing resistance will be available over the areas between the pads, as well as under the pads, and additional passive resistance will be provided by the continuous soil cement layer existing below the pads. Therefore, the soil cement will greatly improve the sliding stability of the cask storage pads.

Since the resistance to sliding of the cask storage pads is provided by the strength of the bond at the interface between the concrete pad and the underlying soil cement and by the bond between the soil cement under the pad and the in situ clayey soils, the sliding stability of the pads at the end of each column or row of pads are no

different than that of the other pads. Therefore, the pads along the perimeter of the pad emplacement area also have an adequate factor of safety against sliding. Further, the soil-cement layer is continuous throughout the pad emplacement area; therefore, the area available to resist sliding of an entire column of pads greatly exceeds the sum of the areas of only the pads in the column. The factor of safety against sliding of an entire column of pads will, therefore, exceed that of an individual pad.

Sliding Stability of the Interface Between the Soil Cement and the Silty Clay/Clayey Silt Underlying the Cask Storage Pads

The sliding stability of the interface between the soil cement and the in situ silty clay/clayey silt layer underlying cask storage pads is presented in Calculation 05996.02-G(B)-4 (SWEC, 2001b). The sliding stability of this interface is demonstrated by ignoring the presence of the soil cement and demonstrating that the factor of safety against sliding of the pads supported directly on the in situ clayey soils is 1.27, which provides an adequate margin against sliding. As discussed above, the soil cement will distribute the loads from the earthquake deeper into the profile, spreading them out over an area that is much greater than that of the pads. Thus, the shear resistance requirements at the bottom of the soil cement will be less than would be required if the pads were constructed directly on the clayey soils. Therefore, sliding will not occur along the interface between the soil cement and the in situ clayey soils.

In these analyses, the factor of safety (FS) against sliding is defined as:

$$FS = \text{resisting force} \div \text{driving force}$$

The resisting force, or tangential (T) shear force, below the base of the pad is defined as:

$$T = N \tan \phi + c B L$$

where, N = normal force

$\phi = 0^\circ$ (for Silty Clay/Clayey Silt)

$c = 2.1$ ksf, as indicated on Figure 7 of SWEC (2000c) for normal stress equal to the vertical stress at the bottom of the fully loaded pads

$B = 30$ feet

$L = 67$ feet

Material directly under and around the pad will be soil cement. In this analysis, however, the presence of the soil cement adjacent to the sides of the pads is ignored to demonstrate that there is an acceptable factor of safety against sliding of the pads along the interface between in situ clayey soils and bottom of soil cement beneath the pads. The potential failure mode is sliding along the surface at the base of the pad. No credit is taken for the passive resistance acting on the sides of the pad above the base. This analysis is applicable for any of the pads at the site, including those at the ends of the rows or columns of pads, since it relies only on the strength of the material beneath the pads to resist sliding.

This analysis conservatively assumes that 100% of the dynamic forces due to the earthquake act in both the horizontal and vertical directions at the same time. The length of the pad in the N-S direction (67 ft) is greater than twice the width in the E-W direction (30 ft); therefore, the dynamic active earth pressures acting on the length of the pad will be greater than those acting on the width, and the critical direction for sliding will be E-W, since passive resistance is ignored.

The soil cement is assumed to have the following properties in calculation of the dynamic active earth pressure acting on the pad from the soil cement above the base of the pad:

$\gamma = 100-110$ pcf Initial results of the soil-cement testing indicate that 110 pcf is a reasonable lower-bound value for the total unit weight of the soil cement adjacent to the pads and that 100 pcf is a reasonable lower-

bound value for the total unit weight of the cement-treated soil to be placed beneath the pads.

$\phi = 40^\circ$

Tables 5 & 6 of Nussbaum & Colley (1971) indicate that ϕ exceeds 40° for all A-4 soils (CL & ML, similar to the eolian silts at the site) treated with cement; therefore, it is likely that ϕ will be higher than this value. This value is not used, however, in this analysis for calculating sliding resistance. It also is used in this analysis only for determining upper-bound estimates of the active earth pressure acting on the pad due to the design basis ground motion.

H = 3 ft

As shown in Figure 4.2-7, the pad is 3 ft thick, and it is constructed such that top of the pad is at the final ground surface (i.e., pads are embedded 3' below grade). Soil cement beneath the pad is 1-ft to 2-ft thick. The dynamic forces (active earth pressure + horizontal inertial forces) are greater for deeper depth of soil cement. Therefore, analyze for 2 ft of soil cement beneath the pad. The depth of the pad is used in this analysis for calculating the maximum dynamic lateral earth pressure.

The value of c is based on the results of the direct shear tests that were performed on specimens obtained from a depth of 5 to 6.3 ft from Sample U-1 in Boring C-2, which was drilled in the pad emplacement area. These test results are consistent with the results obtained from the direct shear tests that were performed on samples obtained from within the Canister Transfer Building area (Borings CTB-6 and CTB-S). All of these direct shear test results are reported in Attachments 7 and 8 of Appendix 2A.

The sliding stability was checked for Load Cases III and IV, conservatively assuming that 100% of the dynamic forces due to the earthquake act in both the N-S and Vertical directions at the same time. In determining the resisting forces in these analyses, no credit is taken for passive resistance acting on the embedded pad. The resulting factor of safety was ~2.3 for Load Case III and 1.27 for Load Case IV, which provides an adequate margin against sliding.

The horizontal force that can be applied to the top of the pad by the casks is limited to the maximum value of the coefficient of friction between the cask and the top of the pad, which equals 0.8, multiplied by the cask normal force. For Load Case III, the maximum frictional force was much less than the maximum cask driving force. Therefore, the sliding stability also was checked for Load Case IV, which has the dynamic forces due to the earthquake acting downward. With the earthquake force acting downward, the frictional force that can be transmitted from the casks to the top of the pad is large enough to transmit the maximum cask driving force.

The horizontal driving force in these analyses includes the inertial forces of the pad and the soil cement beneath the pad and the maximum cask driving forces reported in Calculation 05996.02-G(PO17)-2 (CEC, 2001) that are due to the PSHA 2,000-yr return period earthquake. The dynamic loads due to soil pressures acting on the embedded pad were also included, calculated based on the Mononobe-Okabe method, as described in Seed and Whitman (1970). The driving forces were calculated based on the peak vertical and peak horizontal accelerations; i.e., no credit was taken for the fact that these peaks are not expected to occur at different times.

The driving force due to dynamic active earth pressures acting on the pad in the E-W direction is greater than that acting in the N-S direction, because the dimension of the pad in the N-S direction (67 ft) is greater than twice the width in the E-W direction (30 ft). The maximum dynamic cask driving force also acts in the E-W direction; however,

the maximum horizontal force that can be applied to the top of the pad by the casks is limited to the maximum value of the coefficient of friction between the cask and the top of the pad, which equals 0.8, multiplied by the cask normal force. Therefore, ignoring passive resistance, sliding will be more critical in the E-W direction.

As indicated above, these analyses are very conservative for a number of reasons. They combine the maximum horizontal and vertical forces of the earthquake, rather than using reduced values to account for the fact that the peaks in these motions are not expected to occur at the same time. They also conservatively use the shear strength measured in the static direct shear tests; i.e., no credit is taken for the increase in this strength that is applicable for dynamic loadings, as discussed in Section 2.6.1.11.5, "Dynamic Strength of Cohesive Soils." Therefore, these analyses yield lower-bound factors of safety against sliding where the pads are supported on clayey soils. Even with these conservative assumptions, the factor of safety against sliding exceeds the minimum allowable value of 1.1; therefore the pads overlying 2 ft of soil cement are stable with respect to sliding, assuming the strength of the soil cement underlying the pad is at least as high as the undrained strength of the underlying soils.

These analyses illustrate that if the cask storage pads were constructed directly on the silty clay/clayey silt layer, they would have an adequate factor of safety against sliding due to loads from the design basis ground motion. Because the soil cement is continuous between the pads, its interface with the silty clay will be much larger than that provided by the footprint of the pads and used in the analyses described above. The soil cement will be mixed and compacted into the surface of the silty clay, providing a bond at the interface that will exceed the strength of the silty clay. Therefore, this interface will have more resistance to sliding than is included in these analyses and, thus, there will be adequate resistance at this interface to preclude sliding of the pads due to the loads from the design basis ground motion.

Adhesion between the Base of Pad and Underlying Clayey Soils

The analysis described above demonstrates that the static undrained strength of the soils underlying the pads is sufficient to preclude sliding of the cask storage pads over 2 ft of soil cement for the 2,000-yr return period earthquake with a peak horizontal ground acceleration of 0.711g, conservatively ignoring the passive resistance acting on the sides of the pads. This analysis assumes that the full static undrained strength of the clay is engaged to resist sliding. To obtain the minimum factor of safety required against sliding of 1.1, 76% ($= 1.60 \text{ ksf (required for FS=1.1)} \div 2.1 \text{ ksf available}$) of the undrained shear strength must be engaged, or in other words, the adhesion factor between the base of the concrete storage pads plus 2 ft of soil cement and the surface of the underlying clayey soils must be 0.76. This adhesion factor, c_a , is higher than would normally be used, considering disturbance that may occur to the surface of the subgrade during construction. Therefore, an "engineered mechanism" is required to ensure that the full strength of the clayey soils is available to resist sliding of these pads on 2 ft of soil cement.

Ordinarily, a foundation key would be added to extend the shear plane below the disturbed zone and to ensure that the full strength of the clayey soils are available to resist sliding forces. However, adding a key to the base of the storage pads would increase the stiffness of the foundation to such a degree that it would exceed the target hardness limitation of the hypothetical cask tipover analysis. Therefore, PFS decided to construct the cask storage pads on (and within) a layer of soil cement constructed throughout the entire pad emplacement area.

As shown in Figure 4.2-7, the soil cement will extend to the bottom of the eolian silt or a minimum of 1 ft below the base of the storage pads and up the vertical face at least 2 ft.

In the sliding stability analysis, it is required that the following interfaces be strong enough to resist the sliding forces due to the design earthquake. Working from the bottom up, these include:

1. The interface between the in situ clayey soils and the bottom of the soil cement, and
2. The top of the soil cement and the bottom of the concrete storage pad.

The purpose of soil cement below the pads is to provide the "engineered mechanism" required to effectively transmit the sliding forces down into the underlying clayey soils. The techniques used to construct soil cement are such that the bond between the soil cement and the underlying clayey soils will exceed the undrained strength of the underlying clayey soils.

The shear strength available at each of the interfaces applicable to resisting sliding of the cask storage pads will exceed the undrained strength of the underlying clayey soils. PFS has committed to performing laboratory tests during the design of the soil cement to demonstrate that the required shear strengths can be achieved at the various interfaces, and PFS has committed to performing field tests during construction to demonstrate that the required shear strengths at these interfaces have been achieved.

The soil cement beneath the pads is used as an "engineered mechanism" to ensure that the full static undrained shear strength of the underlying clayey soils is engaged to resist sliding and, as shown above, the minimum factor of safety against sliding of the pads is very conservatively calculated as 1.27 when the static undrained strength of the clayey soils is fully engaged. This value exceeds the minimum value required for the factor of safety against sliding ($=1.1$); therefore, the pads constructed on top of a layer of soil cement have an adequate factor of safety against sliding. See Section 2.6.4.11 for additional details concerning the use of soil cement.

Limitation of Strength of Soil Cement Beneath the Pads

As indicated in Figure 4-2-7, the soil cement will extend at least 1 ft below the storage pads over the entire pad emplacement area, and, as shown in Figures 2.6-5, Pad Emplacement Area Foundation Profiles, it will typically extend ~2 ft below most of the

pads. Thus, the area available to resist sliding will greatly exceed that of the pads alone. The hypothetical cask tipover analysis imposes limitations on the modulus of elasticity of the soils underlying the pad. The modulus of elasticity of the soil cement is directly related to its strength; therefore, its strength must be limited to values that will satisfy the modulus requirement, but it must still provide an adequate factor of safety with respect to sliding of the pads embedded within the soil cement.

Table 5-6 of Bowles (1996) indicates $E = 1,500 s_u$, where s_u = the undrained shear strength. Note, s_u is half of q_u , the unconfined compressive strength.

Based on this relationship, $E = 750 q_u$,

Where E = Young's modulus
 q_u = Unconfined compressive strength

An unconfined compressive strength of 100 psi for the soil cement under the pad will limit the modulus value to 75,000 psi. Thus, designing the soil cement to have an unconfined compressive strength that ranges from 40 psi to 100 psi will provide an adequate factor of safety against sliding and will limit the modulus of the soil cement under the pads to an acceptable level for the hypothetical cask tipover considerations.

Sliding Along Contact Between the Concrete Pad and the Underlying Soil Cement

The soil cement will be designed to have an unconfined compressive strength of at least 40 psi to ensure that it will be stronger than required to provide a factor of safety against sliding that exceeds the required minimum value of 1.1. The shear strength equals half of the unconfined compressive strength, 20 psi, which equals 2.88 ksf. Therefore, the resistance to sliding between the concrete storage pad and the top of the soil cement layer beneath the pad will be greater than:

$$T = \frac{N}{\phi} + c \cdot B \cdot L \cdot T = 6,368 \text{ K} \times \tan 0^\circ + 2.88 \text{ ksf} \times 30 \text{ ft} \times 67 \text{ ft} = 5,789 \text{ K}$$

As indicated above, the driving force, V , is defined as: $V = F_{AE} + EQ_{hp} + EQ_{hc}$

The factor of safety against sliding between the pad and the surface of the underlying soil cement is calculated as the resisting force \div the driving force, as follows:

$$FS_{\text{Pad to Soil Cement}} = \frac{T}{F_{AE\ E-W} + EQ_{hp} + EQ_{hc\ E-W}} = \frac{5,789\text{ K}}{(65.3\text{ K} + 643\text{ K} + 2,212\text{ K})} = \frac{5,789\text{ K}}{2,920.3\text{ K}} = 1.98$$

Thus, designing the soil cement to have an unconfined compressive strength of at least 40 psi results in an acceptable factor of safety against sliding between the concrete at the base of the pad and the surface of the underlying soil cement that exceeds the factor of safety between the bottom of the soil cement and the underlying clayey soils. In other words, the soil cement will have higher strength than the underlying silty clay/clayey silt layer; therefore, the resistance to sliding on that interface will be limited by the strength of the silty clay/clayey silt.

Soil cement with strengths higher than this are readily achievable, as illustrated by the lowest curve in Figure 4.2 of ACI 230.1R-90, which applies for fine-grained soils similar to the eolian silt in the pad emplacement area. Note, $f_c = 40C$ where C = percent cement in the soil cement. Therefore, to obtain $f_c > 40$ psi, the percentage of cement required would be $\sim 40/40 = 1\%$. This is even less cement than would typically be used in constructing soil cement for use as road base. The resulting material will more likely be properly classified as a cement-treated soil, rather than a true soil cement. Because this material is located below the frost zone (which is only 30" below grade at the site), it does not need to comply with the durability requirements of soil cement; i.e., ASTM freeze/thaw and wet/dry tests. The design of the mix for this material will require that the unconfined compressive strength of this layer of material will exceed 40 psi to ensure that the shear strength available to resist sliding of the concrete pads exceeds the shear strength of the in situ clayey soils.

Soil Cement Above the Base of the Pads

Soil cement also will be placed between the cask storage pads, above the base of the pads. Revision 7 of Calculation 05996.02-G(B)-4 (SWEC, 2001b), demonstrated that this soil cement could be designed such that its compressive strength alone would be sufficient to resist all of the sliding forces due to the design earthquake. However, as shown above, this soil cement is NOT required to resist sliding of the pads, because there is sufficient shear strength at the interfaces between the concrete pad and the underlying soil cement and between that soil cement and the underlying clayey soils that the factor of safety against sliding exceeds the minimum required value. The pads are being surrounded with soil cement so that PFS can effectively use the eolian silt found at the site to provide an adequate subbase for support of the cask transporter. The eolian silt, otherwise, would be inadequate for this purpose and would require replacement with imported structural fill. The soil cement surrounding the pad may also help to spread the seismic load into the clayey soil outside the pad area to engage additional resistance against sliding of the pad. This effect would result in an increase in the factor of safety against sliding.

The unconfined compressive strength of the soil cement adjacent to the pads needs to be at least 50 psi to provide an adequate subbase for support of the cask transporter, in lieu of placing and compacting structural fill, but it likely will be at least 250 psi to satisfy the durability requirements associated with environmental considerations (i.e., freeze/thaw and wet/dry cycles) within the frost zone (30 in. from the ground surface).

The beneficial effect of this soil cement on the factor of safety against sliding is demonstrated on page 29 and 30 of Calculation 05996.02-G(B)-4 (SWEC, 2001b). The factor of safety against sliding in the north-south direction increases from 1.5 to 2.3 when the passive resistance of the soil cement above the base of the pads is included, and the factor of safety against sliding in the east-west direction increases to

3.3. Therefore, adding the soil cement adjacent to the pads does enhance the sliding stability of each pad.

Sliding Stability of the Cask Storage Pads on Cohesionless Soils

Adequate factors of safety against sliding due to maximum forces from the design basis ground motion have been obtained for the storage pads founded directly on the silty clay/clayey silt layer, conservatively ignoring the passive resistance of the soil cement that will be placed under and adjacent to the pads. The shearing resistance is provided by the cohesive portion of the shear strength of the silty clay/clayey silt layer, which is not affected by upward earthquake loads. As shown in Figure 2.6-5, Pad Emplacement Area – Foundation Profiles, a layer, composed in part of sandy silt, underlies the clayey layer at a depth of about 10 ft below the cask storage pads. Sandy silts oftentimes are cohesionless; therefore, to be conservative, the sliding stability of the cask storage pads was analyzed assuming that the soils in this layer are cohesionless, ignoring the effects of cementation that were observed on many of the split-spoon and thin-walled tube samples obtained in the drilling programs.

The CPT results (ConeTec, 1999) indicate the presence of a layer of soils that behave like silty sands and sands under the clayey layer at a depth of about 10 ft. Note, however, that recalibrating the SBTs as discussed in Section 2.6.1.6 results in most of these silty sands and sands being more correctly identified as clayey silt/silt with some sandy silt, as shown in Sheets 2 through 14 of Figure 2.6-5. The plots included in Appendix D of ConeTec, 1999) indicate that s_u , the undrained shear strength, or the

THIS PAGE INTENTIONALLY LEFT BLANK

cohesion, drops to 0 and that ϕ is generally greater than 35 to 40° for these soils. If the cohesion available to resist sliding drops to 0 and cementation effects are ignored, the shearing resistance of this layer is directly related to the normal stress.

Analyses were performed to address the possibility that sliding may occur along a deep slip plane at the clayey soil/sandy soil interface as a result of the earthquake forces. To simplify the analysis, it was assumed that cohesionless soils extend above the 10 ft depth and, thus, the pads are founded directly on cohesionless materials. In this analysis, a friction angle of 30° was used to define the strength of the soils to conservatively model a loose cohesionless layer, even though the values measured in the CPTs generally were greater than of 35 to 40°. Without cohesion and ignoring passive resistance acting against the side of the pad, the resistance to sliding is calculated as $N \tan 30^\circ$, or 0.58 N, where N is the normal force. Because of the magnitude of the peak ground accelerations (0.695g) due to the design basis ground motion at this site, the frictional resistance available when N is reduced due to the uplift from the inertial forces applicable for the vertical component of the design basis ground motion is not sufficient to resist sliding. However, analyses were performed to estimate the amount of displacement that might occur due to the design basis ground motion for this case. These analyses, based on the method of estimating displacements of dams and embankments during earthquakes developed by Newmark (1965), indicate that even if these soils are cohesionless and even if they are conservatively located directly at the base of the pads, the estimated displacements would be less than 2.2 inches. Whereas there are no connections between the ground and these pads or between the pads and other structures, this minor amount of displacement would not adversely affect the performance of these structures.

retain its structural integrity and the performance of the structure will not be adversely affected.

Chapter 4 describes the structural analyses of the Canister Transfer Building. The analyses used a finite element model approach and considered the effects of soil-structure interaction. The structural analyses take into account the flexibility of the foundation underlying the building by the use of finite elements with the stiffness properties of the soil. Non-uniform elastic deformation of the soil, which results in bending moments and shear forces in the base mat are accounted for. This analysis is performed in Calculation 0599602-SC-6 (SWEC, 1998a). Induced stresses resulting from these non-uniform displacements were accommodated in the design of the structure.

The Canister Transfer Building is a large and massive building consisting of exterior reinforced concrete walls 2'-0" thick, a reinforced concrete roof 1'-0" thick, and a solid

THIS PAGE INTENTIONALLY LEFT BLANK

including the weight of the block of clayey soils enclosed within the perimeter key is 97,749 K, as shown in Table 2.6-11. For overturning about the N-S axis, the moment arm for the resisting moment equals ½ of ~240 ft, or 120 ft. Therefore,

$$\Sigma M_{\text{Resisting}} = (97,749 - 79,779) \text{ K} \times 120 \text{ ft} = 2,156,400 \text{ ft-K.}$$

As indicated on page 15 of Calculation 05996.02-G(B)-13 (SWEC, 2001c), the driving moments include the 40% of $\Sigma M_{\text{N-S}}$, which is 1,082,784 ft-K, and 40% of the moment due to angular acceleration of the structure about the N-S axis which is 186,292 ft-K. The vertical force due to the earthquake can act upward or downward. However, when it acts downward, it acts in the same direction as the weight, tending to stabilize the structure. Therefore, the minimum factor of safety against overturning will occur when the maximum dynamic vertical force acts in the upward direction, tending to unload the mat and reduce the resisting moment.

The square root of the sum of the squares (SRSS) is used to combine the moments to account for the fact that the maximum responses of earthquake do not act in all three orthogonal directions and angular rotations at the same time. The moments acting about the E-W axis do not contribute to overturning about the N-S axis; therefore,

$$\Sigma M_{\text{Driving}} = \sqrt{1,082,785^2 + (186,292)^2} = 1,098,694 \text{ ft-K}$$

and
$$FS_{\text{OT}} = 2,156,400 \div 1,098,694 = 1.96$$

This is for Load Case IIIA. Calculation 05996.02-G(B)-13 (S&W, 2001c) indicates that the factor of safety against overturning for Load Cases IIIB and IIIC are greater than that for Load Case IIIA. This minimum factor of safety against overturning is greater than the criterion of 1.1; therefore, the Canister Transfer Building has an adequate

factor of safety against overturning due to dynamic loadings from the design basis ground motion.

Sliding Stability of the Canister Transfer Building

The Canister Transfer Building will be founded on clayey soils, as indicated in Figures 2.6-21 through 2.6-23. A 1.5-ft deep key will be constructed around the perimeter of the mat to ensure that the full shear strength of the clayey soils is engaged to resist sliding of the structure due to loads from the design basis ground motion. The sliding stability was evaluated in Calculation 05996.02-G(B)-13 (SWEC, 2001c) based on the loads that were developed in the soil-structure interaction analyses (Calculation 05996.02-SC-5, SWEC, 2001d). The strength of the clayey soils was based on the average of the two sets of direct shear tests performed on samples of soils obtained from beneath the CTB near the elevation proposed for the bottom of the key around the perimeter of the CTB mat. The results of these tests are included in Attachments 7 and 8 of Appendix 2A. As indicated in Section 2.6.1.11.2, this shear strength equaled 1.8 ksf for the normal stress that equals the final vertical stress at the bottom of the key following construction of the building.

This analysis assumed that the backfill to be placed around the Canister Transfer Building mat and 1.5-ft deep key would be the soil cement constructed from the eolian silt that was excavated from the area. For this 5-ft deep layer of soil cement, it is assumed that the lower-bound value of γ is 100 pcf, $\phi = 0^\circ$ & $c = 125$ psi. The passive resistance available is calculated as follows:

$$p_p = 2c$$

For 5 ft soil cement with a FS of 2.0 applied for the passive resistance, the available resistance is

$$P_p = 0.5 \times 5\text{ft} \times 2 \times 125 \text{ psi} \times 0.144 \text{ ksf/psi} = 90 \text{ k/LF}$$

Figure 5 of Calculation 05996.02-G(B)-13 (SWEC, 2001c) indicates that the CTB mat is actually 240' wide in the E-W direction and 279.5' long in the N-S direction. Therefore, the total passive force available to resist sliding is at least $240' \times 90 \text{ k/LF} = 21,600 \text{ k}$ acting in the N-S direction.

Lambe & Whitman (1969, p 165) indicate that little horizontal compression, ~0.5%, is required to reach half of full passive resistance for dense sands. The soil cement will be compacted to a dense state; therefore, this analysis assumed that one-half of the total passive resistance would be available to resist sliding of the building. Note, 0.5% of the 5 ft height of the mat + 1.5-ft deep key = $0.005 \times 6.5 \text{ ft} \times 12 \text{ in./ft} = 0.39 \text{ in.}$ Since there are no safety-related systems that would be severed or otherwise impacted by movements of this small magnitude, it is reasonable to use this passive thrust to resist sliding.

As discussed in Section 2.6.4.11, Techniques to Improve Subsurface Conditions, PFS is performing industry-standard soil cement testing to design the soil-cement mix (SWEC, 2001e), including wet/dry and freeze/thaw tests. These so-called "durability tests" are being performed specifically to ensure that the soil-cement mix to be placed within the frost zone (30" below grade at the site) will be durable enough to withstand the rigors of wetting, drying, freezing, and thawing. These tests are being performed in accordance with ASTM D559 and D560 and will measure the durability of soil cement specimens exposed to 12 cycles of wet/dry and freeze/thaw conditions. PFS is designing the soil-cement in accordance with the criteria specified by the Portland Cement Association (1971). Following these procedures will ensure that the resulting soil-cement will be able to withstand exposure to the elements, as indicated in the paragraphs cited from p. 8 of the "Soil-Cement Laboratory Handbook" (Portland Cement Association, 1971) in Section 2.6.4.11, Techniques to Improve Subsurface Conditions.

As indicated on p.10 of PFS Calculation 05996.02-G(B)-13 (SWEC, 2001c), the unconfined compressive strength of the soil cement is assumed to be 250 psi. This is consistent with the soil cement mix proposed for use within the frost zone adjacent to the cask storage pads and is based on the assumption that the strength will be at least this value to obtain a soil cement mix design that will satisfy the durability requirements of the ASTM wet/dry and freeze/thaw tests.

Further, PFS will construct the soil cement using techniques that will ensure that the bond between the layers is stronger than the shear strength of the underlying clayey soils. These standard practices in design and construction of soil cement have resulted in successful application of soil cement to more extreme environmental considerations than are applicable for this project and, thus, they will ensure that tensile cracking or shear failure does not occur along these interfaces. Therefore, PFS is considering the effects of freeze/thaw cycles on the top layers of soil cement, for both the pad emplacement area and the soil cement surrounding the CTB.

Although the sliding stability analysis of the CTB does not specifically refer to the potential for tensile or shear failure along lift interfaces within the soil cement layer, the analysis does indicate that the soil cement will be designed in accordance with the ASTM requirements for durability. There are also a number of references in Section 2.6.4.11 documenting PFS's commitment to construct the lift interfaces using techniques to ensure that the bond between soil cement layers is adequate to resist the sliding forces due to an earthquake.

The stability analysis of the Canister Transfer Building considers the horizontal displacements required to develop passive resistance from the soil cement. Pages 19 through 21 and 51 of PFS Calculation 05996.02-G(B)-13 (SWEC, 2001c) present the results of the sliding stability analysis of the Canister Transfer Building assuming that

only half of the passive resistance due to the soil cement is available to resist sliding. This is standard practice in geotechnical engineering analyses of sliding of structures where there is assurance that the material that is being relied upon to provide passive resistance will not be excavated. In this case, one-half of the passive resistance is used (p. 19), specifically, to incorporate the effects of strain-compatibility between the horizontal strains required to develop shear strength along the base of the structure and those required to develop a portion of the passive resistance along the side of the mat.

The effects of wall movement on wall pressure are defined in DM-7 (NAVFAC, 1986, p. 7.2-60) as the ratio of horizontal displacement to the height of the wall to emulate the horizontal strain as defined in Lambe and Whitman. For stiff cohesive soils, the wall rotation or yield ratio, y/H , required to fully mobilize passive resistance is 0.02, or 2%.

Based on the shear modulus estimated from the shear wave velocity of the surficial silty clay/clayey silt, the horizontal displacement of the CTB subjected to the full horizontal earthquake load is calculated to be about 1.5 inches using the elastic solution of a buried horizontal rectangle subjected to shear in an elastic half-space. This horizontal displacement corresponds to a yield ratio, defined as horizontal displacement \div height of wall, of 1.9% from translation of the 6.5 ft height of the CTB foundation mat adjacent to the soil cement. This yield ratio is larger than the yield ratio required to mobilize one half of full passive resistance for dense sand or stiff cohesive soils. However, this analysis ignores the build-up of passive resistance as the mat displaces on the elastic half-space. Recognizing that the resistance does gradually build as the foundation displaces horizontally, it is reasonable to expect that the resulting horizontal displacement will be somewhat reduced from the 1.5 inches calculated by the elastic solution. Even if the maximum horizontal displacement were to occur from an earthquake, there would be no safety consequence to the CTB since the building does not rely on any external "Important to Safety" connections.

Page 22 of PFS Calculation 05996.02-G(B)-13 (SWEC, 2001c) discusses further the horizontal displacement to induce the assumed passive resistance. It states:

"Before a complete sliding failure can occur, the full passive resistance of the soil cement must be engaged. Because the strains associated with reaching the full passive state typically are large for soils, in the analyses where the full passive resistance of the soil cement adjacent to the mat is used, the shear strength of the clayey soils under the building is reduced to a conservative estimate of the residual shear strength, based on the results of the direct shear tests.

The results of the direct shear tests, presented as plots of shear stress vs horizontal displacement in Attachment 7 of Appendix 2A of the SAR (annotated copies are included in Attachment C of this calculation), illustrate that the residual strength of these soils is nearly equal to the peak strength for those specimens that were tested at confining stresses of 2 ksf. For example, for Sample U-1C from Boring C-2, at horizontal displacements of ~0.025" past the peak strength, there is ~1.5% reduction in the shear strength indicated. The results for Sample U-1AA from Boring CTB-S showed no decrease in shear strength following the peak at ~0.025" horizontal displacement, and Samples U-3B&C from Boring CTB-6 showed a decrease of ~5%. The specimens that were tested at confining stresses of 1 ksf all show reductions of ~20% at horizontal displacements of ~0.025" past the peak.

The final effective vertical stresses at the base of the Canister Transfer Building, σ'_v , are ~1.5 ksf, now that the mat has been changed to 240 ft x

279.5 ft. This value is approximately half-way between the confining stresses of 1 and 2 ksf used for several of the direct shear tests. The residual strength of the clayey soils beneath the building are expected to show reductions from the peak strength of ~12.5%, since the final effective stresses under the building are ~1.5 ksf. Therefore, based of these results, conservatively assume that the peak strength of the clayey soils beneath the soil cement layer underlying the pads is reduced by 20% to reach residual strength, to account for horizontal straining required to reach a strain applicable to the full passive resistance of the soil cement adjacent to the pad."

The results of the sliding stability analysis of the Canister Transfer Building are presented in Table 2.6-13 and indicate that the factors of safety were ≥ 1.1 for all load combinations examined. The lowest factor of safety was 1.13, which applies for Case IIIC, where 100% of the dynamic earthquake forces acts in the north-south direction and 40% acts in the other two directions. These results assume that only one-half of the passive pressures are available to resist sliding and no credit is taken for the fact that the strength of cohesive soils increases as the rate of loading increases (Casagrande and Shannon, 1948, Das, 1993, and Schimming et al, 1966); therefore, they represent a conservative lower-bound estimate of the sliding stability of the Canister Transfer Building founded on in situ silty clay/clayey silt with 5 ft of soil cement around the building.

Sliding Stability of the Canister Transfer Building on Cohesionless Soils

The Canister Transfer Building will be founded on clayey soils that have an adequate amount of cohesive strength to resist sliding due to the dynamic forces from the design basis ground motion. As shown in Figures 2.6-21 through 2.6-23, however, some of the soils underlying the building are cohesionless within the depth zone of

about 10 to 20 ft, especially near the southern portion of the building. Analyses were performed to address the possibility that sliding may occur along a deeper slip plane at the clayey soil/sandy soil interface as a result of the earthquake forces.

These simplified analyses are presented in Calculation 05996.02-G(B)-13 (SWEC, 2001c). They were performed only for Load Cases IIIA, IIIB, and IIIC, because the resistance to sliding is greatly reduced for frictional materials when the dynamic forces due to the earthquake act upward. As described above, these load cases were defined as follows:

Case IIIA	40%	N-S direction, -100%	Vertical direction, 40%	E-W direction.
Case IIIB	40%	N-S direction, -40%	Vertical direction, 100%	E-W direction.
Case IIIC	100%	N-S direction, -40%	Vertical direction, 40%	E-W direction.

As shown in Figures 2.6-21 through 2.6-23, the top of the cohesionless layer varies from about 5 ft below the mat to about 9 ft, and it generally is at a depth of about 6 ft below the mat. These analyses included the passive resistance of the 5' soil cement and soils acting on a plane extending from grade down to the top of the cohesionless layer, plus the shear strength available at the ends of the silty clay block under the mat, plus the frictional resistance available along the top of the cohesionless layer. The weight of the clayey soils existing between the top of the cohesionless soils and the bottom of the mat was included in the normal force used to calculate the frictional resistance acting along the top of the cohesionless layer. A review of the cone penetration test results (ConeTec, 1999) obtained within the top 2 ft of the layer of nonplastic silt/silty sand/sandy silt underlying the Canister Transfer Building indicated that $\phi = 38^\circ$ was a reasonable minimum value for these soils. The factor of safety against sliding along the top of this layer was found to be >1.1 for all Load Cases IIIA, IIIB and IIIC.

These analyses include several conservative assumptions. They are based on static strengths of the silty clay block under the Canister Transfer Building mat, even though, as reported in Das (1993), experimental results indicate that the strength of cohesive soils increases as the rate of loading increases. For rates of strain applicable for the cyclic loading due to the design basis ground motion, Das indicates that for most practical cases, one can assume that $c_{u \text{ dynamic}} \sim 1.5 \times c_{u \text{ static}}$. In addition, the silty sand/sandy silt layer is not continuous under the Canister Transfer Building mat, and this analysis neglects cementation of these soils that was observed in the samples obtained in the borings. Therefore, sliding is not expected to occur along the surface of the cohesionless soils underlying the Canister Transfer Building.

THIS PAGE INTENTIONALLY LEFT BLANK

in the epicentral area and caused a mine shaft nearby to be thrown out of alignment (Stover and Coffman, 1993). The epicenter is about 48 miles southeast of the PFSF site.

There is no evidence of any effects from any historic earthquake in the PFSF site vicinity.

2.6.2.3 Determining the Design Basis Ground Motion

Federal regulations governing the requirements for siting an ISFSI are contained in 10 CFR 72. These regulations require that seismicity at an ISFSI located west of the Rocky Mountain Front, such as the PFSF, be evaluated using the criteria for determining the safe shutdown earthquake at a nuclear power plant (10 CFR 100 Appendix A) in the same area. Vibratory ground motion design bases were determined by using a "deterministic" approach based upon a single set of earthquake sources. The regulations for siting nuclear power plants (10 CFR 100.23) were amended in 1997 in order to recognize the inherent uncertainties in geologic and seismologic parameters that must be addressed in determining the seismic hazard at a nuclear power plant site. One of the ways to address these uncertainties is through a probabilistic seismic hazard analysis (PSHA). In response to the Part 100 changes and anticipated changes to Part 72 (SECY-98-126), a probabilistic seismic hazard assessment has been performed for the PFSF for vibratory ground motions and surface fault displacement. Methodologies used and the results thereof are detailed in Sections 6 and 7 and Appendix F of Geomatrix Consultants, Inc. (2001a). The hazards results are presented as mean hazard curves that incorporate the uncertainty in input data and interpretations. The seismic source model used 16 capable fault sources and 4 seismic source zones within 100 km. Clarification of the PSHA formulation is provided in SAR Appendix 2F. In addition, sensitivity analyses were performed at the request of the NRC to provide further justification of the design basis ground motions (PFS letter dated May 31, 2001). An evaluation of recent information that indicates a higher slip rate (1 mm/yr) on the

East Great Salt Lake fault, the potential linkage of the East Great Salt Lake fault with other faults, and the possibility that the Stansbury fault could rupture co-seismically with the East fault, West fault, or East-West combined fault is discussed in Appendix 2G.

The NRC staff has recommended a risk-informed graded approach in their proposed changes to 10 CFR 72 when determining the appropriate hazard frequency or return

The dynamic settlements of the nonplastic silts in this layer were estimated based on the method presented in Tokimatsu and Seed (1987). As they indicate, for soils above the groundwater table, dynamic settlements are calculated based on procedures originally developed by Silver and Seed (1971), and the effects of multidirectional shaking are estimated based on studies reported by Pyke, Seed, and Chan (1975). The dynamic settlement mechanism is compaction due to grain slip, and it is a function of the magnitude of the cyclic shear strain developed due to the earthquake, the applied number of cycles of this shear strain, and the relative density of the soils.

Figure 13 of Tokimatsu and Seed (1987) presents the relationship between volumetric strain due to compaction, cyclic shear strain, and corrected penetration resistance (N_1) of dry sands for 15 equivalent uniform strain cycles. The cyclic shear strain is estimated based on the average cyclic shear stress due to shaking caused by the design basis ground motion and the shear modulus of the soil. Figure 13 is used to estimate the volumetric strain due to compaction for 15 equivalent uniform strain cycles. Table 4 of Tokimatsu and Seed (1987) is then used to adjust for differences in the number of representative cycles of applied shear stress due to the design basis ground motion (~12 for Magnitude 7) and the 15 cycles used in Tokimatsu and Seed's studies. The dynamic settlement is calculated as the volumetric strain multiplied by the thickness of the nonplastic silts in the layer. Multidirectional effects of the earthquake are addressed by multiplying this result by 2, based on studies reported by Pyke, Seed, and Chan (1975).

The average cyclic shear stress developed in the field due to earthquake shaking is calculated as:

$$\tau_{avg} = 0.65 \cdot a_{max} \cdot \sigma_v \cdot r_d/g = 606 \text{ psf,}$$

- where: $a_{max} = 0.71$ g for the design basis ground motion
 $\sigma_v = \gamma_{total} \cdot z$ above the groundwater table
 $\gamma_{total} = 92$ pcf
 $z =$ depth below grade
 $r_d =$ stress reduction factor, which varies from 1.0 at $z=0$ to 0.9 at $z=30'$.

An iterative technique is used to determine the cyclic strain in the field due to the earthquake, γ_{field} . For an assumed value of the cyclic strain, G is calculated as $G_{max} \cdot G / G_{max}$, where G / G_{max} for the nonplastic silt is estimated using the curve for $PI=0$ presented in Figure 6 of Vucetic and Dobry (1991). G_{max} equals 2,027 ksf, based on V_s 842 fps and $\gamma_{total} \sim 92$ pcf, as indicated in Table 7 of Calc 05996.02-G(PO18)-2, (Geomatrix, 2001c) for the upper 25 to 30-ft layer. The following table presents the results of these iterations.

Determination of Cyclic Shear Strain Due to the Design Basis Ground Motion

Iteration No.	$\gamma_{assumed}$ $\times 10^{-4}$ in./in.	G / G_{max}	G ksf	γ_{field} $\times 10^{-4}$ in./in.	$\Delta\gamma$ %
1	10	0.250	507	12.0	16
2	15	0.200	405	14.9	0

The cyclic strain in the field, γ_{field} , is calculated as τ_{avg} / G . Note, it is approximately equal to the assumed cyclic strain for Iteration No. 2; therefore, additional iterations are not required, and γ_{field} is 14.9×10^{-4} in./in., or 0.149%.

The volumetric strain due to compaction from 15 cycles is estimated as a function of this cyclic shear strain and N_1 of ~28 blows/ft, based on Figure 13 of Tokimatsu & Seed (1987). This results in a volumetric strain, $\epsilon_{c,N=15}$, of 0.093%.

The design basis ground motion is magnitude 7 (Section 2.6.2.3). Table 4 of Tokimatsu & Seed (1987) indicates this corresponds to ~12 cycles of loading and that the volumetric strain ratio, $\varepsilon_{c,N=12} / \varepsilon_{c,N=15}$, should be ~0.9. Therefore, the volumetric strain corresponding to the design basis ground motion is $\varepsilon_{c,N=12}$, which is $0.9 \times 0.093\%$, or 0.084% .

$$\varepsilon_c = \frac{\Delta\rho_{\text{dyn}}}{\Delta H} \quad \text{where } \Delta\rho_{\text{dyn}} \text{ is the dynamic settlement of the layer,}$$

and ΔH is the thickness of the layer.

The thickness of the nonplastic silts in the upper layer is conservatively estimated to be 15 ft, based on the discussion presented above. Therefore, for unidirectional shaking,

$$\Delta\rho_{\text{dyn},1} = 0.15 \quad \text{inches} = 15 \text{ ft} \times 12 \text{ in./ft} \times \varepsilon_{c,N=12} / 100\%.$$

The dynamic settlement is multiplied by 2 to account for multidirectional shaking due to the earthquake. This results in an estimated dynamic settlement of the nonplastic silts in the upper layer of 0.3 inches.

Examination of these soils, which are deposits from ancient Lake Bonneville, indicates the presence of numerous tiny shells (Ostracodes). Considerable void space was present under some of these shells, and it is believed that these voids are contributing to the high, in situ void ratio measured for the clayey silt.

Calcium carbonate is present in these soils, as evidenced by a vigorous reaction upon application of hydrochloric acid to these soils. Therefore, these soils are believed to be cemented, the result of carbonate cement bonding of the silt and clay-size particles, imparting cohesion to these soils.

The void ratio of 1.9 reported in Section 2.6.1.11 was determined on samples of the clayey silts from the upper layer, not the nonplastic silts. As evidenced by the SPT data,

these nonplastic silts are not loose. The dense nature of these soils, which is most likely the result of carbonate cement bonding of the silt particles, minimizes the potential for dynamically induced settlements due to the design basis ground motion. Ignoring this cementing, the total dynamic settlement is conservatively estimated to be less than ½ of an inch.

This estimated dynamic settlement was determined based on the thickness of nonplastic silts in areas where the nonplastic silts are thickest, not on an average or median thickness. This conservatively overestimates the settlement. In addition, it conservatively neglects the fact that these nonplastic silts are stratified with layers of clay and clayey silt, which will minimize the potential for dynamically induced settlements. Thus, this estimated dynamic settlement is very conservative.

Dynamic settlements will be much less than this over most of the cask storage pad area, since most of the soils in this area are not nonplastic. Rather, these soils are sufficiently stiff and cohesive that they will not experience dynamic compaction due to the shaking caused by the design basis ground motion.

Dynamic settlements of this magnitude are not expected to adversely affect the performance of the facilities.

2.6.4.8 Liquefaction Potential

The soils underlying the proposed PFSF site are not susceptible to liquefaction as a result of the design basis ground motion because they are only partially saturated from grade down to the groundwater level at a depth of 125 ft. The upper ~30-ft thick layer of soils are typically cohesive or cemented and, being essentially dry or only partially saturated, are not subject to liquefaction. The soils from that depth down to the groundwater table at

a depth of 125 ft are similarly only partially saturated and they are very dense. The standard penetration test N-values for these soils typically exceed 100 blows per ft, and they increase with depth. The presence of this greater than 90-ft thick, very dense layer overlying the saturated soils is expected to preclude any surface manifestation of liquefaction (e.g., sand boils) of the saturated soils below the groundwater table, if it were possible for them to liquefy. Below the groundwater table, liquefaction is considered unlikely, however, because the density of the soils encountered in the borings increases with depth, as evidenced by the SPT N-values down to a depth of 226 ft in Boring CTB-1 and the high P-wave velocities (5,100 ft/sec to 5,900 ft/sec) measured for the soils below the groundwater table, reported by Geosphere Midwest, Inc. (Appendix 2B).

2.6.4.9 Design Basis Ground Motion

The design basis ground motion was determined by a probabilistic seismic hazard analysis and is defined as having a peak horizontal ground acceleration of 0.711g and a peak vertical ground acceleration of 0.695g. The development of the design basis ground motion is described in Geomatrix Consultants, Inc. (2001a and 2001b). The site specific response spectra are presented in Table 1 and Figure 4 of Geomatrix Consultants, Inc. (2001b).

2.6.4.10 Static Analyses

Refer to Section 2.6.1.12 for a detailed discussion of static analyses in the stability of foundations for structures.

2.6.4.11 Techniques to Improve Subsurface Conditions

Soil Cement

Discussions presented in Section 2.6.1.12, above, indicate that the soils underlying the eolian silt layer at the surface of the PFSF site are suitable for support of the proposed structures; therefore, no special construction techniques are required for improving the subsurface conditions below the eolian silt. The eolian silt, in its *in situ* loose state, is not suitable for founding the structures at the site. The basemat of the Canister Transfer Building will be founded on the silty clay/clayey silt layer beneath the eolian silt. It was originally intended that the cask storage pads also would be founded on the silty clay/clayey silt layer. However, instead of excavating the eolian silt from the pad emplacement area and replacing it with suitable structural fill, it will be mixed with sufficient portland cement and water and compacted to form a strong soil-cement subgrade to support the cask storage pads. Soil cement will also be utilized around the Canister Transfer Building. The required characteristics of the soil cement will be engineered during detailed design and constructed to meet the necessary strength requirements.

During construction of the storage pads, all of the eolian silt in the quadrant under construction will be excavated. The eolian silt will be mixed with sufficient cement and water and compacted to produce soil cement across the pad area, up to the design elevations of the bottoms of the storage pads. The layer of soil cement beneath the storage pads will have a minimum thickness of 12 inches and a maximum thickness of 24 inches. In the event that the eolian silt layer extends to a depth greater than 2 ft below the elevations of the bottoms of the storage pads, compacted clayey soils will be used to raise the elevation of the subgrade that will support the soil cement layer to an elevation of 2 ft or less below the design elevations of the bottoms of the pads. This will ensure that the layer of soil cement does not exceed a thickness of 2 ft. This is the

maximum permissible thickness of the soil cement layer, since the storage cask hypothetical tipover and drop analyses were performed assuming a 2.0-ft thick layer of soil cement underlying the storage pads.

Strength of Soil Cement and Minimum/Maximum Thickness Requirements

The soil cement underlying the pads shall have a minimum unconfined compressive strength of 40 psi to ensure that there is an adequate factor of safety against sliding of an entire column of pads (S&W Calculation 05996.02-G(B)-4, SWEC, 2001b). This layer of soil cement is required to be no greater than 2-ft thick and have a static modulus of elasticity less than or equal to 75,000 psi to ensure that the decelerations from a hypothetical storage cask tipover event or vertical end drop accident do not exceed HI-STORM design criteria (Section 3.2.11.3).

Following construction of the storage pads on top of this layer of soil cement, additional soil cement will be placed around and between the cask storage pads, extending from the bottoms of the pads to a level that is 28 inches above the bottoms of the storage pads. The remaining 8 inches, from the top of the soil cement up to grade, will be filled with coarse aggregate, placed and compacted to be flush with the tops of the pads to permit easy access by the cask transporter. The soil cement placed around the sides of the storage pads is expected to have a minimum unconfined compressive strength of at least 250 psi to satisfy durability requirements within the depth of frost penetration (based on S&W Calculation 05996.02-G(B)-4 (SWEC, 2001b), as discussed in Section 2.6.1.12.1).

The Canister Transfer Building basemat will be founded on the silty clay/clayey silt layer that is below the eolian silt. The design calls for soil cement to be placed around the Canister Transfer Building base mat to make the free-field soil profile for the building consistent with that for the storage pad emplacement area and to help resist sliding forces due to the higher design basis ground motions. Soil cement will surround the

foundation mat and will extend outward from the mat to a distance equal to the associated mat dimension; i.e., approximately 240 ft out from the mat in the east and west directions and approximately 280 ft out in the north and south directions. Existing soils (eolian silt and silty clay/clayey silt) will be excavated to a depth of approximately 5 ft 8 inches below grade, mixed with cement, and placed and compacted around the foundation mat.

The soil cement placed around the Canister Transfer Building foundation mat will be 5 ft thick and have a minimum unconfined compressive strength of 250 psi to ensure that there is an adequate factor of safety against sliding of the Canister Transfer Building (based on Calculation 05996.02-G(B)-13 (SWEC, 2001c), as discussed in Section 2.6.1.12.2). The top 8 inches will be filled with compacted coarse aggregate, similar to that used in the pad emplacement area.

PFS is developing the soil-cement mix design using standard industry practice. This effort includes performing laboratory testing of soils obtained from the site. This on-going laboratory testing is being performed in accordance with the requirements of Engineering Services Scope of Work (ESSOW) for Laboratory Testing of Soil-Cement Mixes, ESSOW 05996.02-G010 (SWEC, 2001e). This program includes measuring gradations and Atterberg limits of samples of the near-surface soils obtained from the site. It includes testing of mixtures of these soils with varying amounts of cement and the testing of compacted specimens of soil-cement to determine moisture-density relationships, freeze/thaw and wet/dry characteristics, compressive and tensile strengths, and permeability of compacted soil-cement specimens. The entire laboratory testing program is being conducted in full compliance with the Quality Assurance (QA) Category I requirements of the ESSOW.

As part of this effort, PFS is performing so-called durability testing. These tests are performed in accordance with ASTM D559 and D560 to measure the durability of soil cement specimens exposed to 12 cycles of wet/dry and freeze/thaw conditions. As indicated on p. 16 of PFS Calculation 05996.02-G(B)-4 (SWEC, 2001b):

"The unconfined compressive strength of the soil cement adjacent to the pads needs to be at least 50 psi to provide an adequate subbase for support of the cask transporter, in lieu of placing and compacting structural fill, but it likely will be at least 250 psi to satisfy the durability requirements associated with environmental considerations (i.e., freeze/thaw and wet/dry cycles) within the frost zone (30 in. from the ground surface)."

PFS is performing these tests to determine the amounts of cement and water that must be added to the site soils and to determine the compaction requirements to ensure that the soil cement will be durable and will withstand exposure to the elements. As indicated on p. 8 of Portland Cement Association (1971):

"The freeze-thaw and wet-dry tests were designed to determine whether the soil-cement would stay hard or whether expansion and contraction on alternate freezing-and-thawing and moisture changes would cause the soil-cement to soften."

And on p. 32:

"The principle requirement of a hardened soil-cement mixture is that it withstand exposure to the elements. Thus the primary basis of comparison of soil-cement mixtures is the cement content required to produce a mixture that will withstand the stresses induced by the wet-dry and freeze-thaw tests. The service record of projects in use proves the reliability both of the results based on these tests and of the criteria given below.

The following criteria are based on considerable laboratory test data, on the performance of many projects in service, and on information obtained from the outdoor exposure of several thousand specimens. The use of these criteria will provide the minimum cement content required to produce hard, durable soil-cement, suitable for base-course construction of the highest quality.

- 1. Soil-cement losses during 12 cycles of either the wet-dry test or freeze-thaw test shall conform to the following limits:
Soil Groups A-1, A-2-4, A-2-5, and A-3, not over 14 percent;
Soil Groups A-2-6, A-2-7, A-4, and A-5, not over 10 percent;
Soil Groups A-6 and A-7, not over 7 percent.*
- 2. Compressive strengths should increase both with age and with increases in cement content in the ranges of cement content producing results that meet requirement 1."*

The on-going laboratory testing program will also include additional tests to confirm that the bond at the interfaces between concrete and soil-cement, soil-cement and soil-cement, and soil-cement and the site soils will exceed the strength of the in situ clayey soils. These tests will include direct shear tests, performed on specimens prepared from the site soils at various cement and moisture contents, in a manner similar to that used by DeGroot in his testing of bond along soil-cement interfaces.

Based on the above, PFS has adequately defined the measures that will be followed in the design and construction of the soil cement to assure that the assumed bonds can be sustained through the period of interest. PFS has committed to performing site-specific testing to confirm that the required interface strengths are available to resist sliding forces due to an earthquake. As indicated above, this testing will include direct shear tests to be performed in the laboratory in the near-term (pre-construction) during the soil-cement mix development to demonstrate that the required interface strengths can be achieved and during construction to demonstrate that the required interface strengths are achieved. In addition, PFS has committed to augmenting this field testing program by performing additional site-specific testing of the strengths achieved at the interface between the bottom of the soil cement and the underlying soils.

The most recent analyses of the PFSF design basis ground motions assumed the incorporation of a 5 ft thick soil cement layer over the entire pad emplacement area and also surrounding the Canister Transfer Building. The 5 ft soil cement layer around the Canister Transfer Building extends to the free field boundary from the edge of the building basemat. This soil cement layer is assumed to have a minimum shear wave velocity greater than 1,500 fps (Geomatrix 2001a and 2001b). As indicated in Section 2.6.1.2.2, soil cement around the Canister Transfer Building should have a minimum unconfined compressive strength of 250 psi to ensure a factor of safety greater than 1.1 for seismic sliding stability. The design requirements for the 5 ft thick soil cement layer

around the Canister Transfer Building will be based on the results of laboratory and field testing to be conducted during the final design stage.

The surficial layer of eolian silt, existing across the entire site as shown in the pad emplacement area foundation profiles (Figure 2.6-5, Sheets 1 through 14), is a major factor in the earthwork required for construction of the facility. This layer consists of a nonplastic to slightly plastic silt, and it has an average thickness of approximately 2 feet across the pad emplacement area. This layer was expected to be removed prior to construction of the storage pads. However, based on evaluation of the earthwork associated with site grading requirements for flood protection and the environmental impacts of truck trips required to import fill to replace this material, PFS will stabilize this soil with cement and use it as base material beneath the storage pads and adjacent driveways.

Section 2.6.1.12 indicates that there is ample margin in the factor of safety against a bearing capacity failure of the silty clay/clayey silt underlying the site and that the settlements are acceptable for these structures. They indicate that the critical design factor with respect to stability of these structures is the resistance to sliding due to loadings from the design basis ground motion. As discussed in that section, the silty clay/clayey silt layer has sufficient strength to resist these dynamic loadings; therefore, adequate sliding resistance can be provided by constructing the structures directly on the silty clay/clayey silt layer. The soil cement around the storage pads and Canister Transfer Building will be designed and constructed to have a minimum unconfined compressive strength of 250 psi and quality assurance testing will be performed during construction to demonstrate that this minimum strength is achieved. The soil cement directly beneath the storage pads will be designed and constructed to have an unconfined compressive strength of at least 40 psi with static elastic modulus of less than ~75,000 psi. Therefore, the resistance to sliding due to loadings from the design

basis ground motion will be enhanced by constructing the cask storage pads on a properly designed and constructed soil-cement subgrade. See the section titled "Sliding Stability of the Cask Storage Pads Founded on and Within Soil Cement" in 2.6.1.12.1 for additional details.

Using soil cement to stabilize the eolian silt will reduce the amount of spoil materials generated, create a stable and level base for pad construction, and substantially improve the sliding resistance of the storage pads. The soil cement will be placed above the *in situ* silty clay/clayey silt layer and will be designed to improve the strength of the eolian silt so that it will be stronger than the clayey soils that were originally intended for use as the founding medium for the pads. The soil cement will also be used to replace the compacted structural fill that the original plan included between the rows of pads. This continuous layer of soil cement, existing under and between the pads, will spread the loads from the pads beyond the footprint of the pads, resulting in decreased total and differential settlements of the pads. The layer of soil cement above the base of the pads and the bond and friction of the pad foundation with the underlying soil-cement layer will greatly increase the sliding resistance of the pad.

Soil cement has been used extensively in the United States and around the world since the 1940's. It was first used in the United States in 1915 for constructing roads. It also has been used at nuclear power plants in the United States and in South Africa. The largest soil-cement project worldwide involved construction of soil-cement slope protection for a 7,000-acre cooling-water reservoir at the South Texas Nuclear Power Plant near Houston, TX. Soil cement also was used to replace an ~18-ft thick layer of potentially liquefiable sandy soils under the foundations of two 900-MW nuclear power plants in Koeberg, South Africa (Dupas and Pecker, 1979). The strength of soils can be improved markedly by the addition of cement. The eolian silt at the site is similar to the soils identified as Soil A-4 in Nussbaum and Colley (1971), Soils 7 and 8 in Balmer

(1958), and Soil 4 in Felt and Abrams (1957). As indicated for Soil A-4 in Table 5 of Nussbaum and Colley (1971), the addition of just 2.5% cement by weight to the silt increased the cohesion from 5 psi (720 psf) to 30 psi (4,320 psf). The cohesion for Soils 7 and 8 also were increased significantly by the addition of low percentages of cement, as shown on Tables VI and VII of Balmer (1958). Figure 10 in Felt and Abrams (1957) illustrates the continued strength increase over time for these soil-cement mixtures. Other examples of soil-cement strength increases over time are presented in Figure 4.3 of ACI (1998), Table 6 of Nussbaum and Colley (1971), and Figures 6 and 7 of Dupas and Pecker (1979). Therefore, the soil cement will be much stronger than the underlying silty clay/clayey silt and the strength will increase with time, providing an improved foundation material. This will provide additional margin against sliding compared to the original plan to construct the pads directly on the silty clay/clayey silt layer.

As shown in the section titled "Sliding Stability of the Cask Storage Pads Founded on and Within Soil Cement" in Section 2.6.1.12.1 above, the shear resistance required at the base of the pads can be provided easily by the passive resistance of the soil cement acting against the vertical side of the foundation and by bond between the pad foundation and soil-cement contact and the cohesive strength of the soil cement. Shear resistance will be transferred through the approximately 2-ft thick soil-cement layer and into the underlying silty clay/clayey silt subgrade. Additional resistance will be provided by the continuous layer of soil cement under and between the pads; therefore, shear resistance requirements within the silty clay/clayey silt layer will be less with the soil-cement layer compared to the original plan to construct the pads directly on the silty clay/clayey silt without the proposed soil-cement layer.

DeGroot (1976) indicates that this bond strength can be easily obtained between layers of soil cement. He performed nearly 300 laboratory direct shear tests to determine the

effect of numerous variables on the bond between layers of soil cement. These variables included the length of time between placement of successive layers of soil cement, the frequency of watering while curing soil cement, the surface moisture condition prior to construction of the next lift, the surface texture prior to construction of the next lift, and various surface treatments and additives.

His results demonstrated that, with the exception of treating the surface of the lifts with asphalt emulsion, asphalt cutback, and chlorinated rubber compounds, the bond strength always exceeded 6.6 psi, the minimum required value of cohesion if the passive resistance acting on the sides of the pads is ignored. The minimum bond strength he reports, other than for the asphalt and chlorinated rubber surface treatments identified above, is 8.7 psi. This value applied for two tests that were performed on samples that had time delays of 24 hours and did not have a cement surface treatment along the lift line. He reports that nearly all of the specimens that used a cement surface treatment broke along planes other than along the lift lines, indicating that the bond between the layers of soil cement was stronger than the remainder of the specimens. Excluding the specimens that had 24-hr delays between lift placements and which did not use the cement surface treatment, the minimum bond strength was 10.7 psi and there were only two others that had bond strengths that were less than 20 psi. Even these minimum values for the group of specimens that did not use a cement surface treatment exceeded the cohesive strength (6.6 psi) required to obtain an adequate factor of safety against sliding without including the passive resistance acting on the sides of the pads, and all of the rest were much greater, generally more than an order of magnitude greater.

DeGroot reached the following conclusions:

1. Increasing the time delay between lifts decreases bond.
2. High frequency of watering the lift line decreases the bond.

3. Moist curing conditions between lift placements increases the bond.
4. Removing the smooth compaction plane increases the bond.
5. Set retardants decreased the bond at 4-hr time delay.
6. Asphalt and chlorinated rubber curing compounds decreased the bond.
7. Small amounts of cement placed on the lift line bonded the layers together, such that failure occurred along planes other than the lift line, indicating that the bond exceeded the shear strength of the soil cement.

DeGroot (1976) noted that increasing the time delay between placement of subsequent lifts decreases the bond strength. The nature of construction of soil cement is such that there will be occasions when the time delay will be greater than the time required for the soil cement to set. This will clearly be the case for construction of the concrete storage pads on top of the soil-cement surface, because it will take some period of time to form the pad, build the steel reinforcement, and pour the concrete. He noted that several techniques can be used to enhance the bond between these lifts to overcome this decrease in bond due to time delay. In these cases, more than sufficient bond can be obtained between layers of soil cement and between the set soil-cement surface and the underside of the cask storage pads by simply using a cement surface treatment.

DeGroot's direct shear test results demonstrate that the specimens having a cement surface treatment all had bond strengths that ranged from 47.7 psi to 198.5 psi, with the average bond strength of 132.5 psi. Even the minimum value of this range is nearly an order of magnitude greater than the cohesion (6.6 psi) required to obtain a factor of safety against sliding of 1.1, conservatively ignoring the passive resistance available on the sides of the pads. Therefore, when required due to unavoidable time delays, the techniques DeGroot describes for enhancing bond strength will be used between the top of the soil cement and succeeding lifts or the concrete cask storage pads, to assure that the bond at the interfaces are greater than the minimum required value. These

techniques will include roughening and cleaning the surface of the underlying soil cement, proper moisture conditioning, and using a cement surface treatment.

A fundamental assumption in the PFS approach is that sufficient bonding and shear transfer between clay and soil cement interfaces can be achieved using various construction techniques. As indicated above, DeGroot has demonstrated that techniques are available that will enhance the bond between lifts of soil cement. These techniques should be equally effective when applied to the soils at the PFSF site. PFS has committed to perform direct shear tests of the interface strengths during the design phase of the soil cement to demonstrate that the required interface strength can be achieved, as well as during construction, to demonstrate that they are achieved.

PFS has discussed the change to use soil cement beneath the storage pads with the project consultants who have analyses in-place that are based on the storage pads resting on the silty clay/clayey silt. The consultants contacted were Geomatrix (development of seismic criteria and soil dynamic properties), Holtec International (cask stability analysis), and International Civil engineering Consultants (pad design). Each has indicated their analyses would not be adversely affected by this proposed change.

The design, placement, testing, and performance of soil cement is a well-established technology. The "State-of-the-Art Report on Soil Cement" (ACI, 1998) provides information about soil cement, including applications, materials, properties, mix proportioning, design, construction, and quality-control inspection and testing techniques. PFS will develop site-specific procedures to implement the recommendations presented in ACI (1998) regarding mix proportioning, testing, construction, and quality control. The following describes the processes that will be used to develop a proper soil-cement mix design and establish adequate sliding resistance at each material interface in the storage pad and soil system:

- Soil-Cement Mix and Procedure Development – The sliding forces due to the design basis ground motion will be resisted by bond between the base and sides of the foundation and the soil cement and by passive resistance of the soil cement acting against the vertical side of the foundation. The soil-cement mix will be designed and constructed to exceed the minimum shear resistance requirements. During the soil-cement design phase, direct shear testing will be conducted along manufactured soil-cement lift contacts and concrete contacts that represent anticipated field conditions. The direct shear testing, along with other standard soil-cement testing, will be used to confirm that adequate shear resistance and other strength requirements will be provided by the final soil-cement mix design. Procedures required for placement and treatment of the soil cement, lift surfaces, and foundation contact will be established in accordance with the recommendations of ACI (1998) during the mix design and testing process. Specific construction techniques and field quality control requirements will be identified in the construction specifications developed by PFS during this detailed design phase of the project.
- Soil-Cement Lift and Concrete Interface – The soil cement will be constructed in lifts approximately 6-in. thick (compacted thickness) as described in ACI (1998). Construction techniques will be used to ensure that the interface between the soil-cement layers will be adequately bonded to transmit shear stresses. As described in Section 6.2.2.5 of ACI (1998), these techniques will include, but will not be limited to: minimizing the time between placement of successive layers of soil cement, moisture conditioning required for proper curing of the soil cement, producing a roughened surface on the soil cement prior to placement of additional lifts or concrete foundations, and using a dry cement or cement slurry to enhance the bonding of concrete or new soil cement layers to underlying layers that have already set. In addition to conventional quality control testing performed for soil-cement

projects, direct shear testing will be performed on representative samples obtained from placed lift contacts to confirm design requirements are obtained. Sacrificial soil-cement lifts may be used to protect the soil-cement subgrade in the pad foundation areas.

- Soil Cement and *In Situ* Clay Interface – The soil cement and *in situ* clay interface will be constructed such that a good bond will be established between the two materials. Construction techniques will be utilized that will ensure that the integrity of the upper surface of the clay is maintained and that a good interface bond between the two materials is obtained. Specific construction techniques and field quality control requirements will be identified in the construction specifications developed by PFS during the detailed design phase of the project.

An additional benefit of incorporating the soil cement into the design is that it will minimize the environmental impacts of constructing the facility. Using on-site materials to construct the soil cement, rather than excavating and spoiling those materials, will reduce environmental impacts of the project. In addition, replacement of some of the structural fill layer between the rows of pads with soil cement, as shown in Figure 4.2-7, will result in reduced trucking requirements associated with transporting those materials to the site.

Adequacy of the Soil Cement Design

The adequacy of the design of the soil cement surrounding and underlying the pads to ensure the sliding stability of the pads under seismic conditions is demonstrated by S&W Calculation 05996.02-G(B)-04 (SWEC, 2001b). This calculation determined that there is sufficient shear strength at the interfaces between the concrete pad and the underlying soil cement and between that soil cement layer and the underlying clayey soils that the factor of safety against sliding exceeds the minimum required value, with

no credit for the soil cement placed between storage pads above the bottom of the pads. The underlying layer of soil cement is also required to have a static modulus of elasticity less than or equal to 75,000 psi to ensure that decelerations of a cask resulting from a hypothetical storage cask tipover event or vertical end drop accident do not exceed design criteria (Sections 4.2.1.5.1.E and 8.2.6).

The large extent of soil cement in the storage pad emplacement area allows the soil cement layer to be considered as part of the free field soil profile for the site response analyses. The properties of the soil cement, higher shear wave velocity and higher density than the existing soils in the area, help to minimize the response at the surface of the site caused by the design basis ground motions. Soil cement was added around the Canister Transfer Building foundation mat to make the free field soil profile for the building consistent with that for the storage pad emplacement area (as discussed in Section 2.6.4.11), and to help resist sliding forces, in conjunction with the building's perimeter key, due to the revised design basis ground motions. The adequacy of this design feature is demonstrated in Calculation No. 05996.02-G(B)-13 (SWEC, 2001c), which determined that the design of the soil cement surrounding the Canister Transfer Building (in conjunction with the building's perimeter key) is adequate to ensure the stability of the Canister Transfer Building under seismic conditions.

2.6.4.12 Criteria and Design Methods

The allowable bearing capacity of footings is limited by shear failure of the underlying soil and by footing settlement. The minimum factor of safety against a bearing capacity failure from static loads (dead load plus maximum live loads) is 3.0 and from static loads plus loads due to extreme environmental conditions, such as design basis ground motion, is 1.1. Allowable settlements are determined based on Table 14.1, "Allowable Settlement," of Lambe & Whitman (1969) and assume that the differential settlement will be 3/4 of the maximum settlement. Section 2.6.1.12 provides more details.

In order to comply with the requirements of NUREG-75/087, Section 3.8.5, "Foundations," Section II.5, "Structural Acceptance Criteria," the recommended minimum factor of safety against overturning or sliding failure from static loads (dead load plus maximum live loads) is 1.5 and from static loads plus loads due to extreme environmental conditions, such as design basis ground motion, is 1.1. Where the factor of safety against sliding is less than 1 due to the design basis ground motion, the displacements the structure may experience are calculated using the method proposed by Newmark (1965) for estimating displacements of dams and embankments during earthquakes. The magnitude of these displacements are evaluated to assess the impact on the performance of the structure. See Section 2.6.1.12 for details about these analyses.

2.6.5 Slope Stability

There are no slopes close enough to the proposed Important to Safety facilities that their failure could adversely affect the operation of these facilities.

THIS PAGE INTENTIONALLY LEFT BLANK